

Investigating the Reactivity of Marine Bacteria with Copper and other Heavy Metals

by

Sara Maria Tuck

Department of Chemistry  
Duke University

Defense Date: July 22<sup>nd</sup>, 2024

Approved:

Katherine J. Franz, Supervisor

Kenan P. Fears

Michael C. Fitzgerald

Qiu Wang

Ross Widenhoefer

Dissertation submitted in partial fulfillment of the requirements for the degree of  
Doctor of Philosophy in the Department of Chemistry in The Graduate School of  
Duke University

2024

ABSTRACT

Investigating the Reactivity of Marine Bacteria with Copper and other Heavy Metals

by

Sara Maria Tuck

Department of Chemistry  
Duke University

Defense Date: July 22<sup>nd</sup>, 2024

Approved:

Katherine J. Franz, Supervisor

Kenan P. Fears

Michael C. Fitzgerald

Oiu Wang

Ross Widenhoefer

Dissertation submitted in partial fulfillment of the requirements for the degree of  
Doctor of Philosophy in the Department of Chemistry in The Graduate School of  
Duke University

2024

Copyright by  
Sara Maria Tuck  
2024

## Abstract

Marine bioinorganic chemistry is an emerging field that focuses on how inorganic elements impact biological functions within marine organisms. Exploration of heavy metals within marine environments is the connection that holds the world presented herein together.

The work begins with an examination of Interspeed 640, a popular antifouling (AF) coating that utilizes cuprous oxide ( $\text{Cu}_2\text{O}$ ) as the primary biocide, to understand the rationale behind its declining efficacy. This effort was approached in two distinct ways: 1) by designing an assay to characterize the impact of environmental conditions on surface composition and copper (Cu) release to define the interface primary colonizing bacterial species interact with, and 2) by describing the bacterial communities involved in primary colonization to understand acquired Cu tolerance.

First, a newly developed and highly tunable lab-scale assay was utilized to measure the impact of environmental conditions on surface composition and Cu release. This method was utilized to describe the behavior of Interspeed 640 in an inert environment (double-distilled, 18.2 M $\Omega$  water, (ddH $_2$ O)) and under conditions which may facilitate biofilm growth (tryptic soy broth, (TSB)). We utilized x-ray photoelectron spectroscopy (XPS) to characterize the coating surface and inductively coupled plasma optical emission spectroscopy (ICP-OES) to measure Cu release over a 14-day period. Under both immersion conditions, XPS analysis of the coating surface showed signs of

hydrolysis. Coated substrates immersed in TSB demonstrated an increase in both nitrogen and copper as compared to those in water. Additionally, coated substrates immersed for 14 days in TSB released approximately 500% more Cu than those immersed in water.

Next, polyvinyl chloride panels either left blank or coated with Interspeed 640 were deployed at three field sites to collect, isolate, and identify bacterial species involved in the early stages of biofouling. We have created a library of primary colonizing bacteria for all three field sites and, for one site, have completed a preliminary assessment of bacterial Cu tolerance capabilities using broth microdilution assays. These results indicate that Cu tolerance is not unique to species isolated from coated panels.

Further investigations into the interplay between metal ions and marine bacteria continue in the following section where *Marinobacter atlanticus* is evaluated for potential applications in bioremediation. *M. atlanticus* can produce small amounts of electricity and this ability is likely dependent upon labile metal ion concentration and mineral cycling. We hypothesized that *M. atlanticus* may be a promising candidate for applications in heavy metal remediation or as a biosensor. We utilized broth microdilution assays to expose *M. atlanticus* to a concentration range of essential and non-essential metal ions. *M. atlanticus* demonstrated a profound ability to grow in the presence of metal concentrations that significantly exceed those found in native

environments. In a metal detoxification assay, where the ability of *M. atlanticus* to remove metal ions from solution was assessed, we found that this bacterium is unable to significantly reduce metal concentrations.

In one final shift of focus, we provide an examination of bioactive molecules isolated from evolutionarily resilient organisms via an investigation of the Clavanin family of antimicrobial peptides. Prior literature on these peptides indicates the possession of broad-spectrum antimicrobial activity. We focused on the antimicrobial of ClavA against fungal pathogens *Candida albicans* and *Cryptococcus neoformans* and the bacterium *Escherichia coli* strain BW25113; ClavC was tested against *C. albicans* and *E. coli*. Overall, both peptides exhibited enhanced antimicrobial activity under acidic (pH 5.5) and, in most cases, ClavC was more potent than ClavA. When supplemental Cu or Zn were introduced, significant metal modulated activity increases were seen between ClavA and Cu at pH 5.5 against *C. albicans* and *C. neoformans*. Conversely, the combination of ClavC and Cu at pH 5.5 seemed to inhibit peptide activity.

## **Dedication**

To my younger self, thank you for teaching me the value of chasing dreams and believing in magic. I hope I continue to make you proud.

# Contents

Abstract .....	iv
List of Tables.....	xiii
List of Figures.....	xiv
Acknowledgements.....	xvi
1. Introduction.....	1
1.1 Marine Bioinorganic Chemistry .....	1
1.2 Heavy Metal Contamination and Remediation.....	1
1.3 Environmental Impacts of Marine Biofouling .....	4
1.4 Potential within Marine Environments .....	7
1.4.1 Adapting Marine Microorganisms for Applications in Biotechnology .....	8
1.4.2 Leveraging Evolutionary Resilience Present in Marine Life for Advancing Human Health Incentives .....	9
1.5 Summary and Outlook.....	11
2. Assay Development to Characterize Environmental Impacts on the Behavior of a Copper-Based Antifouling Coating .....	12
2.1 Introduction .....	12
2.2 Results and Discussion.....	15
2.2.1 Assay Design to Assess Environmental Impact on Copper Release and Coating Surface Integrity .....	15
2.2.2 Copper Release is Increased Under Conditions which Favor Bacterial Growth .....	18
2.2.3 Characterization of Immersed Surfaces Suggests Differential Changes in Composition and Minor Coating Hydrolysis .....	22

2.3 Conclusions and Future Directions .....	32
2.4 Methods .....	34
2.4.1 Materials and General Methods.....	34
2.4.2 Substrate Preparation .....	34
2.4.3 Sampling Conditions .....	35
2.4.4 Inductively Coupled Plasma Optical Emission Spectroscopy (ICP-OES) .....	36
2.4.4.1 Sample Preparation .....	36
2.4.4.2 Calibration Curves and Analysis Parameters .....	36
2.4.5 X-ray Photoelectron Spectroscopy (XPS).....	37
2.4.5.1 Sample Preparation .....	37
2.4.5.2 Analysis and Quantification .....	38
2.5 Supplemental Materials .....	39
3. Isolation, Identification, and Characterization of Primary Colonizing Bacteria Harvested from Antifouling Coatings.....	40
3.1 Introduction .....	40
3.2 Results and Discussion.....	44
3.2.1 Biofilm Community Development is Influence by Environmental Factors .....	44
3.2.2 Optimization of Cell Culture Conditions .....	50
3.2.3 Copper Tolerance is Not Exclusive to Isolates Harvested from Interspeed 640 Coated Panels .....	52
3.3 Conclusions and Future Directions .....	56
3.4 Methods .....	59
3.4.1 Materials and General Methods.....	59

3.4.2 Panel Preparation, Deployment, and Sampling .....	59
3.4.3 Species Isolation .....	59
3.4.4 Species Identification.....	60
3.4.4.1 16S Amplicon Sequencing .....	60
3.4.4.2 Data Analysis .....	61
3.4.5 Copper Tolerance Profiles.....	62
4. Interactions between <i>Marinobacter atlanticus</i> strain CP-1 and Heavy Metals .....	63
4.1 Introduction .....	63
4.2 Results and Discussion.....	66
4.2.1 <i>Marinobacter atlanticus</i> shows Broad Tolerance Against Multiple Metal Ions...66	
4.2.2 <i>Marinobacter atlanticus</i> Lacks Significant Abilities to Uptake Metal Ions from Solution.....71	
4.3 Conclusions and Future Directions .....	77
4.4 Methods.....	78
4.4.1 Materials and General Methods.....	78
4.4.2 Bacterial Strains and Culture Conditions .....	78
4.4.3 Metal Tolerance Assays.....	78
4.4.3.1 Preparation of Metal Stock Solutions .....	78
4.4.3.2 Microdilution Assays .....	79
4.4.4 Metal Detoxification Assays .....	80
4.4.5 Inductively Coupled Plasma Optical Emission Spectroscopy (ICP-OES) .....	81
4.4.5.1 Sample Preparation .....	81

4.4.5.2 Calibration Curves and Analysis Parameters .....	81
4.5 Supplemental Materials .....	83
5. Investigating metal modulation on the antimicrobial activity of Clavanin A and Clavanin C to describe the role of biometals in primitive innate immunity .....	84
5.1 Introduction .....	84
5.2 Results and Discussion.....	87
5.2.1 Antifungal Activity of Clavanin A and Clavanin C against <i>Candida albicans</i> . ..	87
5.2.2 Clavanin A and Clavanin C Retain Candidacidal Activity in the Absence of Cu and Zn.....	93
5.2.3 Antifungal Activity of Clavanin A Against <i>Cryptococcus neoformans</i> H99 is Potentiated under Acidic Conditions.....	95
5.2.4 Antibacterial Activity of Clavanin and Clavanin C Against <i>Escherichia coli</i> strain BW25113 .....	97
5.3 Conclusions and Future Directions .....	101
5.4 Methods.....	103
5.4.1 Materials and General Methods.....	103
5.4.2 Peptide Synthesis .....	103
5.4.3 Peptide Purification .....	104
5.4.4 Preparation and Quantification of Stock Solutions.....	104
5.4.5 Bacterial Strains, Yeast Strains, and Culture Conditions .....	105
5.4.6 Synthetic Defined (SD+) Media.....	106
5.4.7 Antibacterial and Antifungal Activity Assays.....	107
5.4.7.1 Antibacterial Microdilution Assays .....	107
5.4.7.2 Antifungal Two-Dimensional Microdilution Assays.....	108

5.4.7.3 Antibacterial Two-Dimensional Microdilution Assays .....	109
5.4.7.4 Antifungal Two-Dimensional Microdilution Assays.....	110
6. Conclusion .....	112
References .....	114
Biography.....	137

## List of Tables

Table 1: Bacterial species isolated from site 1 (Chesapeake Bay, Chesapeake Beach, MD, US).....	46
Table 2: Bacterial species isolated from site 2 (Port Marina, Cape Canaveral, FL, US).....	47
Table 3: Bacterial species isolated from site 3 (Indian River Lagoon, Melbourne, FL, US) .....	47
Table 4: Metal Concentrations Chosen for Metal Detoxication Assay.....	73
Table 5: Sequences of Clavanin Antimicrobial Peptides.....	86

## List of Figures

Figure 1: General workflow for assessing the behavior of Interspeed 640 under specifically defined conditions. ....	16
Figure 2: Copper released after 24 hours from Interspeed 640 coated substrates immersed in either ddH <sub>2</sub> O (blue, left axis) or TSB (red, right axis). ....	19
Figure 3: Copper released after 14 days from Interspeed 640 coated substrates immersed in either ddH <sub>2</sub> O (top) or TSB (bottom). ....	20
Figure 4: Environmentally induced changes in surface composition for substrates immersed in ddH <sub>2</sub> O (top) and TSB (bottom). ....	23
Figure 5: Comparison of a coated substrate control to a substrate immersed for 14 days in ddH <sub>2</sub> O. ....	26
Figure 6: Comparison of a coated substrate control to a substrate immersed for 14 days in TSB. ....	28
Figure 7: Deconvoluted C 1s spectra obtained from high-resolution XPS scans. ....	31
Figure 8: Comparison of biofouling in 2006 vs 2018 on Interspeed 640 after static immersion. ....	42
Figure 9: Temperature and salinity data from 2023 for three sites of panel deployment. ....	45
Figure 10: Phylogenetic tree depicting the relationship between species harvested across three field sites from both coated and uncoated panels. ....	50
Figure 11: Growth curves for selected species isolated from site 1 in three different types of culture media. ....	51
Figure 12: Growth curves depicting the behavior of three bacterial species isolated from the uncoated panels deployed at site 1 following incubation with copper. ....	53
Figure 13: Growth curves depicting the behavior of three bacterial species isolated from panels coated with Interspeed 640 (IS640) from site 1 after incubation with copper. ....	55
Figure 14: Growth curves for <i>Marinobacter atlanticus</i> exposed to 10 mM of heavy metals. ....	68

Figure 15: Growth curves for <i>Marinobacter atlanticus</i> in the presence of 100 mM Mn and 100 mM V.....	69
Figure 16: <i>M. atlanticus</i> has Minimal Metal Detoxification Capabilities.....	75
Figure 17: Antifungal activity of Clavanin A with Cu <sup>2+</sup> Supplementation Against <i>C. albicans</i> .....	89
Figure 18: Antifungal activity of Clavanin A with Zn <sup>2+</sup> Supplementation Against <i>C. albicans</i> .....	90
Figure 19: Antifungal activity of Clavanin C with Cu <sup>2+</sup> Supplementation Against <i>C. albicans</i> .....	91
Figure 20: Antifungal activity of Clavanin C with Zn <sup>2+</sup> Supplementation Against <i>C. albicans</i> .....	92
Figure 21: Candidacidal Activity of Clavanin A and Clavanin C under Metal Complete, Zinc Deplete, and Copper Deplete Conditions.....	94
Figure 22: Antifungal Activity of ClavA against <i>C. neoformans</i> is Impacted by Zn <sup>2+</sup> Supplementation.....	96
Figure 23: Antifungal Activity of ClavA against <i>C. neoformans</i> is Increased by Cu <sup>2+</sup> Supplementation.....	97
Figure 24: Antibacterial Activity of Clavanin A with Supplemental Cu <sup>2+</sup> or Zn <sup>2+</sup> against <i>Escherichia coli</i> strain BW25113.....	99
Figure 25: Antibacterial Activity of Clavanin A with Supplemental Cu <sup>2+</sup> or Zn <sup>2+</sup> against <i>Escherichia coli</i> strain BW25113.....	100
Figure 26: Antibacterial Activity of Clavanin C with Supplemental Cu <sup>2+</sup> or Zn <sup>2+</sup> against <i>Escherichia coli</i> strain BW25113.....	101

## Acknowledgements

My academic journey has been full of love and support from the beginning, and I am so incredibly grateful to all the labmates, colleagues, mentors, supervisors, friends, and family members who have been there for me throughout this journey.

I want to thank the members of the Franz lab, past and present, for supporting my non-traditional PhD journey and remaining constant throughout. I'd like to give special thanks to Dr. Catherine Denning-Jannace, who has been a continuous source of friendship and guidance through every high and low. I would also like to give thanks to my advisor Dr. Katherine Franz, who has been a wonderful source of guidance and wisdom. Kathy encouraged me as I forged my own path; she supported my participation in both an internship and in a program that allowed me to build invaluable connections in my future field. Her flexibility and openness to new directions and opportunities greatly enhanced my graduate experience.

I must also express my sincere gratitude to the many friends I have made at the Naval Research Laboratory. To Dr. Kenan Fears, thank you for believing in me and guiding me through new scientific adventures. You have been a wonderful source of advice, support and encouragement. To Brian and Jen, you have both been incredible friends, I am so grateful for the long lunches, science talks, and adventures we have had. To the Dream Team, you know who you are, thank you for all the love, laughs, and hugs

(and sour patch kids). I would also like to recognize Dr. Matt Finn for his assistance (and patience) with my ICP experiments.

I would also like to thank the members of my committee, Dr. Michael Fitzgerald, Dr. Qiu Wang, and Dr. Ross Widenhoefer. I appreciate all the encouragement and feedback I have received throughout this journey; I am grateful to have had for their expertise and support.

I must give special thanks to the wonderful Meg Avery, Christiana Conti-Gooden and Lynn O'Neill; thank you for always advocating for me. Thank you for creating a welcoming and encouraging place to grow; thank you for the unyielding support and the many afternoon chats.

Beyond the lab, I have been supported by friends and family. To my friends at SportRock, thank you for pulling me away from science and reminding me of the importance of maintaining a work-life balance. To my oldest friend, Austin; look how far we've come! Thank you for the video game breaks, late night phone calls, obnoxious photos, and, most of all, showing up for me when I needed it most. Thank you for sending me food when I was too tired to cook and for making me laugh when everything felt too hard.

To my parents: Thank you. Those two words aren't nearly enough to fully explain the depth of my gratitude, but it is a place to start. I am incredibly lucky to have two supportive parents who have unfailingly been there for me. You have both nurtured

my curiosity and have always been the biggest supporters of my dreams. To my mom, my loudest cheerleader, thank you for the endless supply of hugs, phone calls, loving messages, and for constantly encouraging me to do my best despite whatever challenge I face. To my dad, thank you for your continuous love, support, and guidance. I wouldn't be here without the both of you.

# **1. Introduction**

## ***1.1 Marine Bioinorganic Chemistry***

The emerging field of marine bioinorganic chemistry combines knowledge from bioinorganic chemistry with that of trace metal geochemistry to interrogate the role of metal ions within aquatic environments.<sup>1</sup> Specific focus is given to the distribution of inorganic elements, particularly heavy metals, and to the processes in which these metals are utilized throughout natural environments. In aquatic environments, heavy metals are among the least abundant metal ions with typical concentrations in the pico- to nanomolar range.<sup>1,2</sup> Heavy metals, in a biological context, can be broadly categorized as essential or non-essential.<sup>1-4</sup> Essential metals, such as cobalt (Co), copper (Cu), iron (Fe), manganese (Mn), molybdenum (Mo), and zinc (Zn), are crucial for various physiological and biochemical functions.<sup>1-5</sup> However, at high concentrations essential metals may induce deleterious effects in biological systems.<sup>2-6</sup> Non-essential elements, such as cadmium (Cd), lead (Pb), arsenic (As), and mercury (Hg), typically play no vital physiological role and are often toxic at low concentrations.<sup>1-6</sup>

## ***1.2 Heavy Metal Contamination and Remediation***

. While generally low in concentration, heavy metals arise in marine environments from naturally occurring instances including erosion of natural deposits, atmospheric deposition, volcanic activity, and mineral deterioration.<sup>2,5</sup> In the last few decades, increasing environmental concentrations of heavy metals have become a major

concern and is mostly attributed to anthropogenic activity.<sup>7-9</sup> Heavy metal contamination is the result of anthropogenic processes<sup>10, 11</sup> within agriculture, industry, and urbanization, such as the use of inorganic fertilizers,<sup>12, 13</sup> cleaning and scraping of ship hulls,<sup>14-16</sup> oil refining and mining,<sup>17, 18</sup> and electronic waste.<sup>19, 20</sup> Contaminants make their way into aquatic environments, typically through run off and generated wastewater, where they are distributed into the water column and into marine sediments which causes significant ecological damage in multiple ecosystems.<sup>8, 21-23</sup> As heavy metals are resistant to complete degradation they accumulate in the soil and water and ultimately can end up in humans and animals.<sup>24</sup>

Heavy metal aggregation threatens marine ecosystems, contaminates food chains and webs, and induces a litany of damaging effects when toxicity thresholds of biological systems are exceeded. Mechanisms of toxicity can vary, with excess heavy metals known to induce DNA damage, cause protein dysfunction, inhibit cellular respiration, and increase the production of reactive oxygen species.<sup>7, 11, 25</sup> In humans, toxic metals can accumulate in major organs and can severely impact health. Cadmium, a non-essential metal that can bioaccumulate via contamination from pesticides and refined petroleum products,<sup>11</sup> can induce damage to the central nervous system (i.e., development of neurodegenerative diseases) and major organs (i.e., liver, kidneys, heart) upon exposure even to relatively low concentrations.<sup>25-27</sup> Essential metals can also

cause damage. For example, significant environmental Cu contamination arises from the maritime shipping industry and improper disposal of electronics.<sup>23, 25, 26</sup>

Currently employed methods to reduce and remediate heavy metal pollution in aquatic environments include membrane filtration, chemical precipitation, coagulation, hydrolysis, advanced oxidation, and ultrasonic mineralization.<sup>24, 25, 28</sup> Unfortunately, many of these methods are not feasible given the high amounts of metal ions present. An avenue of current research focuses on leveraging native microbial processes to control metal contamination by detoxification (e.g., metal chelation), bioaccumulation (e.g., adsorption, precipitation), and biotransformation (e.g., oxidation, reduction, isomerization, hydrolysis).<sup>7, 24, 26</sup> In the last decade, multiple microorganisms have successfully been employed for the bioremediation of certain trace metals. For example, the bacterium *Pseudomonas veronii* has shown efficacy towards removing Cd, Zn, and Cu,<sup>29</sup> and *Aspergillus nomius*, a fungal species, is effective at mitigating Pb.<sup>30</sup> Given current concerns with heavy metal pollutants accumulating in aquatic environments and evidence that microbes have capabilities to help mitigate this contamination, it is necessary to further our understanding of the interactions between marine-derived microbes and heavy metals. Characterizing this interplay may allow us to harness and fine-tune marine organisms to meet our needs.

### ***1.3 Environmental Impacts of Marine Biofouling***

Attempts to prevent and reduce biofouling, the accretion of unwanted biological material on submerged surfaces, have resulted in significant contributions to heavy metal pollution in aquatic environments.<sup>14</sup> Biofouling has been a concern for over 2000 years with early techniques ranging from sheathing ship bottoms in copper or lead, to applying coatings of oily mixtures containing arsenic, copper, mercury, and sulfur.<sup>31</sup> Copper (Cu) was a widespread biocide until the development of iron-hulled ships that were incompatible with the copper coatings.<sup>31</sup> Around the 1960's, a highly toxic compound, tributyltin (TBT), became commercialized in surface coatings for its efficacy at preventing biofouling.<sup>31, 32</sup> The use of TBT-based coatings was short-lived as environmental concerns resulted in its complete ban in the 1990's.<sup>31, 32</sup> The ban of TBT induced a resurgence of Cu-based coatings, which are still prevalent today. Modern methods of biofouling prevention involve coatings that target different stages of the biofouling process, either settlement or attachment.

The general process by which biofouling proceeds begins with the adsorption of organic materials and minerals on the surface, followed by the settlement of primary colonizers which form the biofilm layer.<sup>33</sup> The biofilm layer is essential for the subsequent adhesion of additional microorganisms that form a microfouling community. Eventually, the settlement of larger organisms such as algae and marine invertebrates that creates the macrofouling community.<sup>33</sup> Macrofouling organisms are

the main cause of increased drag coefficients which induces additional negative impacts such as increased fuel consumption and exhaust emissions.<sup>34</sup> While it is the macrofouling organisms that cause many of the deleterious effects of biofouling organisms, the settlement of these organisms depends on initial biofilm formation that commences shortly after immersion of a foreign object into the marine environment.

Coatings designed to prevent biofouling can broadly be generalized into those that inhibit the settlement of primary colonizers, known as antifouling (AF) coatings, and those that inhibit microbial attachment, known as foul-release (FR) coatings. AF coatings aim to entirely prevent the settlement of microorganisms by providing a chemically modified surface.<sup>35, 36</sup> FR coatings are designed to limit the strength of adhesion between the substrate and microorganisms; these coatings generally rely on hydrodynamic forces generated by currents, swell, and transit of the immersed surface.<sup>37</sup> FR coatings are currently becoming more popular, particularly with the utilization of techniques to preserve the coating when statically immersed, but AF coatings continue to be the most prevalent on marine vessels.<sup>15, 37</sup>

Currently, the most predominately applied coatings are Cu ablative AF coatings.<sup>15, 36</sup> Ablative, or self-polishing, coatings are those that are designed to slowly release biocidal compounds to prevent biofouling settlement.<sup>15, 31, 36</sup> These coatings may contain anywhere from 20 % to 75 % copper oxide (Cu<sub>2</sub>O) by weight and many formulations include additional zinc (as zinc oxide (ZnO) or zinc pyrithione (ZnPT)) as a

booster-biocide.<sup>38</sup> While copper AF coatings have a long history of efficacy, recent investigations suggest that they are declining.<sup>39</sup> The diminishing capabilities of these coatings is currently attributed to increased copper tolerance in primary colonizing bacteria allowing for biofilm formation despite high Cu loads. Our current hypothesis for this decline relies on two key details; the increased prevalence of dissolved copper in aquatic environments as a result of heavy metal pollution and the emergence and persistence of copper tolerant species.

As mentioned briefly in the previous section, efforts to combat marine biofouling have been significant contributors to heavy metal contamination in the marine ecosystem. The release of biocidal compounds in high concentrations poses a significant threat to the marine ecosystem as these toxins accumulate in the sediment and in the water column. It was estimated that upwards of  $15 \times 10^6$  kg/year of Cu is released into aquatic environments from AF paints worldwide.<sup>40, 41</sup> One of the hazards of biofouling accumulation on ships is the potential translocation of bacteria to new environments. Previous studies have discussed the relocation of copper-tolerant species into copper polluted regions where they are able to outcompete native bacteria, thus bolstering the spread of copper tolerance.<sup>33</sup> Additionally, marine biofilms are considered hotspots for the transfer of genes between species using a process known as horizontal gene transfer (HGT).<sup>42, 43</sup> Many species are known to utilize HGT to share genetic information conveying coping mechanisms for environmental stresses which contributes greatly to

physical and chemical tolerances possessed within multispecies biofilms. Thus, current methods for combating biofouling may be promoting the spread of Cu-tolerant species in various aquatic environments.

### ***1.4 Potential within Marine Environments***

The marine habitat is incredibly diverse: salinity gradients, temperature variation, nutrient restriction, and great depths are characteristics of extreme physical environments that have yielded evolutionarily sophisticated microorganisms.<sup>44</sup> Microorganisms that have adapted to survive in these extreme environments are promising sources for unique biological mechanisms and bioactive compounds that can be leveraged in a litany of applications.<sup>45</sup> Marine environments contain the highest biomass and the greatest biodiversity which is suggested to indicate wide chemical variation.<sup>46-48</sup> Bioactive compounds and metabolites harvested from marine micro- and macro-organisms are already proving to be useful in biomanufacturing and medical applications.<sup>46, 49-51</sup> Enzymatic processes in marine organisms are also garnering attention for their ability to perform under stressful physiological conditions that would render enzymes in their terrestrial counterparts inactive.<sup>52</sup> Recent estimates suggest that only 0.01% of all marine bacteria have been investigated, thus there is seemingly endless potential in continued research revolving around marine organisms.<sup>44, 52</sup>

### 1.4.1 Adapting Marine Microorganisms for Applications in Biotechnology

Marine ecosystems contain a plethora of diverse microorganisms which present an understudied goldmine of unique biological processes and metabolites that may be utilized for biotechnological advancement. Biotechnology is a multidisciplinary field that combines chemistry, biology, engineering, and manufacturing with the goal to meet societal and commercial needs in industrial realms ranging from agricultural to biomedical by leveraging either directly obtained or bio-inspired compounds and processes.<sup>51</sup> As previously discussed, marine organisms are promising due to unique adaptations required to survive in their harsh and pathogen-laden environment.

Multiple marine-derived organisms have shown potential valorization for biotechnical applications. Many microorganisms produce bioactive compounds that are recognized for properties such as antimicrobial, anticancer, and antioxidant activities.<sup>53</sup> Many promising pharmaceutically active metabolites, such as the well-known cephalosporin antibiotics, have been isolated from marine fungal species.<sup>45, 51</sup> Additionally, enzymes from marine organisms have been applied in a wide range of systems, for example, xylanases isolated from *Pseudoalteromonas haloplanktis* have been implemented in bioremediation and in the food industry, glucanases from *Shewanella spp.* are used in cattle raising, and chitinases from some *Athrobacter spp.* are involved in the production of prebiotics.<sup>53-55</sup> Microalgae have been used for their ability to synthesize biomass for use in biofuels and bioproducts used in pigments, and vitamins.<sup>45, 49, 51, 56</sup> To

further utilize the capabilities of these microorganisms, research has turned towards synthetic biology to adapt marine systems for biosensors. Biosensor development involves meticulous fine-tuning of intracellular functions to program cells to produce a detectable output once certain conditions are met.<sup>57</sup> Biosensors have been applied environmentally by detecting pollutants such as pesticides, metal ions, waterborne pathogens, and explosives, and in human health monitoring (i.e., detecting pathogenic biomarkers in clinical samples or glucose in blood samples).<sup>58, 59</sup>

#### **1.4.2 Leveraging Evolutionary Resilience Present in Marine Life for Advancing Human Health Incentives**

As briefly alluded to above, many bioactive compounds isolated from marine organisms have applications as antimicrobial agents. With the continued emergence and persistence of treatment-resistant pathogens, research has taken a closer look at marine organisms to better understand immunological responses and for novel therapeutic strategies. Surviving in an environment rich in pathogens, while limited in nutrients and critical cofactors, implies the presence of sophisticated defense mechanisms in marine derived micro- and macro-organisms.<sup>60, 61</sup> Mechanisms for protection against pathogenic microbes make up the immune system and are generally classified as either innate or adaptive.<sup>62-64</sup> An in-depth discussion of the difference between innate and adaptive immunity is beyond the scope required here, but is explained in many excellent review articles.<sup>62-70</sup> In brief, the innate immune system exists in both invertebrate and vertebrate organisms. Innate immunity, sometimes called natural immunity, is present at the start

of life and responds quickly and non-specifically to threats. Conversely, adaptive, or acquired immunity, is slow acting but highly specific as it develops upon repeated exposure to pathogens. The presence of an adaptive immune system separates vertebrate and invertebrate organisms.

Over 99% of living species are wholly reliant on innate immunity for host defense, these organisms rely on a variety of molecules including phagocytotic cells, signaling receptors, pattern-recognition receptors, antimicrobial metabolites, and antimicrobial peptides.<sup>67, 70</sup> The pathogen-rich environment coupled with the long evolutionary history of marine invertebrates makes these organisms worthwhile candidates in the search for novel natural-product based therapeutics as their defense mechanisms are robust and broad-spectrum.<sup>71, 72</sup> There are multiple examples of successfully applied marine-derived natural products, some prominent examples include: a new polyketide mayamycin, isolated from the marine sponge *Halichondria panicea*, with impressive antimicrobial activity against methicillin-resistant *Staphylococcus aureus* (MRSA), *Pseudomonas aeruginosa*, and extended-spectrum beta-lactamase *K. pneumoniae*,<sup>73</sup> the metabolite dentigerumycin E, isolated from co-culture of marine strains *Streptomyces* and *Bacillus*, has shown antimetastatic and antiproliferative activity against human carcinoma,<sup>74</sup> and a cyclic hexapeptide, bacicyclin, isolated from the mussel *Mytilus edulis* demonstrated antibacterial activity against *Enterococcus faecalis* and *Staphylococcus aureus*.<sup>75</sup> Marine environments have already proven to be a profound

source of bioactive compounds, continuing investigations into currently identified species as well as into isolating and identifying new species will continue to further efforts in combating antimicrobial resistance and in novel therapeutic development.

### ***1.5 Summary and Outlook***

The work presented here serves many purposes centering around the role of metals in marine-based biological systems. Chapters 2 and 3 center around the role of copper as a biocide in popular ablative antifouling coatings. Chapter 2 focuses specifically on the surface chemistry and copper-release from a commercially available copper based self-polishing antifouling coating in the presence and absence of various media components. Chapter 3 assesses biofilm community diversity from biofilms harvested at three field sites along the East Coast (MD, United States and FL, United States) and how these communities respond to supplemental copper to begin elucidating copper tolerance mechanisms. Chapter 4 deviates to a discussion of the potential of *Marinobacter atlanticus*, a marine bacterium, for applications in electrogenic biosensor development, heavy metal detoxification, and biomanufacturing based on its ability to persist in metal-contaminated environments. Finally, in Chapter 5, a family of antimicrobial peptides isolated from the marine tunicate *Styela clava*, are investigated for metal-modulated antimicrobial activity based on the putative metal binding sites present in their amino acid sequences.

## **2. Assay Development to Characterize Environmental Impacts on the Behavior of a Copper-Based Antifouling Coating**

### ***2.1 Introduction***

Marine biofouling is defined as the settlement and accumulation of organisms including bacteria, fungi, algae, and animal species such as bryozoans, mollusks, barnacles and tunicates on submerged surfaces. Biofouling induces a myriad of deleterious effects in multiple systems including potentiating corrosion on submerged ships and structures,<sup>76, 77</sup> inhibiting efficacy within the maritime shipping industry,<sup>34, 78, 79</sup> and facilitating the translocation of pathogens.<sup>80, 81</sup> It is estimated that microbially induced corrosion amounts to approximately 20% of all corrosion costs each year with impacted surfaces ranging from submerged pipes to ship hulls and other structures.<sup>76, 77</sup> In the maritime shipping industry, the presence of biofouling is primarily associated with increased drag coefficients which has cascading effects by impacting fuel consumption, exhaust emissions, and operational costs.<sup>34, 78, 79</sup> Biofouling accumulation on vessels has also been highlighted as a vector for the translocation of non-indigenous marine microorganisms which may induce extensive damage to native aquatic and terrestrial biodiversity and to human health.<sup>42, 43, 81, 82</sup>

Traditionally, biofouling is inhibited by the application of surface coatings which can be broadly categorized into antifouling (AF) coatings, those which contain biocides

to prevent fouling growth,<sup>15, 35</sup> or foul-releasing (FR) coatings, those which restrict the settlement and adhesion of fouling communities.<sup>37</sup> While FR coatings have begun to gain popularity due to rising concerns surrounding biocide-based environmental contamination, ablative AF coatings continue to be the most prevalent world-wide.<sup>15, 35, 83</sup> Within the realm of ablative AF coatings, which slowly release biocidal molecules, those containing copper are the most utilized.<sup>15, 35, 83</sup> Copper (Cu) ablative AF coatings may contain up to 75% cuprous oxide (Cu<sub>2</sub>O) by weight dispersed within the paint matrix.<sup>15</sup> The coatings are rosin based which allows the coating to dissolve slowly as it hydrates to expose fresh Cu<sub>2</sub>O nanoparticles.<sup>84</sup> The release of Cu<sub>2</sub>O coupled with the percentage of fouled surface area are the main metrics used to define the efficacy of these coatings.

In previous studies, salinity, Cu content, zinc (Zn) content, temperature and paint matrix formulation were assed for their independent roles in the release of Cu.<sup>15</sup> It was determined that, of the five parameters, salinity and Cu content were able to significantly influence Cu release rates. However, knowledge of salinity and Cu content only allow for a rough estimation of Cu release rates due to the high variation within the other parameters.<sup>15</sup> Of almost equal importance in influence Cu release, are the composition of the paint matrix (binder erosion potential, content of additional soluble pigments) and the solubility of the active Cu source (usually either Cu powder or Cu<sub>2</sub>O). A separate study investigated the impact of pH and swell on Cu leaching and

determined that lower pH values and consistent flow (high swell), simulated by shaking incubation, also increased Cu release.<sup>85</sup>

Previous investigations of Cu release have been limited to field-based studies, where water samples are taken near deployed panels, or lab-based immersion experiments that mimic natural environments using artificial sea water. This work has two main aims, the first being to design an assay that allows for the expansion of the systems in which Cu release and surface quality may be measured in parallel. The second being to evaluate coating performance in an environment that will facilitate bacterial growth. Here, we utilized Interspeed 640 (International Marine) which is an AF coating prevalent commercially and privately. Interspeed 640 contains between 25-50% Cu<sub>2</sub>O as the primary biocide and up to 25% ZnO as a booster biocide both of which are interspersed in the paint matrix which is mostly comprised of N-ethyl-(o/p)-toluenesulfonamide.

Towards the first aim, we present the developed experimental method and provide suggestions for future improvements. For the second aim, we tested our method design to measure the Cu release under conditions which will favor bacterial growth via the use of a rich bacterial medium tryptic soy broth (TSB) as an immersion environment. The method described in this chapter is a scalable laboratory-based method designed to assess the Cu release and the surface environment in parallel. We measured Cu release over a 14 day timeframe through the use of glass coverslips coated in our AF coating

immersed in either double-distilled 18.2M $\Omega$  water (ddH<sub>2</sub>O), which served as a control condition, and in TSB, which served as a test conditions. Released Cu was quantified using inductively coupled plasma optical emission spectroscopy (ICP-OES). Surface characterization of immersed coated coverslips was conducted using X-ray photoelectron spectroscopy (XPS) to assess changes in both surface composition and in the chemical environment. We found that, in the presence of TSB, there is an approximate 500% increase in Cu release. Surface characterization suggests minor surface hydrolysis and depicts alterations in surface composition under both treatment conditions.

## ***2.2 Results and Discussion***

### **2.2.1 Assay Design to Assess Environmental Impact on Copper Release and Coating Surface Integrity**

Previous investigations of this AF coating have been conducted in natural environments, sterilized sea water, and artificial seawater for time periods ranging from 14 days to an excess of 5 years.<sup>15, 85-87</sup> While biofouling does occur in natural environments, the assessment of coating response is challenging due to the complex nature of the marine ecosystem. The method described here was designed to evaluate the behavior of the antifouling coating Interspeed 640 (International-Marine) under conditions which favor bacterial growth to facilitate the characterization of coating response to biofouling under controlled laboratory conditions.

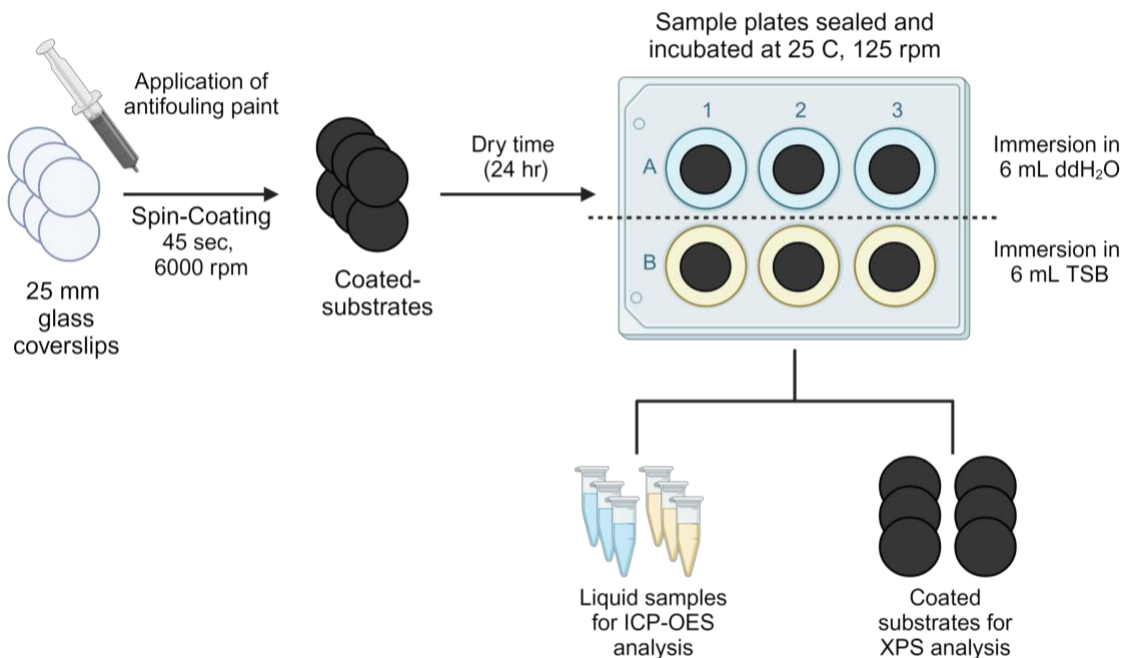


**Figure 1: General workflow for assessing the behavior of Interspeed 640 under specifically defined conditions. In this method, multiple 25 mm diameter glass coverslips were coated with a thin film of Interspeed 640 using a spin coating instrument. Coated substrates were immersed in either double-distilled 18.2 MΩ water (as a control environment) or in tryptic soy broth (as a test environment) for 14 days to measure copper release and changes in surface character in parallel.**

With the goal of establishing a baseline for coating response to conditions which favor bacterial growth we designed a simple workflow (**Figure 1**). Substrates were prepared by spin coating a thin layer of Interspeed 640 onto the surface of 25 mm diameter circular glass coverslips (Fisher Scientific). Coated glass coverslips were immersed in 6-well culture plates (Thermo Scientific) that were sealed with AeraSeal plate film (Sigma-Aldrich) and stored in a large incubator set to 25 °C with shaking at 125 rpm to mimic environmental temperature and mild water swell over the 14-day assessment period. We utilized double-distilled 18.2 MΩ water (ddH<sub>2</sub>O) as a control

environment and tryptic soy broth (TSB) as the environment to facilitate bacterial growth. TSB media was chosen as it is a nutrient-rich medium composed of tryptone and soytone (protein digests that may partially mimic the presence of biological matter), sodium chloride (to provide salinity and osmotic pressure control), dextrose (as an energy source), and dipotassium phosphate (to buffer against pH changes).

As depicted above in **Figure 1**, 6-well plates were divided horizontally, the top row contained 6 mL of ddH<sub>2</sub>O and the bottom row contained 6 mL of TSB, additionally, each 2-well column was representative of one timepoint. Timepoints were collected over a 14-day window with initial collections following a pseudo-logarithmic timescale to best capture the first 24 hours of immersion. Each coated substrate was representative of a single timepoint to allow for characterization of both surface composition and Cu release. Replicate samples were arranged across three different 6-well sample plates to prevent total timepoint loss in the event of plate contamination. Additionally, consecutive timepoints were organized so that sampled plates were only removed from the incubator once in a 24 h period. For each timepoint, liquid samples were collected from the respective wells and the coated substrate was removed from the remaining solution and transferred to a clean 6-well plate to dry prior to subsequent surface analysis.

The method described thus far has provided a strong foundation to allow for the simultaneous investigation of alterations in the surface composition and Cu release in

response to the sampling environment. For future applications of this method, we suggest the inclusion of pH monitoring as Cu release has been shown to both impact and be impacted by environmental pH.<sup>15, 86, 87</sup> It is also suggested to include multiple control wells containing either ddH<sub>2</sub>O, TSB, or other desired solutions to track evaporation over the course of the assay, especially if the duration is to be extended beyond 14 days or if the temperature is to be increased.

### **2.2.2 Copper Release is Increased Under Conditions which Favor Bacterial Growth**

The evaluation of Cu release from Interspeed 640 was performed in accordance with the method previously described in Section 2.2.1 and depicted in **Figure 1**. Briefly, 25 mm diameter circular glass coverslips were coated with the copper-based antifouling coating Interspeed 640 using a spin coating system to create uniformly coated surfaces. Coated substrates were immersed in 6-well plates divided so the top 3-well row contained 6 mL ddH<sub>2</sub>O and the bottom 3-well row contained 6 mL TSB. Sampling plates were sealed and stored in a large incubator at 25 °C set to 125 rpm for the entirety of the 14-day sampling period.

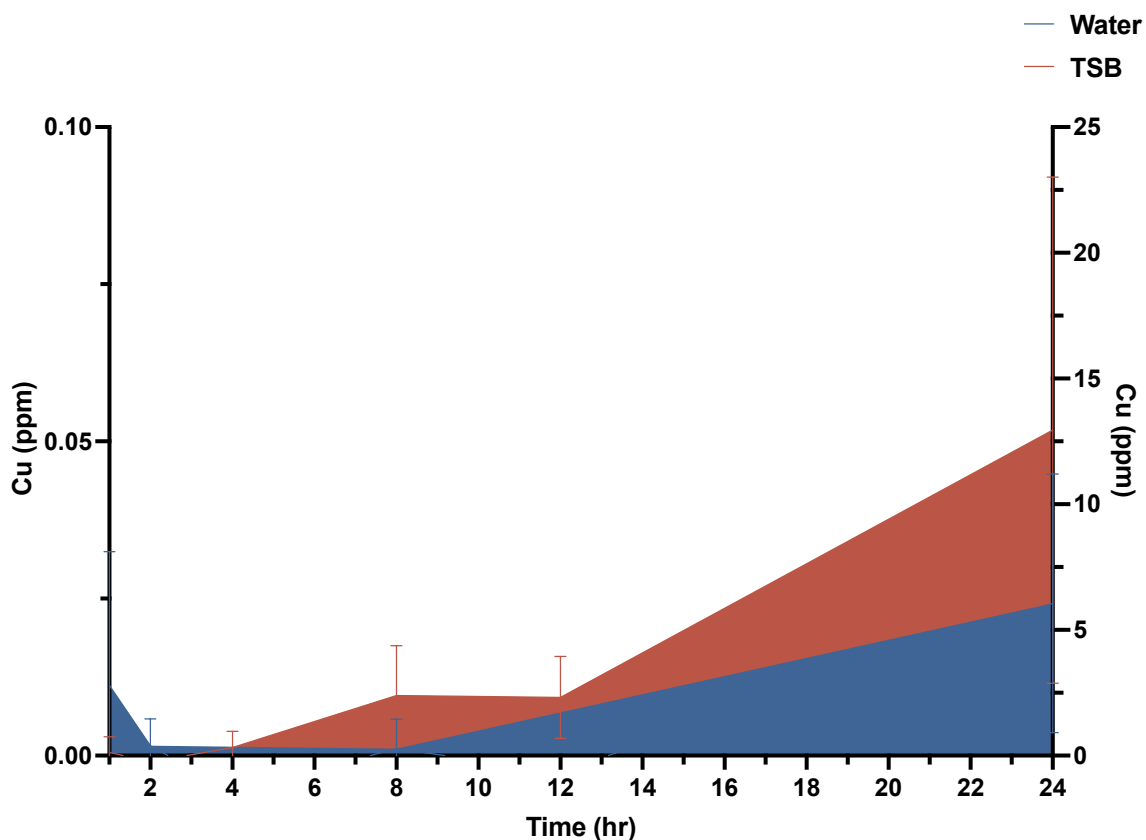


**Figure 2: Copper released after 24 hours from Interspeed 640 coated substrates immersed in either ddH<sub>2</sub>O (blue, left axis) or TSB (red, right axis). Note the difference in scale between the left and right axis. Copper concentrations shown were obtained from elemental analysis conducted using ICP-OES and converted from intensity to ppm using calibration curves for 324 nm (see supplemental). Data are presented as the average of three replicate samples with triplicate measurements taken for each. Error was calculated as standard deviation and shown with error bars in the figure.**

For each timepoint, 4.5 mL was collected for subsequent elemental analysis using inductively coupled plasma optical emission spectroscopy (ICP-OES). Initial sampling times followed a logarithmic-like scale to best capture the first 24 hours of immersion (Figure 2). Samples collected from coated substrates immersed in ddH<sub>2</sub>O, depicted in blue, reveal low levels of Cu with approximately 24 ppb (~40 μM) detected after 24

hours. Conversely, samples collected over the same period immersed in TSB contained 13 ppm (~200  $\mu$ M) after 24 hours. While differences in Cu release prior to 12 hours cannot be resolved due to the limits of detection in ICP-OES, it is evident that solution composition plays an immediate role on the release of Cu from Interspeed 640. This trend continues across the 14-day sampling period (Figure 3).

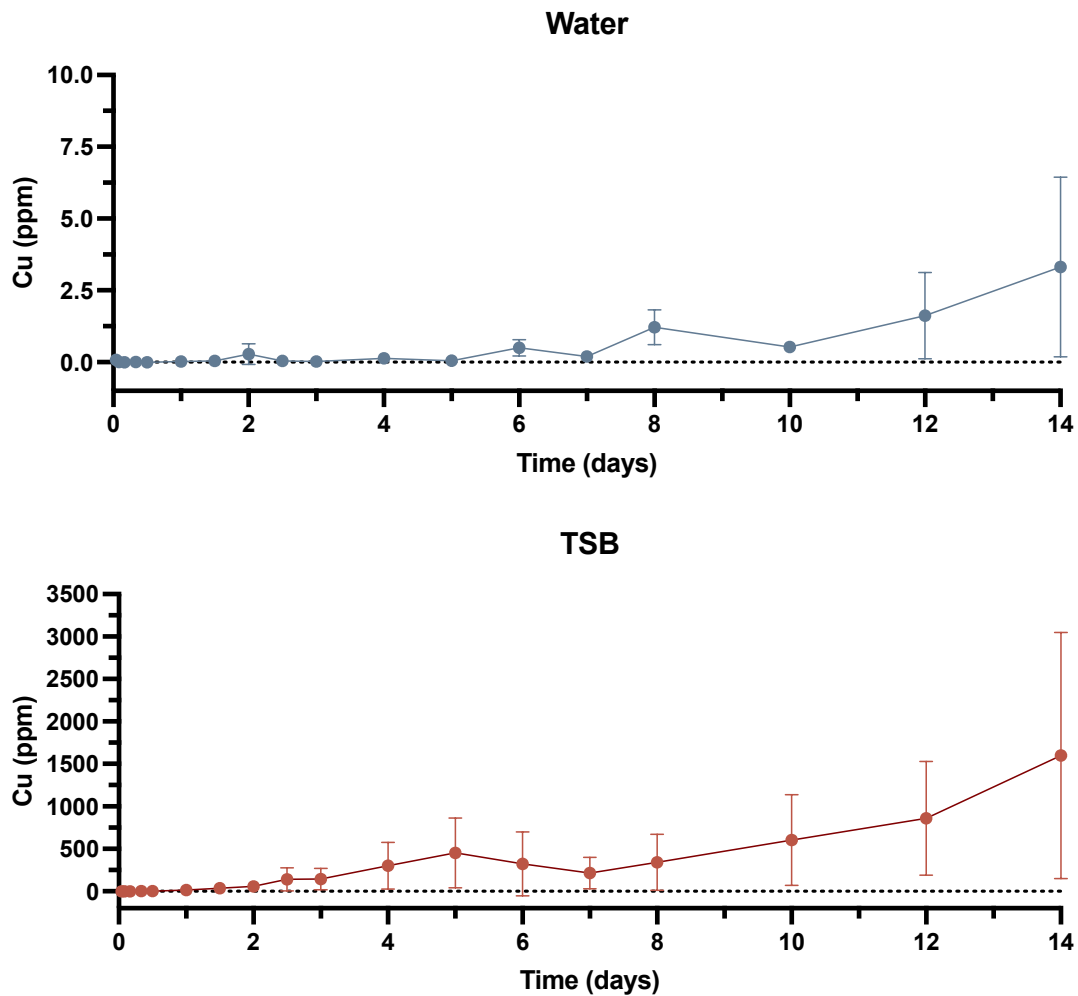


Figure 3: Copper released after 14 days from Interspeed 640 coated substrates immersed in either ddH<sub>2</sub>O (top) or TSB (bottom). Note the difference in scale between the axis for ddH<sub>2</sub>O and TSB. Copper concentrations shown were obtained from

**elemental analysis conducted using ICP-OES and converted from intensity to ppm using calibration curves for 324 nm (see supplemental). Data are presented as the average of three replicate samples with triplicate measurements taken for each. Error was calculated as standard deviation and shown with error bars in the figure.**

After 14 days of constant immersion, samples collected from ddH<sub>2</sub>O contained an average of 3 ppm (~50 μM) Cu while those collected from TSB contained 1600 ppm (~25 mM) Cu. These results indicate that Cu release from Interspeed 640 has an environmental dependence. Previous literature has shown that factors such as temperature, agitation, salinity, and pH impact Cu release from similar AF coatings.<sup>86, 87</sup> In this method temperature and agitation (simulated with shaking at 125 rpm) were controlled across all samples. Only samples immersed in TSB were exposed to saline conditions as TSB contains 5 g/L NaCl. Since Cu release has been shown to have a linear relationship with salinity,<sup>86</sup> typically expressed as the presence of chloride ions in solution, the salt content in TSB contributes to the increased Cu release. However, additional discrepancies between treatment conditions, such as pH and the presence of media components beyond salt, likely contribute to Cu release.

While solution pH was not monitored in the initial application of this method, the starting pH of each treatment solution differed with ddH<sub>2</sub>O at approximately pH 5.5 and TSB with approximately pH 7.6. Release of Cu from other systems in, such as metallurgical slag (waste matter generated from ore mining) and metal sheets, are pH dependent with enhanced Cu release under acidic conditions.<sup>88, 89</sup> Small changes in pH may induce significant changes in metal concentration in solution and the dissolution of

Cu will have different effects in unbuffered ddH<sub>2</sub>O and in TSB which includes dipotassium phosphate for buffering. Further complexity is added to the system by considering the solution chemistry of Cu given its propensity to oxidize from Cu(I) to Cu(II) and potential complexation with multiple solution components such as dissolved organic carbon, chloride ions in solution and other molecules that may be present. Unlike substrates immersed in ddH<sub>2</sub>O, substrates immersed in TSB were exposed to media components that provide organic ligands for potential Cu complexation. Given the known ability of Cu to interact with proteins and peptides,<sup>90-95</sup> it is possible that the amino acids and peptide fragments present in TSB play roles in increasing Cu release from Interspeed 640.

### **2.2.3 Characterization of Immersed Surfaces Suggests Differential Changes in Composition and Minor Coating Hydrolysis**

Glass coverslips coated with Interspeed 640 were immersed in ddH<sub>2</sub>O as a control environment or TSB as a test environment to measure the impact of conditions that favor bacterial growth on the surface activity of this AF coating. Collected substrates were removed at the respective timepoints, stored in a sterile 6-well culture plate, and allowed to dry prior to surface characterization. Surface characterization was conducted using x-ray photoelectron spectroscopy (XPS) to measure the impact of environmental conditions on the coating surface. XPS analysis was chosen as it allows for the study of surfaces on the nanoscale (< 10 nm) by providing chemical composition and elemental information used to deconvolute chemical environments.<sup>96</sup>

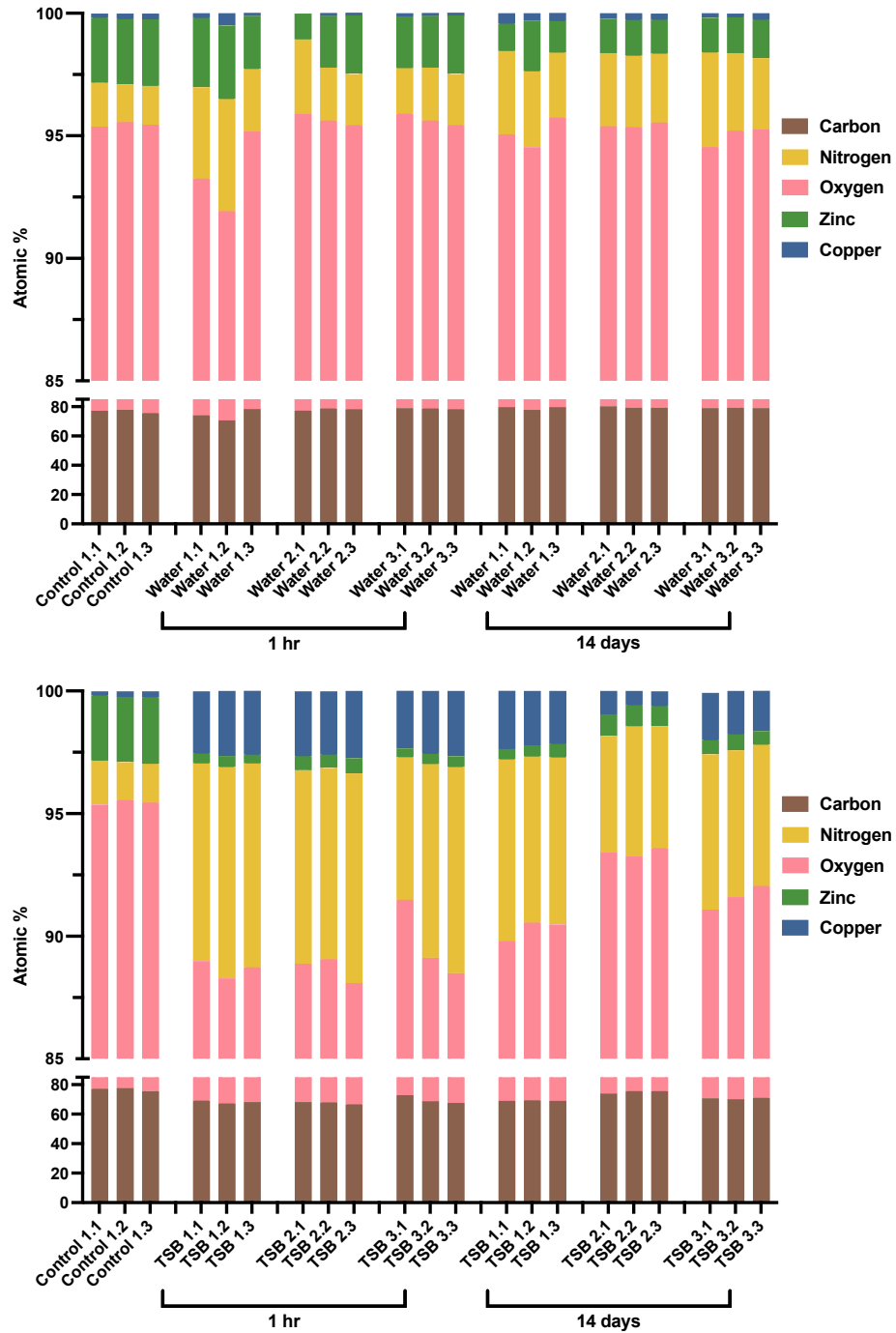


Figure 4: Environmentally induced changes in surface composition for substrates immersed in ddH<sub>2</sub>O (top) and TSB (bottom). Note the break on the y-axis. Bar graphs depicting the atomic percentage of major elements detected by XPS on the surface of

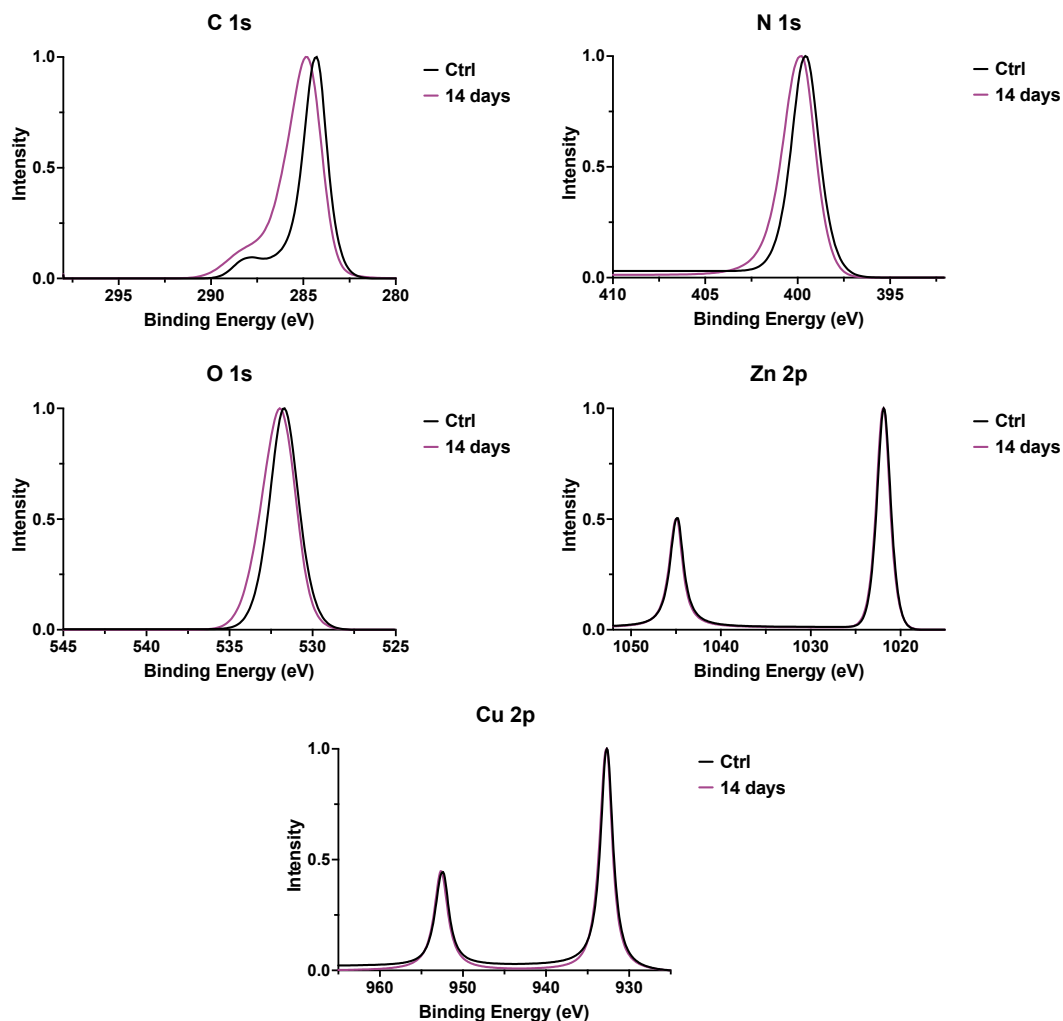
**substrates coated with Interspeed 640 after immersion for either 1 hour or for 14 days. High-resolution scans were recorded at three different positions for replicate sample to capture potential surface heterogeneity, labeling on the x-axis indicates replicate number and scan number for all conditions. Both figures include the surface composition of a control substrate for comparison on the far left.**

For all samples, the “atomic %” elemental compositions were calculated using built-in Avantage (Thermo Avantage V.5.9931, Thermo Fisher Scientific) software processing tools which rely on calibrated analyzer transmission functions, effective attenuation lengths (EALs), and Scofield sensitivity factors.<sup>97-99</sup> In the atomic % calculation, the EAL term allows for the comparison of elements with different signal intensities.<sup>100</sup> High-resolution scans of carbon (C) 1s, nitrogen (N) 1s, oxygen (O) 1s, zinc (Zn) 2p, and copper (Cu) 2p were taken at three different positions on a coated substrate that did not undergo any immersion and were utilized as a control for comparison (**Figure 4**). On average, the control surface contained 76.8% C, 1.6% N, 18.6% O, 2.7% Zn, and 0.2% Cu. Immersion in ddH<sub>2</sub>O for one hour induces minor changes in composition with averages across all three replicates of 77.0%, 2.7%, 17.9%, 2.2%, and 0.2% for C, N, O, Zn, and Cu, respectively. After 14 days of immersion in ddH<sub>2</sub>O, the following averages for all three replicates were obtained 79.3%, 3.1%, 15.9%, 1.5%, and 0.3% for C, N, O, Zn, and Cu, respectively. When compared to the control, 14 days of immersion in ddH<sub>2</sub>O induces a subtle increase in C, N, and Cu, and a decrease in O and Zn. Over the course of the assay, the surface composition of substrates immersed in ddH<sub>2</sub>O remained relatively constant.

Substrates immersed for one hour in TSB yielded an average of 68.6%, 7.9%, 20.4%, 0.5%, and 2.6% for C, N, O, Zn, and Cu, respectively across all replicate conditions. After 14 days of immersion, replicate substrates in TSB contained an average of 71.6%, 6.0%, 20.1%, 0.6%, and 1.6% C, N, O, Zn, and Cu, respectively. analysis of immersed substrates indicates rapid environmentally induced changes in surface composition when compared to controls. In comparison to the control, immersion for 14 days in TSB induced an increase in N, O, and Cu, and a decrease in C and Zn on the surface. Substrates immersed in TSB between one hour and 14 days, on average, had a relatively consistent surface composition.

Interspeed 640 is an AF coating designed for long term use so consistent surface composition over the course of the sampling period is not surprising. Minor undulations in composition are likely the result of the hydrate and dissolve cycle the coating is designed to perform to release biocide. However, the immediate difference in surface composition between ddH<sub>2</sub>O substrates and TSB substrates indicate some degree of environmental dependency in coating response. Solution-dependent impacts are most evident in the average percentage of N, Zn, and Cu. As previously discussed in Section 2.2.2, there are great differences in the composition of ddH<sub>2</sub>O and TSB. The additional components present in TSB are likely contributing not only to increased Cu release but also to differences in surface composition. Protein digest components such as peptide fragments and amino acids interacting with the surface of the coating are a likely

explanation for the increased presence of nitrogen. Additionally, the ratio of surface Zn to Cu appears to be dependent on the solution environment. Coated substrates immersed in ddH<sub>2</sub>O consistently contain a higher percentage of surface Zn than Cu both initially (2.2% Zn vs 0.2% Cu) and after 14 days (1.5% Zn and 0.3% Cu). Whereas an opposite trend is observed for samples in TSB which consistently contain more surface Cu than Zn both initially (2.6% Cu vs 0.5% Zn) and at the end of the assay (1.6% Cu vs 0.6% Zn). These differences may be due to differences in ionization behavior between Cu and Zn in addition to the different solution compositions.



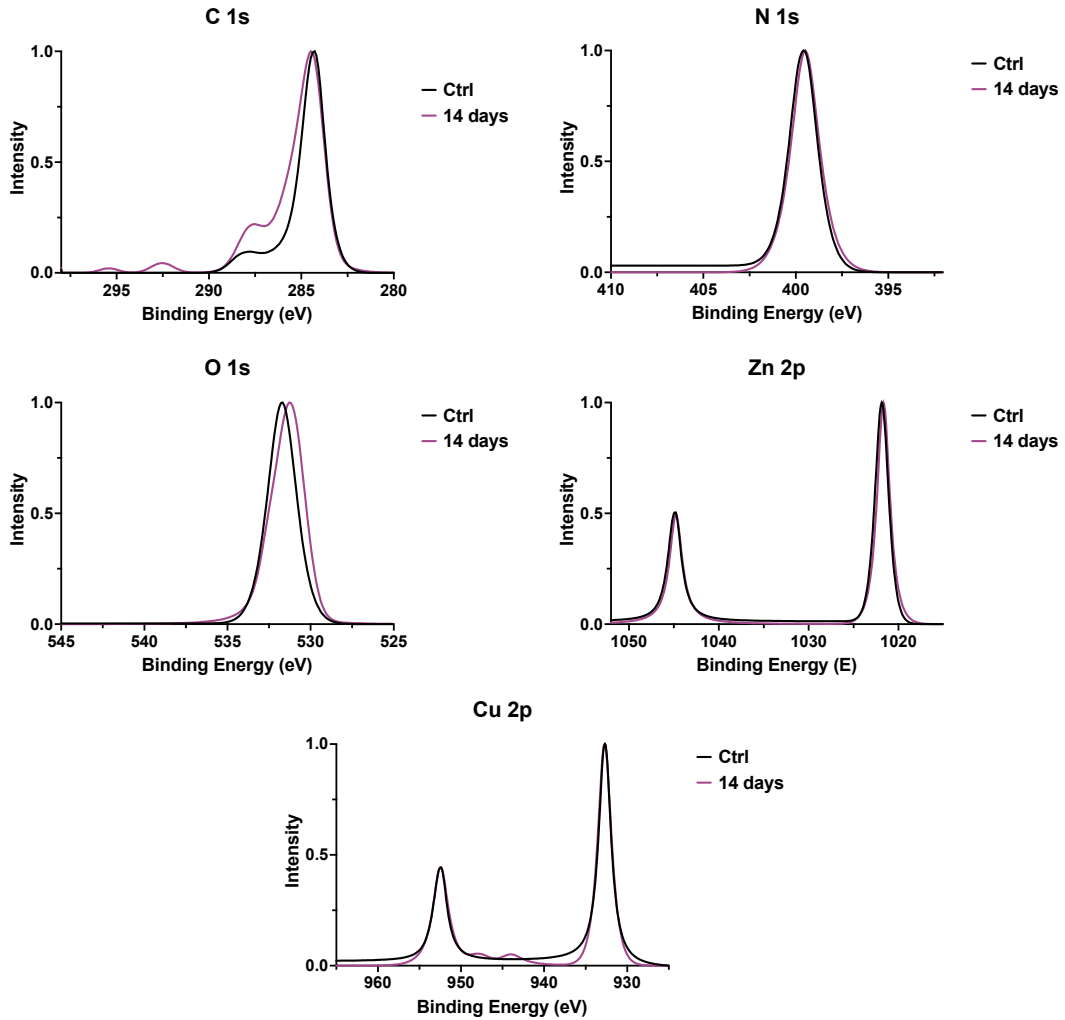
**Figure 5: Comparison of a coated substrate control to a substrate immersed for 14 days in ddH<sub>2</sub>O. Normalized high-resolution scans of carbon (C 1s), nitrogen (N 1s), oxygen (O 1s), zinc (Zn 2p), and copper (Cu 2p) obtained for substrates coated with Interspeed 640. Control substrates (Ctrl, black) were not immersed and substrates immersed in ddH<sub>2</sub>O (purple) were immersed for 14 days. Data presented are background adjusted and normalized to maximum peak intensity of best visualize changes in peak shape.**

Figure 5 shows an overlay of high-resolution XPS data for C 1s, N 1s, O 1s, Zn 2p, and Cu 2p for both a control coated substrate and for a coated substrate immersed for two weeks in ddH<sub>2</sub>O. Data presented are normalized and overlaid to best visualize

immersion-induced alterations in peak shape. To establish a baseline for comparison an analysis of the control coating is discussed first. In the C 1s scan, there are two clear peaks one centered at binding energy (BE) = 284.3 eV which is characteristic of aliphatic carbon.<sup>101</sup> The next peak centered at BE = 288.1 eV may be indicative of C interacting with a nearby O or N atom.<sup>101</sup> For N 1s, the singular peak is centered at BE = 399.6 eV which is the region in which amides and amines are expected to appear.<sup>101</sup> The O 1s signal is centered at BE = 531.8 eV which falls in the range for organic carbonyl signals.<sup>101</sup> Both Zn 2p and Cu 2p produce doublet signals due to split spin-spin orbital coupling. For Zn, the 2p<sub>3/2</sub> signal is found at BE = 1021.8 eV and the 2p<sub>1/2</sub> signal is found at BE = 1044.8 eV, the signals have the large separation of 23 eV characteristic of Zn.<sup>101</sup> In Cu, the 2p<sub>3/2</sub> signal is at BE = 932.7 eV and the 2p<sub>1/2</sub> signal is centered at BE = 952.5 eV, the separation between these signals is 19.8 eV which is a characteristic of Cu XPS spectra.<sup>101</sup>

The overlay of normalized scans collected from the control sample with those collected from the surfaces of samples immersed in ddH<sub>2</sub>O reveal subtle differences in peak shape and shifts in binding energies. The most obvious of which is present in the shape of the C 1s scan, after 14 days of immersion which will be discussed below (**Figure 7**). Peaks for C 1s are found at BE = 284.7 eV and BE = 288.3 eV, the signal for N 1s is at BE = 399.8 eV, and O 1s has BE = 532.0 eV. The doublet signals for Zn 2p are BE = 1021.7 eV and 1045 eV, and for Cu 2p are BE = 932.7 eV and 952.7 eV. In all analyzed spectra of

samples submerged for 14 days in ddH<sub>2</sub>O revealed binding energy shifts of less than 0.5 eV.



**Figure 6: Comparison of a coated substrate control to a substrate immersed for 14 days in TSB. Normalized high-resolution scans of carbon (C 1s), nitrogen (N 1s), oxygen (O 1s), zinc (Zn 2p), and copper (Cu 2p) obtained for substrates coated with Interspeed 640. Control substrates (Ctrl, black) were not immersed and substrates immersed in TSB (purple) were immersed for 14 days. Data presented are background adjusted and normalized to maximum peak intensity of best visualize changes in peak shape.**

Similarly, an overlay of normalized scans collected from the control sample compared to those collected from samples immersed in TSB reveal subtle differences in both the shape of elemental peaks and in binding energies (**Figure 6**). Like the ddH<sub>2</sub>O samples, all observed shifts were less than 0.5 eV. The most obvious spectral difference is present in the shape of the C 1s scan, all of which will be discussed in detail below (**Figure 7**). C 1s major peaks are found at BE = 284.4 eV and BE = 287.8 eV, satellite peaks are visible at BE = 292.6 eV and 295.5 eV. These satellite features may be indicative of substantial sp<sup>2</sup> content in the sample. The signal for N 1s is at BE = 399.5 eV, and O 1s has BE = 531.3eV. The doublet signals for Zn 2p are found at BE = 1021.7 eV and 1044.8 eV. The doublet signals for Cu 2p are BE = 932.7 eV and 952.6 eV with additional satellite peaks at BE = 944.1 eV and 947.9 eV. Analysis of satellite signals in Cu spectra can assist in the identification of the oxidation state present on the substrate. XPS spectra for Cu<sup>2+</sup> is easily differentiated from Cu<sup>+</sup> and Cu<sup>0</sup> as it features a large satellite peak approximately 9 eV above the doublet signals, landing around 961 eV. Conversely, differentiating between Cu<sup>+</sup> and Cu<sup>0</sup> can be quite challenging as it is reliant on the peak broadening and often requires analysis of other spectral regions or complimentary analytical techniques. In this case, however, the minor satellite signals between the main doublet peaks are likely indicative of trace Cu<sup>2+</sup> on the surface. Interspeed 640 contains cuprous oxide nanoparticles within the matrix (Cu<sub>2</sub>O) and exposure to aerobic environments over time likely induces oxidation to generate Cu<sup>2+</sup>.

Beginning to decipher chemical environment that may induce the variations in peak shape seen in C 1s XPS scans discussed early requires a deeper analysis. By deconvoluting the envelopes obtained for the raw scans we can identify which chemical environments are contributing to the overall scan and their relative abundance. In the control sample, scan A makes up the majority of the signal which indicates a composition rich in aliphatic carbon.<sup>101</sup> Scan B accounts for roughly 6% of measured carbon and scan C accounts for the remaining ~8%, both signals are in regions that indicate interactions with O or N. Scan B exists in a region associated with C-(O/N) interactions whereas scan C indicates the presence of carbonyl interacting with O or N.<sup>101</sup> Overall, the carbon detected on the surface of control samples coated with Interspeed 640 is primarily aliphatic with minor interactions with either N or O.

In contrast, samples immersed in ddH<sub>2</sub>O have a significantly different surface environment with a sharp decrease in aliphatic carbon (scan A, **Figure 7**) and an increase in the percentage of C-(O/N) content (scan B). The relative amount of carbonyl carbon detected (scan C) on the surface is largely unchanged when compared to the control surface. The general increase in carbon associated with either O or N may suggest hydrolysis of the surface which is consistent with the mechanism of action AF coatings are designed to employ.

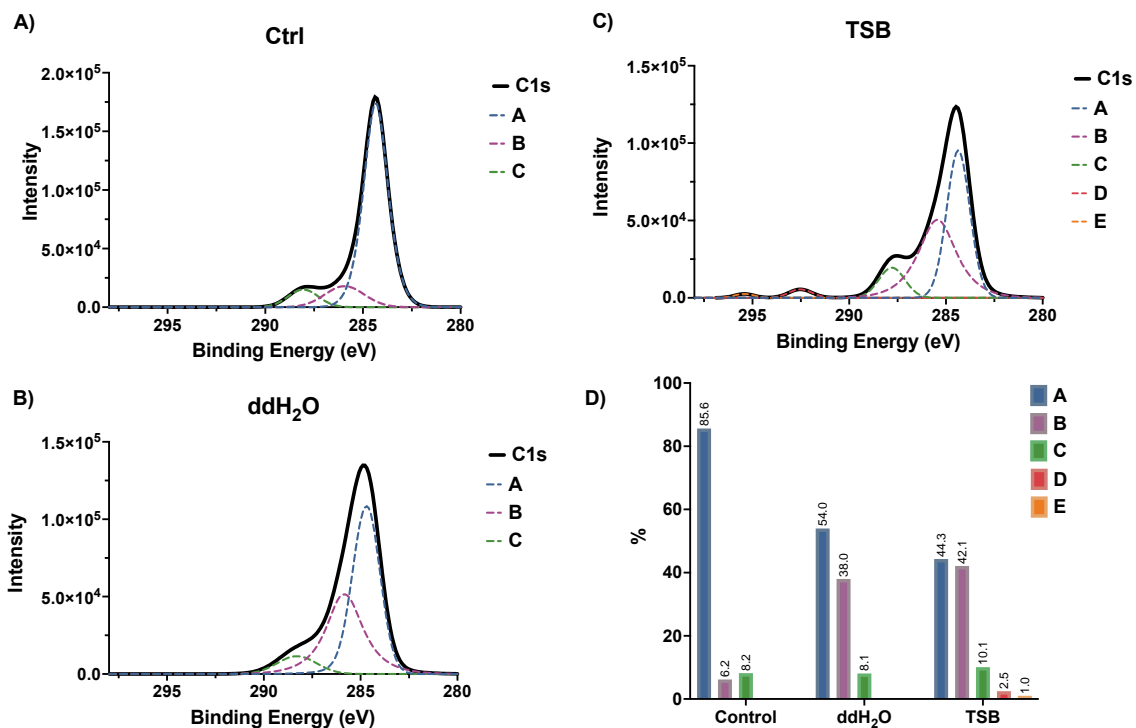


**Figure 7: Deconvoluted C 1s spectra obtained from high-resolution XPS scans. C 1s spectra deconvoluted for the control substrate coated with Interspeed 640 (A), coated substrates immersed in ddH<sub>2</sub>O (B) and in TSB (C). In A-C, black lines depict the envelope (summation of all deconvolutions) and deconvolutions are labeled A-E with increasing binding energies. Bar graph presented in D depicts the percentage each deconvolution contributes to the overall envelope.**

Surfaces immersed in TSB for 14 days also show a decrease in aliphatic carbon (scan A, **Figure 7**) coupled with an increase in C-(O/N) signal as shown by scan B. The presence of carbonyl signals (scan c) is increased by roughly 2% when compared to other samples. Unlike the control or the ddH<sub>2</sub>O samples, the TSB surface analysis includes to satellite peaks represented by scan D and scan E. These satellites are commonly associated with the presence of sp<sup>2</sup> carbon.<sup>101</sup> Similar the ddH<sub>2</sub>O immersed surfaces, the increase in scan B and scan C may suggest surface hydrolysis. Additional

satellite peaks and increased carbonyl signal may be a byproduct of an unknown interaction between TSB and the coating surface, or it may indicate the presence of molecules or other media components from TSB adhered to the surface.

### ***2.3 Conclusions and Future Directions***

Great steps have been taken towards the establishment of a method for the analysis of coating behavior under controlled laboratory conditions. In this work, we originally sought to develop an assay that would allow us to assess how Interspeed 640 responds to conditions that favor bacteria growth. However, we created an assay that allows for the fine-tuning of solution conditions while monitoring changes in Cu release and surface chemistry in tandem. In the application of this method described here we were able to successfully measure Cu release under our established conditions and characterize the coating surface.

Glass coverslips coated with Interspeed 640 were immersed for 14 days in either ddH<sub>2</sub>O or TSB. Here, ddH<sub>2</sub>O was chosen as an inert control environment and TSB was chosen as the environment to favor bacterial growth. After 14 days, coated substrates immersed in ddH<sub>2</sub>O released an average of 3 ppm Cu into solution while substrates immersed in TSB released 1600 ppm Cu. Interestingly, the increase in Cu release is apparent within one day of immersion. Previous literature has emphasized the measurement of Cu release in natural environments and in artificial seawater, from these investigations we know that Cu release increases with salinity.<sup>15, 85-87</sup> The results

obtained here agree with prior literature as we see over a 500% increase in Cu release from samples immersed in TSB compared to those in ddH<sub>2</sub>O. However, TSB contains additional components, such as protein digests, that may impact Cu release. Future method development and assessment of Interspeed 640 should focus on the inclusion of single components to elucidate their importance in Cu release under simplified conditions. Furthermore, this method would benefit from the implementation of pH monitoring as solution pH will directly affect both Cu speciation and Cu release.

Surface analysis of coated substrates can be divided into two main sections, elemental composition and chemical environment. When compared to untreated coated substrates, immersion in ddH<sub>2</sub>O induced little change in the elemental composition of the surface. Conversely, TSB induced substantial increases in both nitrogen and copper. Our current theory to explain this increase revolves around the presence of protein digests in the TSB. We suspect that peptide fragments and amino acids may be interacting with the surface in a currently unknown way, or that these increased signals are the result of residual TSB dried on the surface, or a combination of the two.

Our assessment of the chemical environment relies upon high-resolution XPS data collected for C 1s, N 1s, O 1s, Zn 2p, and Cu 2p. In either ddH<sub>2</sub>O or TSB, we observed no shifts in binding energy greater than 0.5 eV when compared to the control substrate. This implies that alterations in the chemical environment of the surface are minor. In depth analysis of C 1s reveals that immersion in both test environments

decreases the proportion of aliphatic carbon and increases the proportion of carbon associated with either oxygen or nitrogen. These results suggest hydrolysis of the surface which is in line with the standard behavior of antifouling coatings. For samples immersed in TSB, we observed the presence of additional satellite signals in the C 1s region which indicate  $sp^2$  carbon. We also observed satellite signals in the Cu 2p which indicate trace  $Cu^{2+}$  on the surface. The presence of additional satellite signals coupled with the slight increase in carbonyl carbon content observed in TSB immersed sample surfaces may imply more complex surface chemistry.

Ultimately, the work presented herein has provided a foundational method to assess environmental impacts on antifouling coatings. More specifically, the assay conditions chosen here set the stage for future analyses in which bacterial species will be included to determine the impact of bacterial growth on Cu release and the coating surface. Deciphering the role of bacteria, particularly those implicated in the facilitation of marine biofouling, and how they impact the microenvironment at the coating surface will inform the development of future AF coatings.

## ***2.4 Methods***

### **2.4.1 Materials and General Methods**

Chemicals and solvents were obtained from commercial suppliers and used as received unless otherwise described.

## 2.4.2 Substrate Preparation

25 mm diameter circular glass coverslips with a thickness of 0.19-0.22 mm (Fisher Scientific) were coated with a thin layer of Interspeed 640 (International-Marine), an antifouling (AF) coating that utilizes  $\text{Cu}_2\text{O}$  as a primary biocide. The coverslip was placed onto the spin vacuum chuck of a spin coating system (POLOS) and a 10 mL syringe was used to dispense approximately 200 - 300  $\mu\text{L}$  of AF paint onto the surface. The tip of the syringe was used to roughly distribute the paint across the surface and the sample was spun at 6000 rpm with an acceleration of 1200 rpm/sec for 45 seconds. Samples were allowed to dry for at least 24 hours.

## 2.4.3 Sampling Conditions

Clear, flat-bottom, 6-well cell culture plates (Thermo Scientific) were used as vessels for the immersion assay described in Section 2.2.1. The top 3-well row was filled with 6 mL of double-distilled 18.2 M $\Omega$  water (ddH<sub>2</sub>O) to serve as the control environment. The bottom 3-well row was filled with 6 mL of tryptic soy broth (Difco, (TSB)) to serve as the test environment. TSB was prepared according to the manufacturer's instructions, briefly, to one liter of ddH<sub>2</sub>O 30 g of premixed powder were added prior to autoclaving at 121 °C for 15 min. The final composition of TSB per one liter is 17 g casein digest, 3 g soybean digest, 2.5 g dextrose, 5 g sodium chloride, and 2.5 g dipotassium phosphate. Using sterilized tweezers, a single coated coverslip was added to each well coating side up. Plates were sealed with an AeraSeal plate film (Sigma-

Aldrich) and covered with the provided lid. Sealed sample plates were stored in a large shaking incubator set to 25 °C and 125 rpm.

Timepoints were collected initially in a pseudo-logarithmic manner (1 h, 2 h, 4 h, 8 h, and 12 h) before switching to 12 h increments for the first three days. Timepoints continued daily from day 4 to day 8, then every other day until the final timepoint at day 14. For each timepoint, three separate 1.5 mL aliquots of each condition were collected into 2 mL snap-cap microcentrifuge tubes and coated glass substrates were transferred into clean 6-well culture plates. Samples were stored at 4 °C and coated substrates were left to dry in preparation for subsequent analysis. Liquid samples were analyzed for copper content using inductively coupled plasma optical emission spectroscopy (ICP-OES) (section 2.4.4) and coated coverslips were analyzed via x-ray photoelectron spectroscopy (XPS) for surface composition (section 2.4.5).

## **2.4.4 Inductively Coupled Plasma Optical Emission Spectroscopy (ICP-OES)**

### **2.4.4.1 Sample Preparation**

Samples for ICP-OES were made gravimetrically; dry acid-rinsed (3% HNO<sub>3</sub>) 15 mL centrifuge tubes were labeled, and the mass was recorded. Aliquots of each collected sample were passed through 0.22 µm filters to remove any solid particulates and transferred into the appropriate centrifuge tube. Samples were brought up to 5 mL using dilute nitric acid. Masses were recorded for each sample before and after dilution.

#### 2.4.4.2 Calibration Curves and Analysis Parameters

Copper (Cu) curves were prepared to span a wide range of Cu concentrations, and all glassware used was prewashed with nitric acid and dried to remove adventitious metals. Calibration curves were prepared gravimetrically in 3% HNO<sub>3</sub> in ddH<sub>2</sub>O using metal standards purchased from Inorganic Ventures. A copper stock solution was made in a 50 mL volumetric flask in 3% HNO<sub>3</sub> and serially diluted 2-fold. Serially diluted copper stock solutions were divided in half, one half was brought to volume with 3% HNO<sub>3</sub> and the other half was brought to volume with 3% HNO<sub>3</sub> with the addition of 1% TSB to account for media present in the samples.

Elemental analysis was performed on an Agilent 5800 ICP-OES system. Instrument calibration occurred initially and half-way through sample analysis for both the control (ddH<sub>2</sub>O) sample set and the test (TSB) sample set. Multiple wavelengths were selected to ensure adequate signal resolution, but the wavelength with the highest linearity and lowest error in the calibration curve was chosen for data analysis (Cu = 325 nm). Samples were measured in triplicate and the average intensity is the value reported by the instrument. Intensities were converted to concentration (in ppm) using the line-of-best fit generated from the prepared calibration curves.

## **2.4.5 X-ray Photoelectron Spectroscopy (XPS)**

### **2.4.5.1 Sample Preparation**

Coated substrates were kept in 6-well culture plates between collection and analysis. Surfaces were untouched between collection and XPS analysis. For each timepoint, all three replicates from both ddH<sub>2</sub>O immersion and TSB immersion were measured together. In some cases, the surface coating had signs of cracking and flaking, in these situations the coverslip was lightly tapped to remove loose particulates.

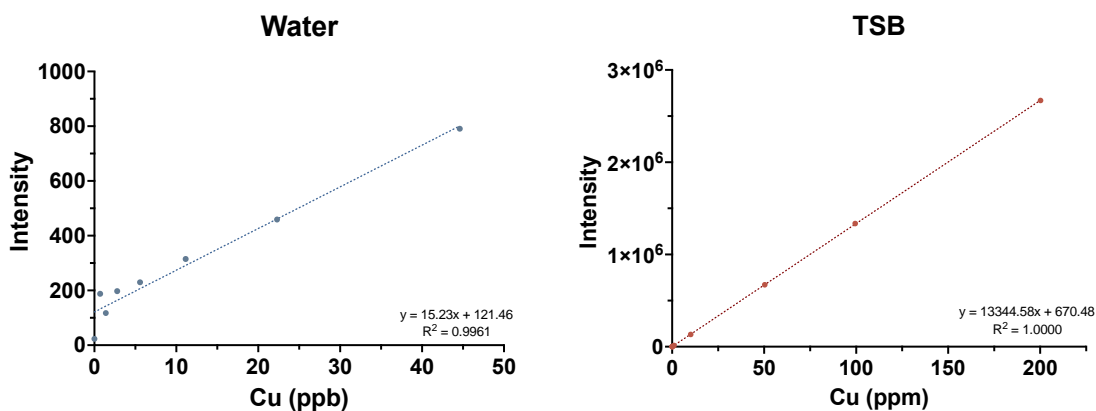
### **2.4.5.2 Analysis and Quantification**

XPS was performed using a Thermo Fisher Nexsa G2 surface analysis system. Data was acquired at room temperature (~27 °C) in an ultra-high vacuum analysis chamber with a base pressure of  $<5 \times 10^{-9}$  mbar. The instrument was equipped with a monochromated, micro-focused, low-power Al K $\alpha$  x-ray source that is regularly calibrated and maintained at  $1486.6 \pm 0.2$  eV. For analysis, the x-ray source illuminated a 400  $\mu$ m spot and three separate positions were analyzed per sample. Samples were irradiated using a low energy (< 10 eV) Ar<sup>+</sup> flood gun to mitigate surface charging.

Survey spectra were acquired with one eV resolution (step size) and a pass energy of 200 eV (resolution of 1.7 eV) for a total of four scans per spot. High-resolution spectra were acquired with a 0.1 eV resolution and a pass energy of 50 eV for a total of ten scans per spot. For each sample, normal-emission high-resolution spectra in the C 1s, N 1s, O 1s, Zn 2p, and Cu 2p regions were acquired. High-resolution spectra were fit

with Smart background and symmetrical Guassian-Lorentzian peaks using the Avantage software package (Thermo Avantage V.5.9931, Thermo Fisher Scientific). Binding energies were not charge corrected; the primary aliphatic C 1s peak was observed at a binding energy (BE) of  $284.4 \pm 0.4$  eV. Deconvolution was performed from lowest to highest BE. Elemental compositions represented as atomic % were generated by the software package but are generally quantified using calibrated analyzer transmission functions, Scofield sensitivity factors, and effective attenuation lengths.

## 2.5 Supplemental Materials



**Supplemental Figure 2.1: Calibration curves generated for ICP-OES measurement of Cu in both ddH<sub>2</sub>O and TSB. Line of best fits were generated and used to convert raw intensity to ppb or ppm.**

### **3. Isolation, Identification, and Characterization of Primary Colonizing Bacteria Harvested from Antifouling Coatings**

#### ***3.1 Introduction***

Accumulation of marine biofouling on ship hulls and other submerged structures creates a foundational problem within the maritime shipping industry. Biofouling build-up increases the drag coefficient which in turn negatively impacts fuel consumption, exhaust emissions, and operational costs.<sup>34, 78, 79</sup> In addition to deleterious industrial impacts, biofouling also poses substantial risks to human health as fouled vessels are recognized for the transfer of microorganisms to non-native environments.<sup>42, 43, 81, 82</sup> Biofouling is commonly inhibited by the application of antifouling coatings containing biocides to prevent the growth of microbial communities. Currently, the most utilized coatings are ablative antifouling coatings that rely on copper oxide ( $\text{Cu}_2\text{O}$ ) as the main biocide.<sup>15, 35, 83</sup>

Copper (Cu) is the most widely used biocide in antifouling coatings.<sup>83</sup> Cu is also a vital micronutrient, serving as a critical cofactor for enzymes involved in a multitude of biological pathways. All organisms possess mechanisms to manage copper levels including pathways for its acquisition, trafficking, storage, and detoxification.<sup>102-104</sup> Minor alterations in copper concentration disrupt intracellular metal homeostasis and induces a myriad of damaging effects including the production of reactive oxygen species (ROS), impairment of membrane function, protein dysfunction, and disruption

of enzymatic activity.<sup>102, 105-107</sup> To combat Cu dyshomeostasis, bacteria utilize various regulation mechanisms to ensure that vital cuproproteins, proteins that require Cu for proper function, are metalated while other cellular regions are protected from toxic Cu levels. Due to the differences in their ability to regulate Cu, bacterial organisms typically exhibit widely varied sensitivities to copper.<sup>108-110</sup> While there is likely substantial variation in Cu handling mechanisms, those within *Escherichia coli* are currently the most well defined.

With the main goal of maintaining Cu homeostasis, bacteria have evolved a variety of proteins and small molecule-based systems responsible for the efflux, oxidation, and sequestration of copper.<sup>111</sup> In *E. coli*, both Cu(I) and Cu(II) may permeate the outer membrane to enter the periplasm, but only Cu(I) may pass through the inner membrane to the cytoplasm.<sup>112, 113</sup> Efflux of Cu(I) from the cytosol is controlled by the *cue* system, which directly activates CueR; a copper-selective protein that coordinates one Cu(I) ion per monomer.<sup>113, 114</sup> Activation of CueR induces upregulation of *copA* and *cueO* genes, which are related to copper efflux and oxidation, respectively.<sup>111</sup> CopA, a P<sub>1B</sub>-type ATPase, is an efflux pump that traverses the inner membrane to export Cu(I) from the cytoplasm to the periplasm.<sup>113, 115</sup> Additional copper concentration control is carried out by the two-component Cus system comprised of CusCFBA and CusRS which, upon activation, is responsible for minimizing periplasmic copper.<sup>116</sup> Oxidation of Cu(I), the more damaging form of copper, to Cu(II) is mediated by the multicopper oxidase

CueO.<sup>111, 117</sup> Cu sequestration is conducted by a variety of Cu chaperones, siderophores, and cuproproteins. A well-known Cu chaperone is CopZ, a protein encoded by CopA, which transport copper intracellularly.<sup>92, 115</sup> Though mechanisms may not be as well defined in other species, the toxicity of Cu and the necessity of tight regulation is constant across all domains of life.

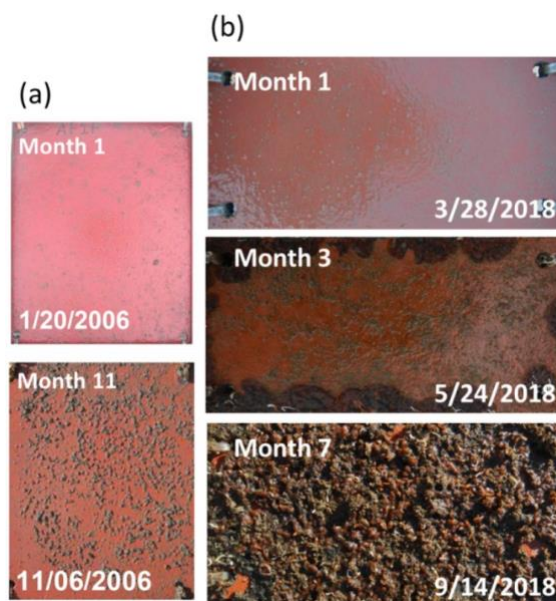


**Figure 8: Comparison of biofouling in 2006 vs 2018 on Interspeed 640 after static immersion. Depiction of the declining efficacy of Interspeed 640 over months of static immersion over the course of a decade. Images used with permission from the 2006 study<sup>118</sup> and the 2018 study<sup>39</sup>**

Commercially available Cu antifouling coatings can contain up to 75 % Cu<sub>2</sub>O by weight in an attempt to release sufficient levels of Cu to prevent biofouling over the extended coating lifetime.<sup>105, 107, 119</sup> Despite these high loading, the efficacy of these coatings has been in decline with what is hypothesized to be the emergence and spread of Cu tolerant species. In 2006, the biofouling on Interspeed 640, a standard Cu ablative

coating, was limited to small aggregates of slime after eleven months of static immersion.<sup>118</sup> When the study was replicated in 2018, a thick slime layer had formed within the first month, followed by the appearance of a diverse macrofouling community after only seven months of static immersion.<sup>39</sup> (**Figure 8**) This progression of biofouling suggests that the biofilm community forming on these Cu-rich surfaces have become increasingly capable of tolerating high levels of Cu.

The process of biofouling is dependent on the formation of the initial biofilm as this is what facilitates the settlement and accumulation of macrofouling organisms (e.g., algae, sponges, ascidians, barnacles, etc.). Thus, investigating the composition and Cu tolerance of the organisms contained in the initial biofilm, hereby referred to as primary colonizers, is of interest. Additionally, previous literature indicates that a combination of surface character and environmental conditions play substantial roles on the diversity of biofilm communities.<sup>120-124</sup> For example, when panels are deployed in one location with different types of AF coatings applied, the isolated biofilms present differences in composition and richness (defined as the number of different species), indicating a surface-dependence in biofilm diversity.<sup>124</sup> Similarly, when panels coated with the same AF paint are deployed at different locations, the biofilms isolated will have differing species compositions.<sup>120, 123</sup> In this study, panels coated with Interspeed 640 were deployed alongside uncoated polyvinyl chloride panels at three different field sites and biofilms were collected after two weeks of immersion. Bacterial species were isolated

and identified to better define the species involved in primary colonization across the three different field sites.

Towards the goal of capturing biofilm diversity after early immersion across field sites, we were able to generate a library of isolated bacteria. The library contains species from both coated and uncoated panels from each site. Based off the methods employed here we were able to identify 10 species from site 1, 7 species from site 2, and 21 species from site 3. Species isolated from site 1 and site 2 had higher similarity to each other than to site 3. From the species isolated at the estuarine site in Maryland (site 1), we found that Cu tolerance was not restricted to species harvested from coated panels as species harvested from both coated and uncoated panels displayed similar levels of Cu tolerating abilities.

## ***3.2 Results and Discussion***

### **3.2.1 Biofilm Community Development is Influence by Environmental Factors**

Diversity within biofilm communities is influenced by surface characteristics and environmental factors, mainly temperature and salinity.<sup>120-122</sup> To capture this diversity, uncoated panels and panels coated with Interspeed 640 were deployed in three different locations: Chesapeake Bay, Chesapeake Beach, MD, US (site 1), Port Marina, Cape Canaveral, FL, US (site 2), and Indian River Lagoon, Melbourne, FL, US (site 3). Panels were deployed for 14 days in June of 2023, temperature and salinity data are provided in

**Figure 9** for all three field sites. At the time of sampling, the average temperature and salinity were 22 °C and 9.3 ppt for site 1, 28 °C and 36 ppt for site 2, and 26 °C and 21 ppt for site 3. Additionally, the sites differ in the frequency of marine traffic, as site 2 is an active marina there is significantly more in- and out-bound vessel traffic than site 1 or site 3.

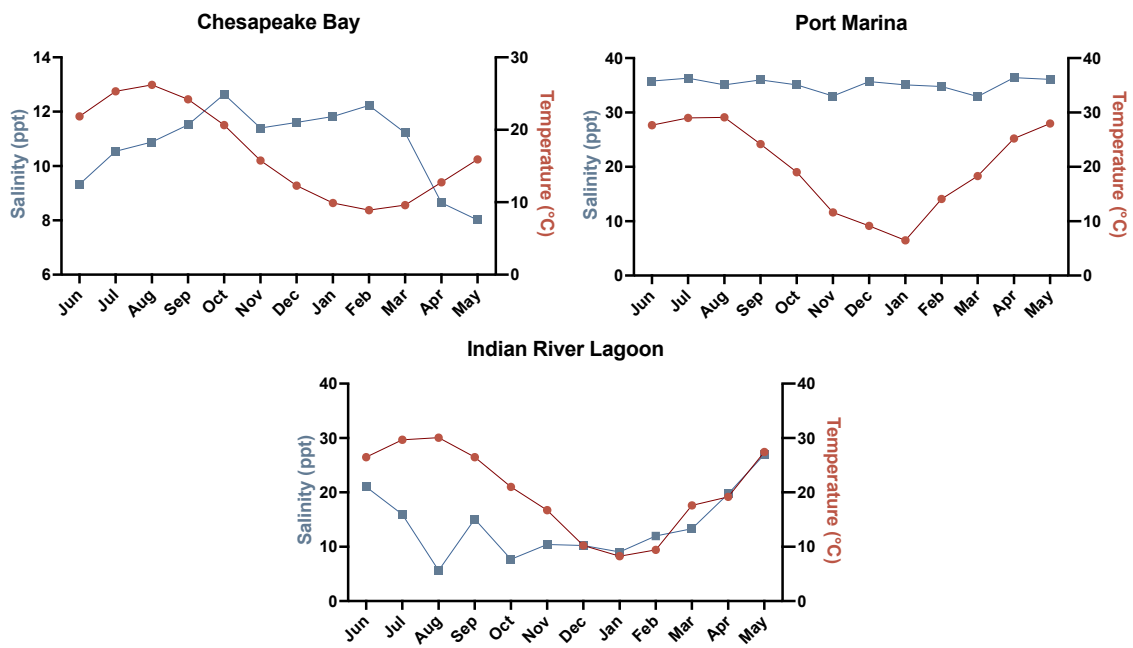


**Figure 9: Temperature and salinity data from 2023 for three sites of panel deployment.** Temperature (red, right axis) and salinity (blue, left axis) data for all three field sites where panels were deployed to assess biofilm community diversity. The data for site 1 was extracted from the National Oceanic and Atmospheric Administration and the data for site 2 and site 3 were provided by Kailey Richard (FIT).

Polyvinyl chloride (PVC) panels were either deployed uncoated or coated with a commercially available copper-based self-polishing antifouling coating. Panels were attached to 10' × 6' racks and immersed at a depth of approximately 2 m in late May of 2023 for site 1. Racks were left undisturbed for two weeks and, in early June, biofilms

were collected in triplicate using cell scrapers and stored in glycerol (25% glycerol in Difco Marine Broth (MB) 2216). Collections at site 2 and site 3 followed the same protocol and sampling schedule with collections two weeks after site 1.

Species isolation was carried out using serial plating techniques. Briefly, 2  $\mu$ L aliquots of replicate collections were combined and plated onto Difco Marine Agar (MA) 2216 and incubated at 30 °C until visible colonies formed (approximately 72 h). From these consortium plates single colonies were picked and replated onto fresh MA for another round of incubation. This process was repeated until single, homogeneous colonies were obtained and then three additional rounds of plating to ensure pure colonies. A library of isolated bacteria was created for each field site (**Tables 1–3**) for future reference and species were identified using 16S amplicon sequencing techniques. The following tables indicate the species isolated successfully from each field site grouped by the substrate from which the biofilm was originally collected. The leftmost column present in each table indicates the alignment grade which is a measurement of how well the isolated bacterial DNA overlaps with the sequences present in the NCBI database.

**Table 1: Bacterial species isolated from site 1 (Chesapeake Bay, Chesapeake Beach, MD, US)**

Panel Treatment	Identified Species	Alignment Grade
Blank	<i>Fictibacillus sp.</i> strain AFS043915	99.9%

Blank	<i>Bacillus xiamenensis</i> P2	100%
Blank	<i>Bacillus pumilus</i> strain BM1Q2009	100%
IS640	<i>Erythrobacter aquimaris</i> strain 4m129	99.2%
IS640	<i>Pontixanthobacter luteolus</i> strain SW-109	99.1%
IS640	<i>Priestia aryabhatai</i> strain NPH4	100%
IS640	<i>Altererythrobacter luteolus</i> strain Hal078	100%
IS640	<i>Pontixanthobacter luteolus</i> strain M72	100%
IS640	<i>Priestia aryabhatai</i> strain R12	100%
IS640	<i>Pontixanthobacter luteolus</i> strain ROD208	100%

**Table 2: Bacterial species isolated from site 2 (Port Marina, Cape Canaveral, FL, US)**

Panel Treatment	Identified Species	Alignment Grade
Blank	<i>Halobacillus</i> sp. strain PK-M7	99.8%
Blank	<i>Halobacillus</i> sp. strain JSM ZJ206	100%
Blank	<i>Alkalihalobacillus algicola</i> strain M160	100%
Blank	<i>Microbulbifer</i> sp. strain CCB-MM1	99.9%
IS640	<i>Alkalihalobacillus algicola</i> strain M160	99.7%
IS640	<i>Alkalihalobacillus algicola</i> strain ROD204	97.0%
IS640	<i>Bacillus cereus</i> strain G50	96.9%

**Table 3: Bacterial species isolated from site 3 (Indian River Lagoon, Melbourne, FL, US)**

<b>Panel Treatment</b>	<b>Identified Species</b>	<b>Alignment Grade</b>
Blank	<i>Halobacillus</i> sp. strain FJATT-53063	98.4%
Blank	<i>Bacillus pumilus</i> strain BM1Q2009	98.5%
Blank	<i>Cytobacillus kochii</i> strain V75	99.7%
Blank	<i>Bacillus</i> sp. PRL6	92%
Blank	<i>Cytobacillus kochii</i> strain V51	98.9%
Blank	<i>Bacillus xiamenensis</i> strain P2	27.5%
Blank	<i>Rossellomorea</i> sp. YZS02	94.3%
Blank	<i>Cytobacillus firmus</i> strain HIB-085	99.1%
Blank	<i>Fictibacillus phosphorivorans</i> strain V6146	99.5%
Blank	<i>Fictibacillus phosphorivorans</i> strain V6547	72.2%
Blank	<i>Cytobacillus homeckiae</i> strain AN479	80.3%
Blank	<i>Rossellomorea</i> sp. strain OTU36M16	72.6%
IS640	<i>Priestia aryabhatai</i> strain 22414	99.5%
IS640	<i>Priestia aryabhatai</i> strain V6191	99.7%
IS640	<i>Bacillus pumilus</i> strain MB1Q2009	99.7%
IS640	<i>Bacillus</i> sp. strain 11R-A	99.1%
IS640	<i>Bacterium</i> strain BS1358	99.3%
IS640	<i>Halobacillus</i> sp. strain GSP43	98.4%

IS640		<i>Bacillus altitudinis</i> strain L9		99.6%
IS640		<i>Bacillus sp.</i> strain S112T		99.6%
IS640		<i>Bacillus sp.</i> strain 22LB5		99.8%

Of all 38 successfully identified isolates, 21 were collected from site 3. This may be indicative of generally higher species richness and diversity at this location in comparison to site 1 and site 2. Importantly, the method used to collect biofilms at each field site included the use of MB which may induce a down-selection for the collected bacterial communities as the species that are incompatible with MB would be unlikely to survive. Additionally, not all collected bacteria are compatible with culture techniques.

A phylogenetic tree was constructed to best interpret the relationship between the three field sites while also relating both coated and uncoated panels (**Figure 10**). In the phylogenetic tree below, each branch or horizontal line, represents a lineage and where the branch diverges is a node. The scale bar at the bottom represents the length of the branch that corresponds to a difference of 7 nucleotides; essentially the shorter the branches on the node connecting two species the more closely related those species are. Conversely, long branches indicate species that are less related. Isolates from site 1 appear to have higher similarity to isolates from site 2 based off the length of the branches connecting them. We also observe very short branch lengths between the species from the coated panels, this is because only four unique species were isolated from site 1 and different strains were identified. Isolated species from site 2 appear in

the clusters of site 1 and site 3. Interestingly, site 2 is unique as it is an active marina which allows for the introduction of new species that may not natively exist in that location. While further analysis is required to fully characterize the biofilm communities at each site, it is interesting to consider that site 2 is an amalgamation of native and non-native bacterial species brought about by marine vessel traffic. Finally, the isolates of site 3 follow a similar trend to those in site 1 the overall group of both coated and uncoated panels are mostly separated from the other sites. Within the isolates for site 3, species from the coated and uncoated panels are also separated.

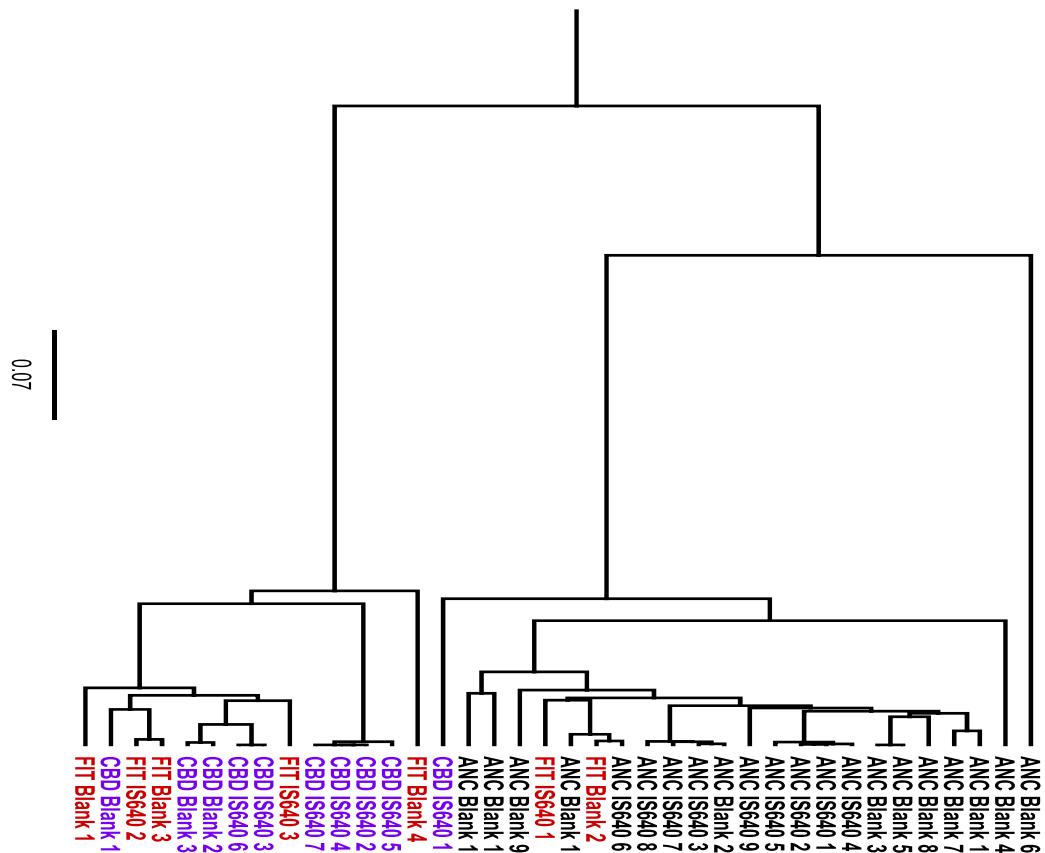
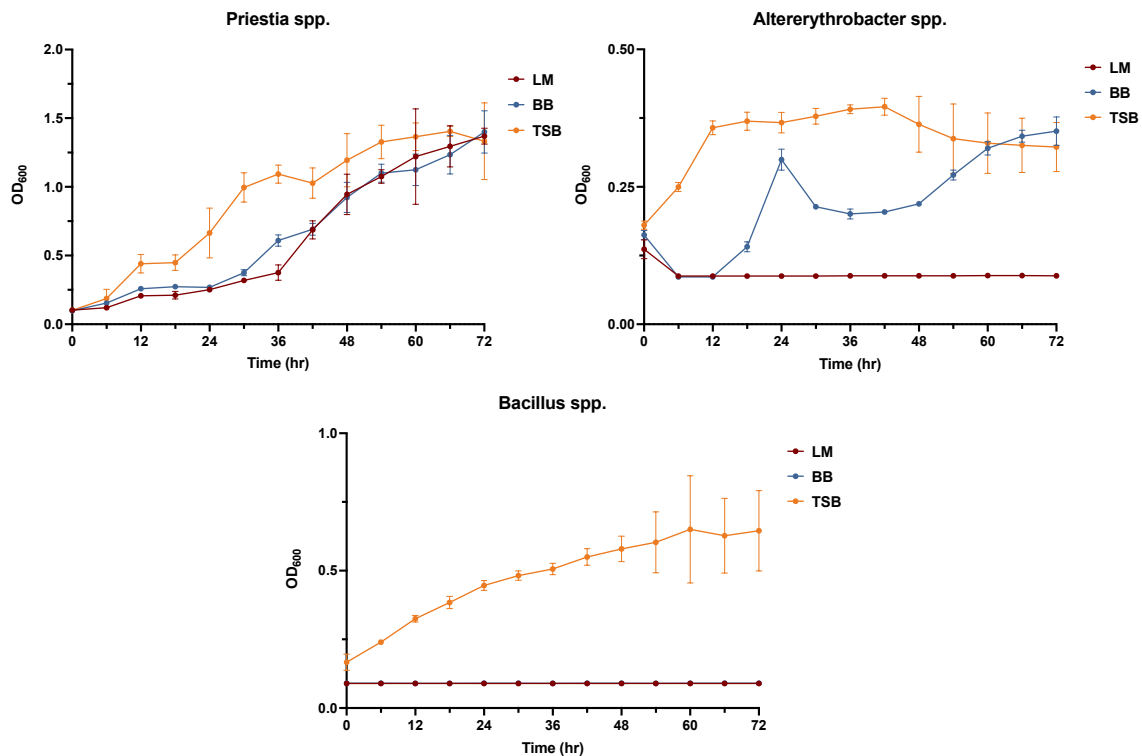


Figure 10: Phylogenetic tree depicting the relationship between species harvested across three field sites from both coated and uncoated panels. Relationship between

species collected from site 1 (CBD, purple), site 2 (FIT, red), and site 3 (ANC, black) across both uncoated (label: blank) and coated (label: IS640). The scale bar at the bottom shows the length of the branch that represents the amount of genetic change.

### 3.2.2 Optimization of Cell Culture Conditions

Bacterial species were originally isolated on Difco marine agar (MA) 2216 plates and cultured using Difco marine broth (MB) 2216, however due to the high salinity in the media precipitation from MB is common and is thus optically unfavorable. In all assays, bacterial growth was measured using the optical density at 600 nm ( $OD_{600}$ ) and assays originally completed using MB were unable to differentiate between precipitation and bacterial growth. To circumvent this problem, growth assays were completed using alternative culture media; LM (standard LB broth with an additional 10 g/L sodium chloride, NaCl), BB (one part LB to one part MB), or tryptic soy broth (TSB).



**Figure 11: Growth curves for selected species isolated from site 1 in three different types of culture media. Single colonies of selected species were used to inoculate 3 mL of MB and incubated overnight at 30 °C, 225 rpm. Overnight cultures were diluted into test media to a final OD<sub>600</sub> of 0.05 in 96-well culture plates. Data are representative of three biological replicates and plotted as the average with error calculated as standard deviation, represented by the error bars in the figure.**

Representative strains of each major species group collected and isolated from site 1 were used for general growth optimization as shown in **Figure 11** above. The tested bacterial isolates all grew best when supplemented with TSB, which is mildly surprising given the general affinity for marine bacteria and high salinity. LM is a nutrient rich medium, with LB as a base, but with a much higher salinity with an additional 10 g NaCl per L added (for a total of 15 g per L). BB is a media rich in both nutrients and salinity as it is composed of one-part LB and one-part MB. MB contains

approximately 20 g NaCl per L with multiple additional metal salts making it the highest salinity media assayed. TSB is considered a nutrient-rich medium with a moderate salinity originating from the 5 g NaCl per L prepared. The *Priestia spp.* isolated do not appear to be sensitive to nutrient variability or salinity where the isolated *Bacillus spp.* have the opposite reaction. From these observations, subsequent cell culture assays for field site isolations were carried out in TSB.

### **3.2.3 Copper Tolerance is Not Exclusive to Isolates Harvested from Interspeed 640 Coated Panels**

Given the diversity in the bacterial species isolated from the uncoated and coated panels, it was hypothesized that there would be variation in copper tolerance depending on the origin of the sampled bacteria. Additionally, we hypothesized that species isolated from coated panels would have a substantially higher tolerance to supplemental Cu.

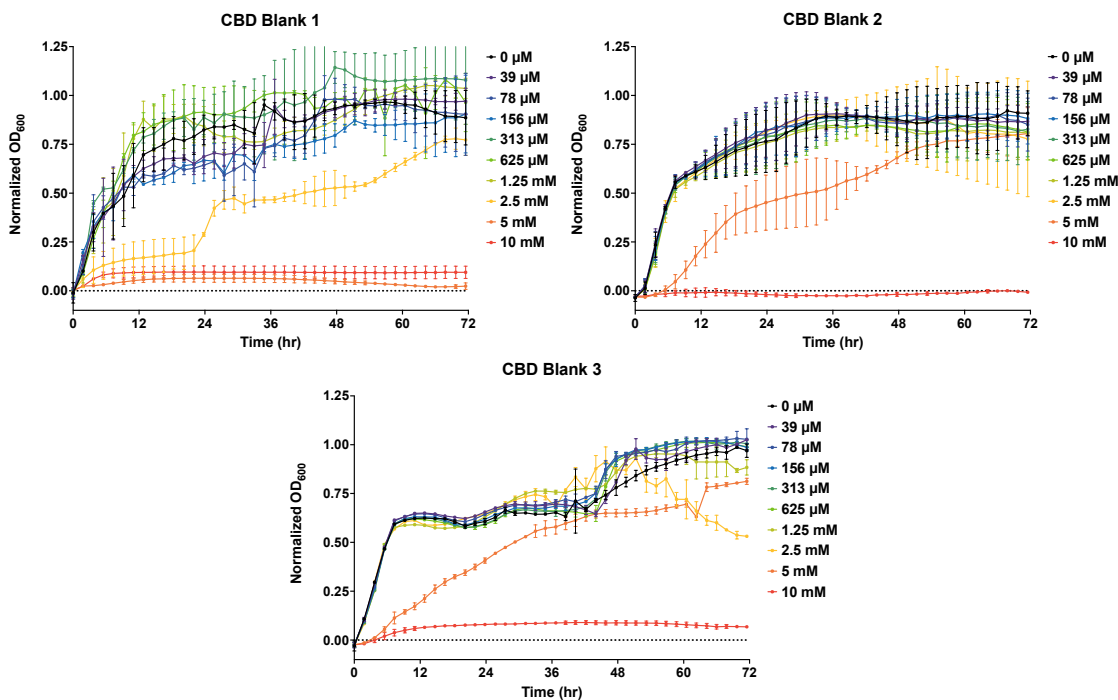


**Figure 12: Growth curves depicting the behavior of three bacterial species isolated from the uncoated panels deployed at site 1 following incubation with copper. Single colonies from each isolate were used to inoculate 3 mL of TSB media and incubated at 30 °C overnight at 225 rpm. Overnight cultures were diluted to a final OD<sub>600</sub> of 0.05 in 96-well culture plates containing increasing concentrations of copper sulfate. Data represented are the average of three biological replicates that have been background subtracted, to correct for media signals and copper absorbance, and normalized. Error was calculated as SD and represented by error bars in the figures.**

To investigate this, individual species harvested from site one (CBD, MD) were studied using a one-dimensional broth microdilution technique. In a simple 96-well plate format, each strain was exposed to a dilution series of copper sulfate diluted into TSB and bacterial growth was measured using OD<sub>600</sub> over a 72-h period. The upper limit of 10 mM supplemental CuSO<sub>4</sub> was originally chosen as an arbitrary starting point, however the isolated bacterial strains show an ability to tolerate levels of Cu that are

significantly higher than anticipated based off the concentrations typically detected in aquatic environments. The upper Cu concentrations have an absorbance band that overlaps with the OD<sub>600</sub> reading; to account for this each assay included a Cu dilution in media in the absence of cells to provide a sufficient background control.

Bacterial species isolated and cultured from uncoated (**Figure 12**) and coated panels (**Figure 13**) showed similar abilities to survive when challenged with high concentrations of CuSO<sub>4</sub>. Species isolated from uncoated or 'blank' panels demonstrated a collective ability to tolerate up to 1.25 mM Cu across all three species without significant growth inhibition. The Cu-tolerance may be a result of high concentrations of dissolved Cu in the sampling area or due to the proximity of blank panels to coated panels. Based off of the results discussed in the previous chapter and the literature precedent for the direct relationship between Cu-release and salinity, we can suppose that there is a substantial spike in local copper concentration immediately surrounding the racks to which the panels were attached.

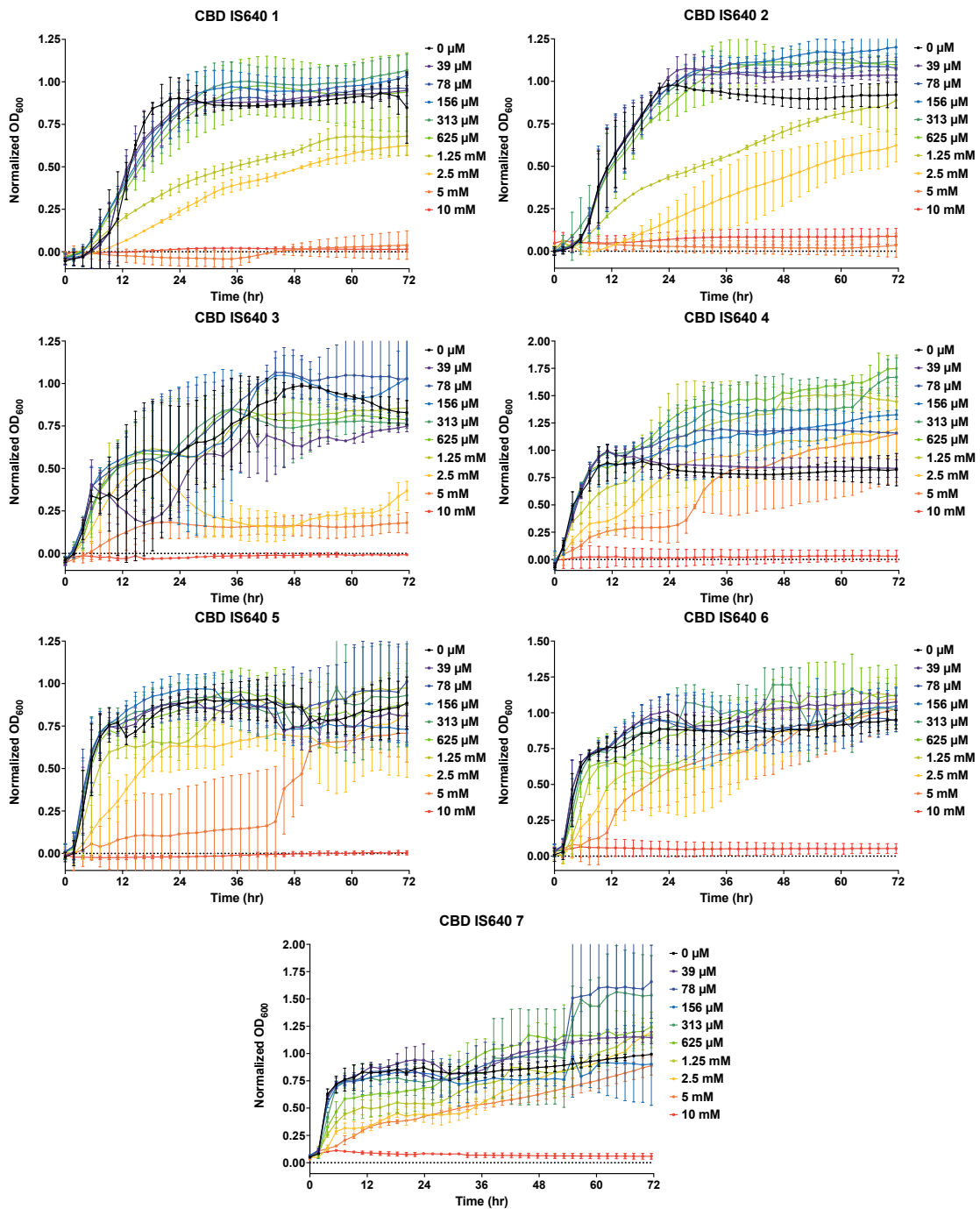


Figure 13: Growth curves depicting the behavior of three bacterial species isolated from panels coated with Interspeed 640 (IS640) from site 1 after incubation with copper. Single colonies from each isolate were used to inoculate 3 mL of TSB media and incubated at 30 °C overnight at 225 rpm. Overnight cultures were diluted to a final

**OD<sub>600</sub> of 0.05 in 96-well culture plates containing increasing concentrations of copper sulfate. Data represented are the average of three biological replicates that have been background subtracted, to correct for media signals and copper absorbance, and normalized. Error was calculated as SD and represented by error bars in the figures.**

Panels treated with our antifouling coating of interest yielded species with copper tolerating abilities similar to those detected in species isolated from blank panels. A noticeable trend prevalent in the isolates from coated panels is their growth recovery ability. This phenomenon, in which concentrations of Cu may initially inhibit growth but over the course of the assay, growth recovers to almost match that of the positive, or untreated control, can best be visualized in isolate 6 and 7. Within the first 24 hours of Cu exposure, concentrations between 5 mM and 0.625 mM Cu inhibited bacterial growth compared to no Cu. Perhaps the most interesting of the seven isolated species is isolate number 4, which appears to have enhanced growth in the presence of supplemental Cu. Growth in this species was completely inhibited at 10 mM Cu, concentrations between 1.25 mM and 5 mM Cu appear to initially inhibit growth but these and lower concentrations of Cu seem to promote growth beyond the abilities of untreated cells.

### ***3.3 Conclusions and Future Directions***

We originally hypothesized that there would be substantial species diversity both across field sites and across testing conditions (coated vs. uncoated panels). Additionally, it was postulated that the bacterial species isolated from panels treated with the AF coating of interest would exhibit enhanced abilities to tolerate high levels of copper when compared to species isolated from uncoated panels. These hypotheses

were investigated first by deploying panels at field sites with critical differences in environment such as temperature and salinity as well as in marine vessel traffic.

Biofilms formed on these panels after two weeks were collected to isolate what we refer to as primary colonizing bacteria. From this, we have created a library of primary colonizers that we may use to evaluate copper tolerance present now. This library may also be utilized in the future as these bacteria will become a point of comparison for future collections.

Overall, we observed bacterial diversity across all field sites as expected.

Diversity between coated and uncoated panels was also detected as expected.

Interestingly, the copper tolerating abilities assessed for site 1 using broth microdilution techniques did not reveal any substantial difference based on the origin of the bacteria sample. There was no significant increase in Cu tolerance from isolates taken from Cu AF coating panels. A potential explanation for this observed trend is related to the position of coated panels in relation to uncoated panels, as they are both in close proximity (within inches) it is likely that released Cu from coated panels is concentrated in the area and exposing bacteria to a similar environment regardless of the surface interface.

The efforts presented here go together with those presented in Chapter 2 as both chapters aim to tackle the same problem, the decline of self-polishing antifouling coatings that use Cu as a biocide, from two different angles. Chapter 2 provides

information regarding how environmental conditions impact Cu release and coating surface composition in the 14 day period in which primary colonization occurs; chapter 3 focuses on building a foundation for a larger effort towards evaluating the emergence and persistence of potential copper tolerance in bacteria. These results will serve as a foundation for future studies in which bacterial species are included in the sample set to begin investigating how primary colonizing bacteria interact with the surface.

Based on experimental evidence and literature surrounding marine bacteria, there are at least a few potential possibilities: 1) Modern marine bacteria have acquired advanced mechanisms to handle copper, either through sequestration or detoxification, 2) these bacteria possess extremely efficient copper efflux processes which allow leached Cu to essentially bypass the adhering bacteria and release into open water, or 3) bacterial adhesion inhibits the Cu release rate thus allowing biofilm formation and subsequent fouling to occur. Assessment of copper handling mechanisms within bacteria can be a complex process and the results are likely unique to each species. This study has provided a library of bacterial species known to form biofilms on coated panels as well as Cu tolerance profiles to better understand how these species respond to Cu. These results provide a launch point for future research that may involve full genomic analysis of acquired species to determine which Cu handling mechanisms are present and RNA sequencing to determine global responses to different levels of Cu

treatment. Ultimately, we hope to understand the biological processes that are contributing to the decline of this prominent antifouling coating.

### ***3.4 Methods***

#### **3.4.1 Materials and General Methods**

Chemicals and solvents were obtained from commercial suppliers and used as received unless otherwise noted.

#### **3.4.2 Panel Preparation, Deployment, and Sampling**

Polyvinyl chloride panels, 4"x8", were either coated with Interspeed 640 with a commercially available paint roller or left untouched prior to static immersion at estuarine and marine field test sites. Coated panels were allowed to dry for at least 24 h before deployment.

Triplicate sets of coated and uncoated panels were submerged for 14 days prior to sampling. Plastic cell scrapers were used to collect biofilms from the panel surface. Field site samples were collected and immediately stored in cryogenic vials containing 25% glycerol in Difco marine broth 2216 (MB). Cryogenic vials were stored at -80 °C when not in use.

#### **3.4.3 Species Isolation**

For each condition, 3  $\mu$ L of collected stocks in replicate conditions (i.e., all collections from coated panels from one field site) were combined in a 250  $\mu$ L snap-cap tube and mixed. To create consortia plates, a 1  $\mu$ L inoculation loop was used to streak

the combined sample on Difco Marine Agar 2216 (MA) plates and incubated at 30 °C for 72 h. After inoculation, visual characteristics (color, morphology, opacity, etc.) were used to pick single colonies which were then used to inoculate a fresh MA plate. The fresh plate was again incubated at 30 ° for 72 h. This process was repeated until each MA plate contained homogenous colonies and then an additional three rounds of plating to ensure pure colonies were obtained.

A single pure colony was used to inoculate 3 mL of MB prior to incubation at 30 °C, 225 rpm for 48 h. Inoculated cultures were used to generate glycerol stocks with a final concentration of 25% glycerol (v/v) in MB. Glycerol stocks were stored at -80 °C.

### **3.4.4 Species Identification**

#### **3.4.4.1 16S Amplicon Sequencing**

Initial DNA extraction was completed using single colonies grown from frozen glycerol stocks and plated onto fresh MA plates. A single colony was picked using a sterile toothpick and placed into one well of a 24-well PCR plate containing 200 µL of 10% chelex (w/w) solution. Plates were sealed with adhesive PCR plate seals (ThermoFisher) and placed into a thermocycler (ThermoFisher ProFlex PCR System) for DNA extraction. DNA extraction plate was held at 60 °C for 90 min then the temperature was increased to 99 °C for 10 min before being reduced and maintained at 10 °C. Extracted DNA samples were used for PCR amplification in fresh 24-well PCR plates containing Hot Start Taq 2x Master Mix (NEB; M0496L) and the 27F/1492R primer

pair in nuclease free water. PCR plates were sealed and placed in the thermocycler. Aliquots were electrophoresed on a 1% agarose gel, then stained with SYBR Safe DNA gel stain (Invitrogen) and checked for the presence of a band around 1500 base pairs. Successfully amplified PCR products were cleaned using ExoSap-IT Express to remove excess nucleotides prior to submission for sequencing. Sequenced results were blasted against the NCBI nucleotide collection for species analysis.

#### **3.4.4.2 Data Analysis**

All sequence analysis was performed using Geneious 11.1.5 software and tools included in the base software. Forward and reverse nucleotide sequences were returned for each DNA extraction performed as described in the previous section. Sequences were trimmed from both the 5' and 3' ends with a 5% error probability limit. Alignment of the forward and reverse sequences was completed using a global alignment with free end gaps. Consensus sequences were generated submitted to the basic local alignment search tool (BLAST) for sequence alignment in the NCBI Nucleotide collection. A total of 100 BLAST hits were obtained for each sequence and used to provide preliminary species identification. Phylogenetic trees were constructed using the previously assembled consensus sequences. These sequences were aligned using Muscle (3.8.425 by Robert C. Edgar) with anchor optimization. The Geneious Tree Builder tool was used to build trees using the unweighted pair group method with arithmetic mean (UPGMA) method with the Tamura-Nei genetic distance model.<sup>125</sup>

### 3.4.5 Copper Tolerance Profiles

A single colony of selected bacterial isolates was cultured overnight in 2 mL of Tryptic Soy Broth (TSB) at 30 °C, 225 rpm. Overnight cultures were diluted to an OD<sub>600</sub> of 0.1 in fresh TSB media and used as the working culture. An aqueous stock of copper sulfate TSB media to 20 mM working solutions and serially diluted from right to left along the rows of a clear, flat-bottomed, 96-well plate. Aliquots of 100 µL of the working culture were added to the inner wells of the 96-well plate to a final OD<sub>600</sub> of 0.05 and final volume of 200 µL. Aliquots of 100 µL of fresh TSB were added to the wells of the top and bottom rows to achieve a final volume of 200 µL. The top and bottom rows of the plate serve as metal dilution controls to allow for background subtraction of copper solution. The right and left columns of the plate contained only 200 µL media and served as sterility controls for the assay. Bacterial growth was evaluated via OD<sub>600</sub> using a Tecan plate reader set at 30 °C, over a 72-hour period with readings taken every 10 minutes with constant double orbital shaking (1.5 mm). OD<sub>600</sub> values were normalized to the positive growth control and adjusted for both background signal and metal signals using either the values from the right and left columns or the top and bottom rows, respectively. Data presented are representative of biological triplicates with error calculated as standard deviation represented by error bars in the figures. GraphPad Prism 10 (version 10.2.3) was used for data visualization

## 4. Interactions between *Marinobacter atlanticus* strain CP-1 and Heavy Metals

### 4.1 Introduction

Over two decades ago, it was discovered that certain bacteria, microorganisms that typically couple the oxidation of organic compounds to the reduction of insoluble compounds such as metals (i.e., iron (III) chloride,  $\text{FeCl}_3$ ), were capable of extracellular electron transport (EET) to electrodes. Microorganisms have been isolated from cathodes, in which electron acceptors reduce compounds by reacting with electrons and protons, as well as from anodes, where organic compounds are oxidized to release electrons and protons,<sup>126, 127</sup> although the majority of characterized electroactive microorganisms have been isolated from anodes.<sup>127</sup> Microorganisms capable of EET are referred to as electroactive bacteria and include model organisms such as *Shewanella oneidensis*<sup>128</sup> and *Geobacter sulfurreducens*,<sup>129</sup> which can produce electrical current using redox mediators, cytochromes, and/or nanowires as charge carrying mechanisms.<sup>130, 131</sup> *S.*<sup>130, 131</sup> *S. oneidensis* and *G. sulfurreducens* are model electroactive bacteria due to their ability to produce high currents through organic acid oxidation and electrode respiration under oxygen-depleted conditions. Since the initial discovery of electroactive bacteria, EET capabilities have been revealed in a wide range of genera.<sup>132</sup> Additionally, some electroactive bacteria are capable of both electrogenesis (the deposition of electrons onto an electrode, (e.g., to produce electricity) and electrotrophy (the consumption of

electrons from an electrode (e.g., to consume electricity). Despite the wide diversity of organisms capable of EET, the range of electrical current production for many of these species utilizing EET is much lower than those observed for *S. oneidensis* and *G. sulfurreducens*. For example, *Marinobacter atlanticus* produces electrical current four orders of magnitude lower than that of the model species.<sup>129, 133, 134</sup> However, lower current production may be favorable for the development of a biosensor or a biomanufacturing chassis organism than an organism that produces high current, where EET is likely an important aspect of the microorganism's metabolism.<sup>135</sup>

*M. atlanticus* is a Gram-negative, heterotrophic marine bacterium isolated from Biocathode MCL (*Marinobacter*, *Chromatiaceae*, *Labrenzia*),<sup>136</sup> an electrode biofilm community isolated from the Atlantic Ocean.<sup>137, 138</sup> In the presence of oxygen, *M.*<sup>137, 138</sup> In the presence of oxygen, *M. atlanticus* produces small amounts of electrical current via oxidation of organic acids despite not possessing critical charge-carry mechanisms native to model electroactive bacteria.<sup>133, 138-140</sup> In particular, differential gene expression<sup>137</sup> revealed an absence of genes known to be linked to EET, no evidence of large multi-heme *c*-type cytochromes, and no evidence of soluble shuttle (redox mediator) production despite the electroactive capabilities of *M. atlanticus*.<sup>135</sup> Thus, despite EET capabilities, the mechanisms for EET in *M. atlanticus* remain unknown.

A study characterizing the electrochemical qualities of *M. atlanticus* noted that the addition of trace metals, such as those present in Wolfe's trace mineral solution (i.e.,

cobalt, copper, manganese, iron, and zinc) increased anodic current by an order of magnitude.<sup>133</sup> Additional studies have indicated that *M. atlanticus* modifies its extracellular environment in response to electrode potential which is further supported by the increased prevalence of genes for protein secretion and metal uptake under current-producing conditions.<sup>137</sup> Overall, this suggests that currents produced by *M. atlanticus* are likely linked to mineral cycling and metal concentrations within the local environment, both of which could affect EET abilities.

The dependence of mineral bioavailability on the current production by *M. atlanticus* may be linked to the bacterium's ability to tolerate or leverage environmental metal ions. We aimed to determine if there are specific concentration ranges that are tolerated without significant impact on growth or if there are concentrations that potentiate bacterial growth in order to promote the development of *M. atlanticus* as a biosensor.<sup>141-143</sup> For instance, *M. atlanticus* may be capable of detecting lower concentrations of metal ions than other organisms or may remain responsive in the presence of toxic heavy metals whose concentrations may nullify other marine biosensors. The response of *M. atlanticus* to changing metal concentrations also likely impacts the organism's EET capabilities, and results from the experiments described here can inform future biosensor design. Further, expanding our knowledge of metal tolerance in *M. atlanticus* would enhance ongoing biomanufacturing efforts when using

waste streams, should the waste stream composition change or acquire heavy metal contamination.<sup>144-146</sup>

In this study, we sought to determine the extent of metal-tolerance for ten different metals commonly found in marine environments to assess the ability of *M. atlanticus* to grow under metal-contaminated conditions. Broth microdilution techniques were initially employed to determine concentration ranges in which the growth of *M. atlanticus* was impacted by the presence of additional metal ions. Then, the ability of *M. atlanticus* to detoxify metals from solutions was investigated using a large-scale culture assay in which changes in metal content were assessed using inductively coupled plasma optical emission spectroscopy (ICP-OES). In this instance, detoxification was defined as a measurement of metal concentration reduction in the supernatant. We found that *M. atlanticus* tolerates up to 2.5 mM of all metal ions tested with the exception of cadmium which inhibited growth above 313  $\mu$ M. In the ICP-OES assessment of metal detoxification, *M. atlanticus* exhibits a marginal ability to remove metal ions from media.

## ***4.2 Results and Discussion***

### **4.2.1 *Marinobacter atlanticus* shows Broad Tolerance Against Multiple Metal Ions**

The electroactive properties of *M. atlanticus* may be linked to labile heavy metals and trace mineral cycling. Due to these attributes the potential ability of *M. atlanticus* to tolerate metals found in both marine and biological environments was of interest.

Additionally, to our knowledge, no study has been reported that assesses the heavy metal tolerance of *M. atlanticus*. Identifying bacterial species with the ability to tolerate or process metals commonly implicated in heavy metal toxicity is of interest as these species may be leveraged to aid in efforts to detoxify water sources or to recover precious metals.

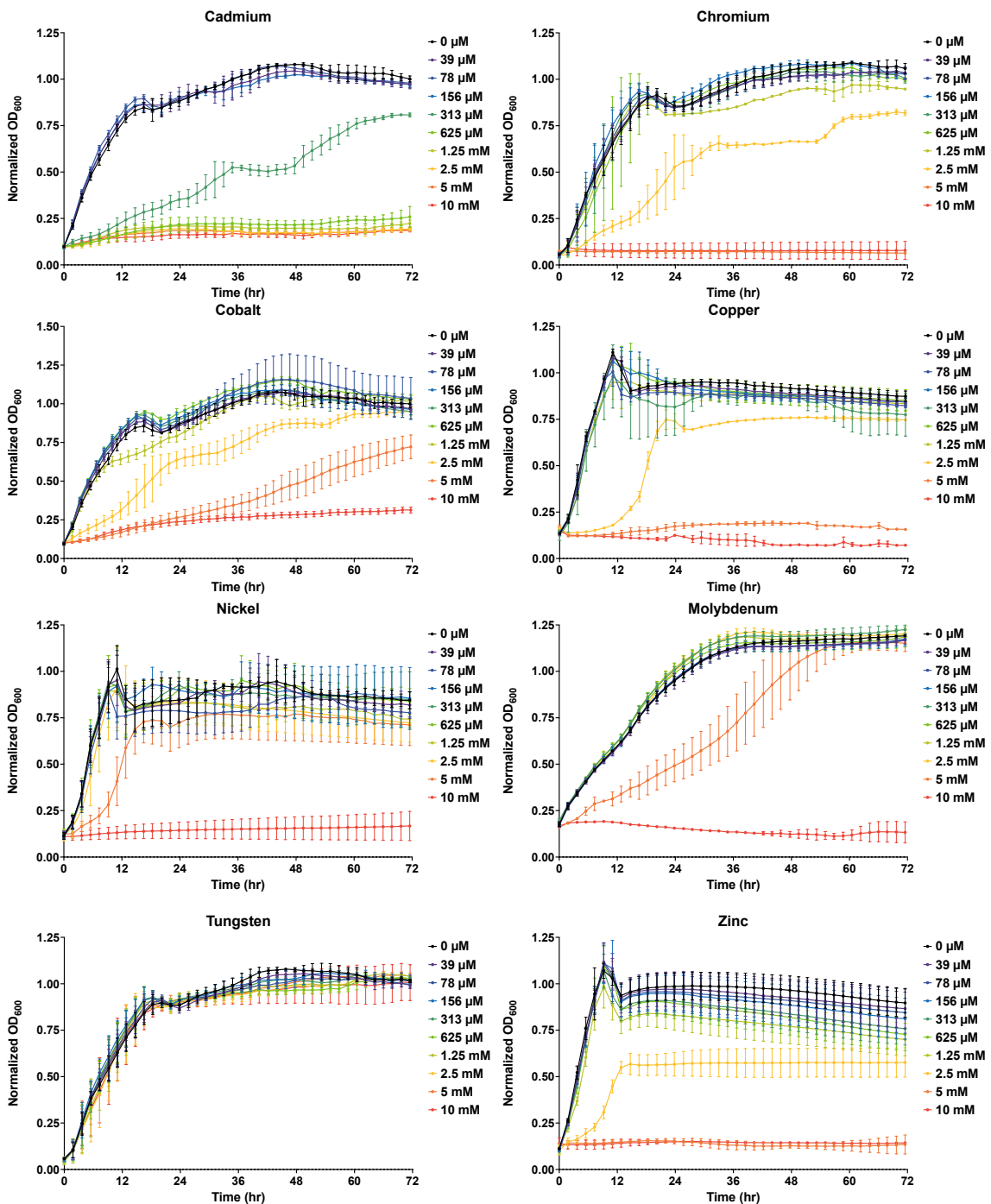


Figure 14: Growth curves for *Marinobacter atlanticus* exposed to 10 mM of heavy metals. *M. atlanticus* was cultured overnight in 3 mL BB at 30 °C, 225 rpm in angled racks (~45°). Overnight cultures were diluted to a final OD<sub>600</sub> of 0.05 in 96-well plates containing increasing concentrations of heavy metals (see individual figure titles).

Data represented are the average of three biological replicates that have been background subtracted to correct for metal absorbance and media background signals. Error was calculated as SD and is represented by error bars in the figures.

The assessment of metal handling potential in *M. atlanticus* was completed using one-dimensional broth microdilution techniques in which the bacteria were exposed to a series of metal concentrations over a three-day period. Metals were chosen due to known toxicity, presence in marine ecosystems, or known biological importance. *M. atlanticus* was tested against a series of 10 metals which included biologically essential and non-essential metals common to marine environments: cadmium (Cd), chromium (Cr), cobalt (Co), Copper (Cu), Manganese (Mn), Molybdenum (Mo), Nickel (Ni), Tungsten (W), Vanadium (V), and Zinc (Zn). Against all but Cd, *M. atlanticus* showed the ability to tolerate up to 2.5 mM of each metal salt and up to 5 mM in the case of Mn, W, and V without significant impact on growth (Figure 14 & Figure 15). *M. atlanticus* has demonstrated the ability to persist in environments containing metal contamination levels substantially higher than those detected in natural bodies of water.<sup>147</sup>

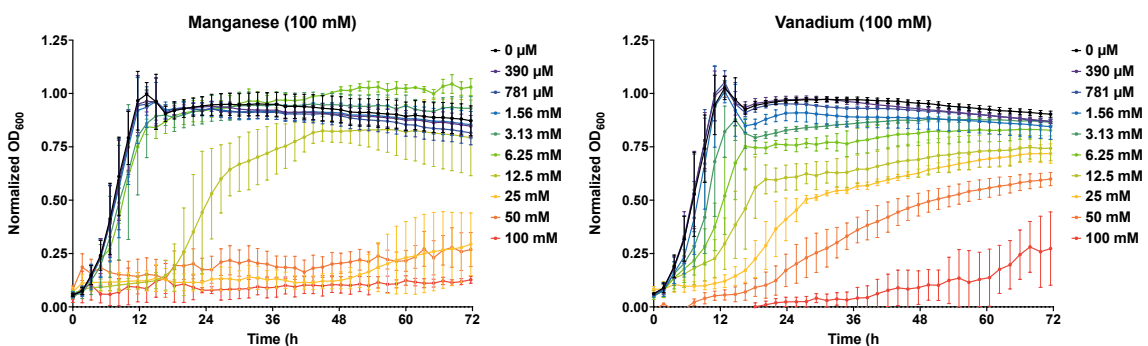


Figure 15: Growth curves for *Marinobacter atlanticus* in the presence of 100 mM Mn and 100 mM V. *M. atlanticus* was cultured overnight in 3 mL BB at 30 °C, 225 rpm in

angled racks (~45°). Overnight cultures were diluted to a final OD<sub>600</sub> of 0.05 in 96-well plates containing increasing concentrations of either Mn or V. Data represented are the average of three biological replicates that have been background subtracted to correct for metal absorbance and media background signals. Error was calculated as SD and is represented by error bars in the figures.

*M. atlanticus* was tested against higher concentrations of Mn and V (Figure 15).

Manganese is a vital metal in marine ecosystems as it is intricately involved in almost every elemental cycle currently known within the marine microbiome.<sup>148</sup> Mn plays important roles in biology, in marine microbes specifically Mn has the ability to oxidize toxic organic and inorganic compounds, plays roles as enzymatic cofactors in Mn-specific and nonspecific metalloenzymes, and provides defense against oxidative stress.<sup>148</sup> Additionally, Mn has been shown to participate in microbially-mediated redox reactions that are either independent of or linked to metabolism.<sup>148</sup> Under these conditions, *M. atlanticus* displays the ability to tolerate up to 12.5 mM Mn.

Interestingly, *M. atlanticus* seems have an initial sensitivity to high concentrations of V with concentration dependent inhibitions of cell growth. Despite the decrease in initial growth, it appears that *M. atlanticus* may have the ability to recover even under extraordinarily high (100 mM) concentrations of vanadium as we can see growth increasing after approximately 36 hours. This may suggest sophisticated intracellular mechanisms for tolerating V, likely by methods including detoxification, accumulation, sequestration, or efflux. Current literature suggests that vanadium-resistant bacteria isolated from marine ascidians are typically associated with accumulating vanadium.<sup>149</sup>

Another potential avenue for the unique response of *M. atlanticus* and V may revolve around the different biological roles V may step into. An interesting characteristic of V, the vanadate anion specifically, is its ability to substitute for the phosphate anion as the two are similarly sized structural analogues.<sup>150</sup> Additionally, there are multiple known bacteria capable of utilizing V in respiration, particularly under conditions in which the native metal ion is depleted.<sup>150</sup> In marine species particularly, there are V-dependent haloperoxidases whose function typically involved halide oxidation.<sup>150</sup> Ultimately, it is impossible to postulate the intracellular fate of vanadium in *M. atlanticus* with the currently available data. Regardless, the general ability of *M. atlanticus* to tolerate such high metal loads without growth inhibition is promising for future applications of this bacteria in both biosensing and biomanufacturing.

#### **4.2.2 *Marinobacter atlanticus* Lacks Significant Abilities to Uptake Metal Ions from Solution**

As shown above, *M. atlanticus* has demonstrated the ability to tolerate metal concentrations substantially higher than those found in native marine environments. Due to the ability of *M. atlanticus* to survive when challenged with high concentrations of heavy metals we hypothesized that this bacterium may have potential applications in heavy metal remediation. To investigate this potential, 30 mL cultures of *M. atlanticus* were grown in BB broth overnight and aliquots were used to inoculate fresh media containing a high and low concentration of each metal of interest (**Table 4**). Metal concentrations were selected based off the results of the metal tolerance assay discussed

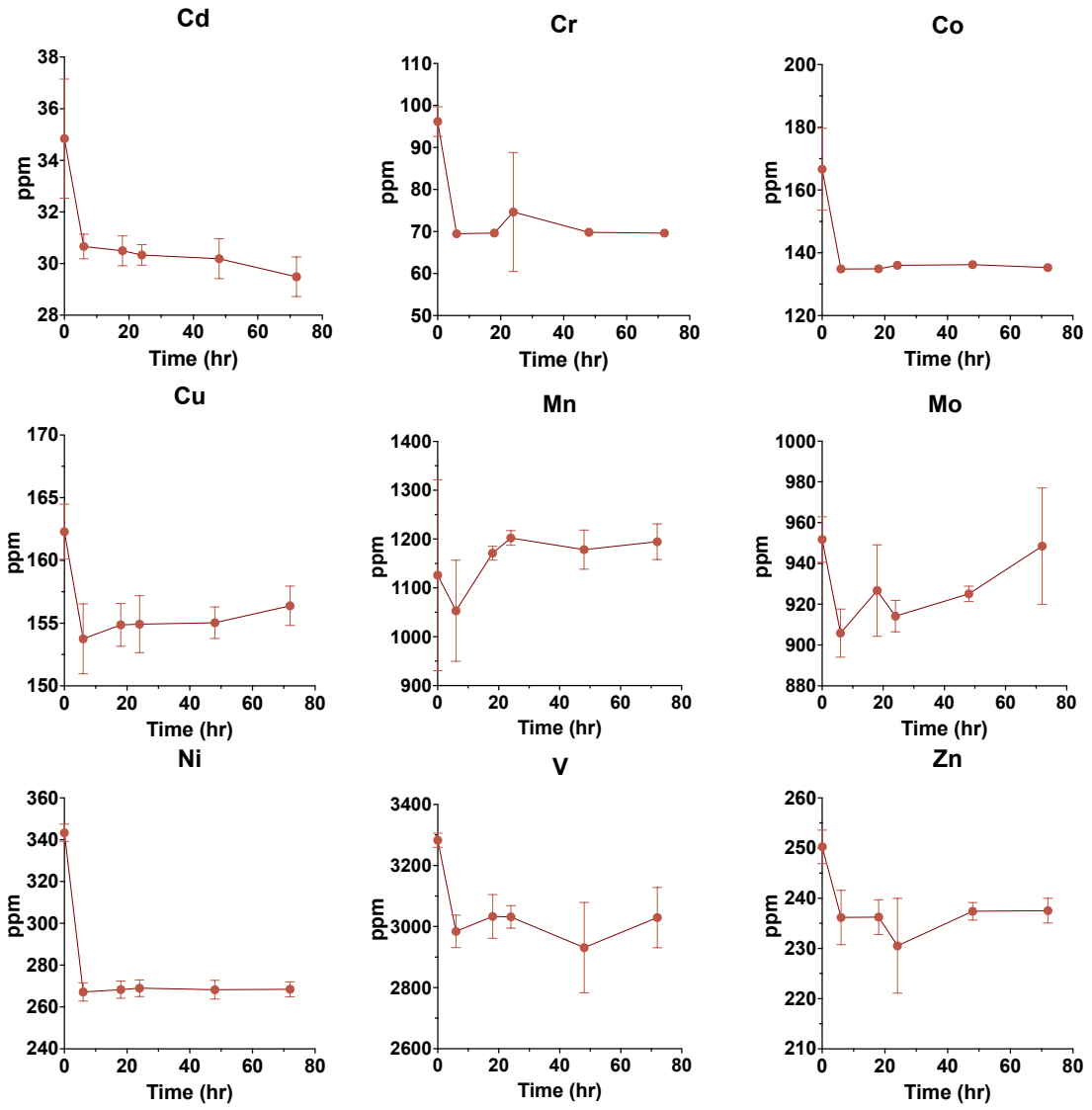
in the previous section. Generally, most care was given to the selection of the high concentration which was identified by the highest concentration where bacterial growth was still present but may be inhibited. Three large cultures of *M. atlanticus* were grown in BB media and aliquots were used to inoculate the metal-containing BB media samples. These cultures were grown for three days with aliquots taken at 6, 18, 24, 48 and 72 hours to capture metal content throughout the growth phases of *M. atlanticus*. Aliquots were centrifuged to isolate biological material and inductively coupled plasma optical emission spectroscopy (ICP-OES) was used to measure metal content in the supernatant.

**Table 4: Metal Concentrations Chosen for Metal Detoxication Assay**

<b>Metal Ion</b>	<b>High Concentration (mM/ppm)</b>	<b>Low Concentration (mM/ppm)</b>
<b>Cadmium</b>	0.313/35.1	0.156/17.6
<b>Chromium</b>	2.5/130	0.625/32.5
<b>Cobalt</b>	2.5/147.3	0.625/36.8
<b>Copper</b>	2.5/158.7	0.625/39.7
<b>Manganese</b>	12.5/686.8	3.13/171.7
<b>Molybdenum</b>	5/479.6	2.5/240
<b>Nickel</b>	5/293.5	0.625/36.9
<b>Tungsten</b>	100/18390	10/1839
<b>Vanadium</b>	50/2547	1.56/79.6
<b>Zinc</b>	2.5/163.5	0.625/40.9

Changes in metal concentration within the collected supernatant were attributed to metal uptake or detoxification, meaning the loss of detectable metal ions in the supernatant, by *M. atlanticus*. Samples containing W were unable to be measured as significant amounts of insoluble oxides precipitated out and the amount of hydrofluoric acid required to solubilize these insoluble species was incompatible with the ICP-OES instrument available. For both the high and low metal ion concentrations tested, the only significant, detectable change occurs early in the time frame. Between 0 h and 18 h, during the exponential growth phase of *M. atlanticus*, metal concentrations in the supernatant decrease slightly before appearing to stabilize **Figure 16**. As the metal ion concentration reaches stabilization around when the exponential growth phase completes, this initial decrease may be representative of an ability of *M. atlanticus* accumulate or sequester small concentrations of these metal ions. In all cases, *M. atlanticus* displays minor abilities to remove metal ions from solution.

A)



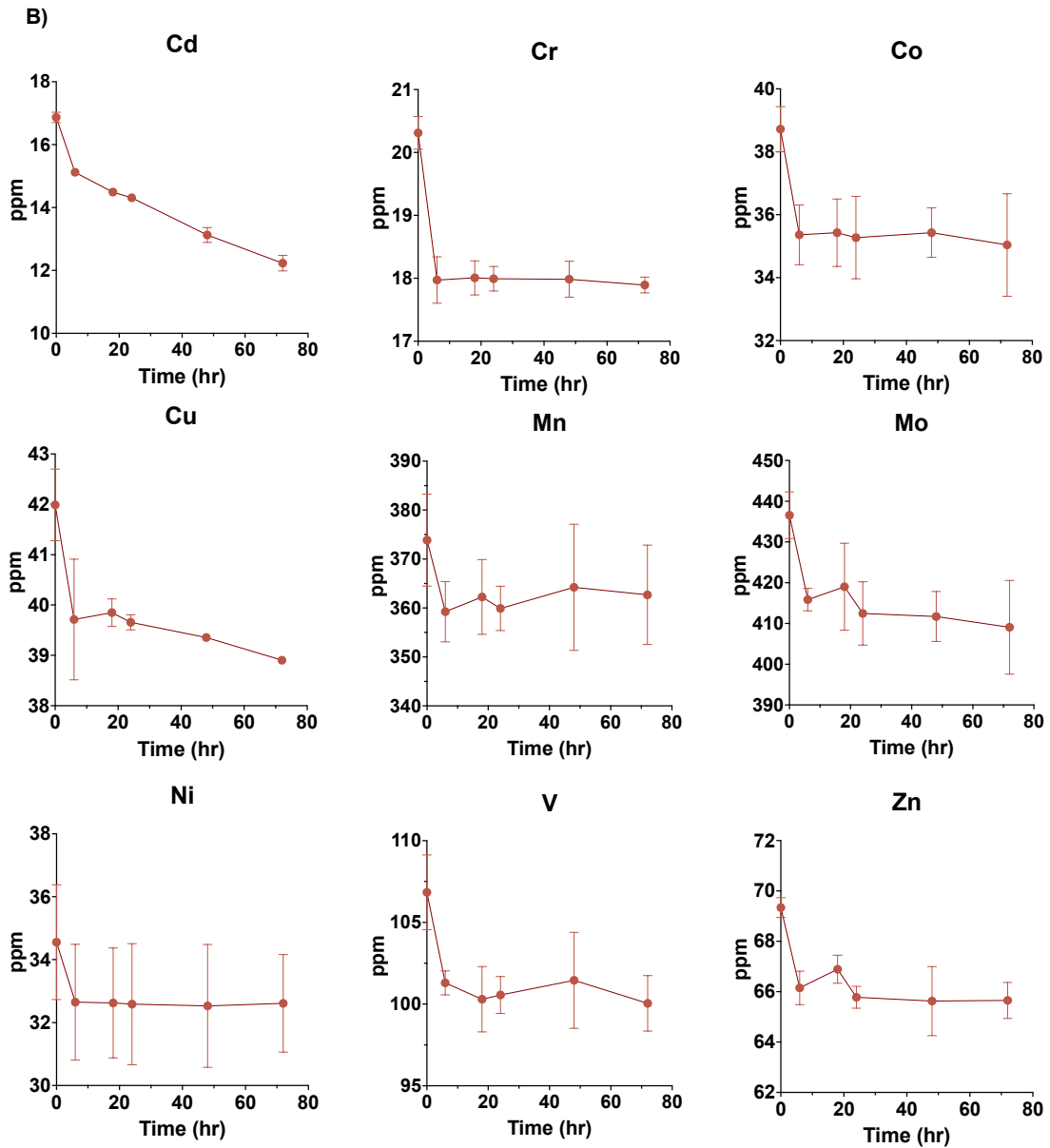


**Figure 16: *M. atlanticus* has Minimal Metal Detoxification Capabilities.** *M. atlanticus* was grown in three 30 mL aliquots of BB overnight at 30 °C, 225 rpm in angled racks (~45°). Overnight cultures were used to inoculate 50 mL centrifuge tubes containing either a high (A) or a low (B) concentration of metal (see individual figure titles).

The results above suggest a marginal ability for *M. atlanticus* to remove select metal ions from solution however, the data above do not indicate what method the

bacterium may be utilizing to induce this decrease. Bioremediation methods commonly employed by marine bacteria include biosorption, bioaccumulation, and bio-reduction<sup>21</sup>.

<sup>151</sup> Biosorption is the most simple way in which bacterial species may take up labile heavy metals as it is a metabolically passive process that ceases when the cellular surface has reached an equilibrium with bound pollutant.<sup>152</sup> Bioaccumulation begins in the same way as biosorption but the process continues to involve active transport of the pollutant inside of the cells where binding to intracellular components takes place; this is generally a slower process that facilitates the uptake of more pollutant.<sup>152</sup> Bio-reduction, unlike the other two methods, does not necessarily remove heavy metal toxins from solution, rather it is a process in which bacteria reduce toxic metals to a more innocuous state. The reduction of Cr(VI) to Cr(III) by some *Bacillus spp.* is a prominent example of bio-reduction.<sup>153</sup> Bio-reduction products are highly dependent on the toxin and the pH of the environment, some examples for Cr include the formation of insoluble CrO(OH), organic Cr(III) complexes bound to the cell surface, or water soluble organic-Cr(III) complexes.<sup>153-155</sup> Given the results we have obtained, we cannot completely rule out the potential of *M. atlanticus* for use in heavy metal bioremediation, but significantly more investigation is necessary to fully explore this potential. Regardless, the ability of this bacterium to persist in metal contaminated environments is promising for its future development as a biosensor.

### ***4.3 Conclusions and Future Directions***

We hypothesized that, because *M. atlanticus* likely relies on the presence of trace minerals and available metal ions to facilitate EET this bacterium may be useful for applications in bioremediation and biosensing. In this work, we present the first evaluation of heavy metal tolerance for *M. atlanticus* for a range of both essential and non-essential heavy metals that are prominent in marine ecosystems. In all cases, *M. atlanticus* exhibited the ability to persist in the presence of metal concentrations significantly higher than those detected in the average marine ecosystem. Based on this discovery, we investigated the potential for *M. atlanticus* to remove heavy metals from contaminated solutions using ICP-OES. The results of this effort are inconclusive, while we do observe some decreases in metal ion concentration, we are unable to definitively discern the actions of *M. atlanticus*. In combination, this study has provided a foundation for future endeavors regarding the full characterization of *M. atlanticus* as a biosensor and for use within other biotechnological applications. Future efforts towards characterizing *M. atlanticus* should certainly involve further investigation into its interaction with vanadium as there is likely a metal-dependent response that may be tied to the electroactivity of *M. atlanticus* or a separate not-yet defined characteristic. Characterization of EET in the presence of assayed metal ions may be an interesting future avenue as it may allow for fine-tuning the behavior of *M. atlanticus*.

## **4.4 Methods**

### **4.4.1 Materials and General Methods**

Chemicals and solvents were obtained from commercial suppliers and used as received unless otherwise noted.

### **4.4.2 Bacterial Strains and Culture Conditions**

Bacterial strains of *Marinobacter atlanticus* strain CP-1 were maintained at -80 °C in 25% glycerol in rich medium that is one half lysogeny broth (LB)<sup>156</sup> and one half Difco marine broth 2216 (MB) (Becton Dickinson, Franklin Lakes, NJ, United States) that will be referred to here as BB medium.<sup>157</sup> For 1 L of BB medium 18.7 g MB, 5.0 g tryptone, 2.5 g yeast extract, and 5.0 g of sodium chloride are added. To prepare agar plates, 15.0 g of agar were added to prior to autoclaving. Before all experiments, *M. atlanticus* were streaked onto BB agar plates from frozen stocks and incubated at 30 °C for 72 h. A single colony was used to inoculated 3 mL BB which was then incubated at 30 ° in an angled rack (~ 45 °) at 225 rpm for 18-24 h.

### **4.4.3 Metal Tolerance Assays**

#### **4.4.3.1 Preparation of Metal Stock Solutions**

Stock solutions of the following metals salts purchased from Sigma-aldrich were prepared at 0.5 M in Milli-Q water: cadmium (Cd), chromium (Cr), cobalt (Co), copper (Cu), nickel (Ni), manganese (Mn), molybdenum (Mo), tungsten (W), vanadium (V), and zinc (Zn). All metal stocks were stored in sealed scintillation vials in the dark.

Sodium orthovanadate (Sigma-aldrich) was prepared at 1 M concentration in water according to vendor instructions. Briefly, sodium orthovanadate was dissolved in water to approximately 1 M and the solution pH was adjusted to ~10 using NaOH pellets. The solution was then boiled to allow the decavanadate to polymerize to monovanadate, indicated by a color change from orange to clear. The precise solution concentration was determined using the molar extinction coefficient ( $3,550 \text{ M}^{-1}\text{cm}^{-1}$ ) at 260 nm at pH 10.5.

#### **4.4.3.2 Microdilution Assays**

A single colony of *M. atlanticus* was cultured overnight in 2 mL BB media (0.5 parts LB and 0.5 parts MB) at 30 °C, 225 rpm. Overnight cultures were diluted to an OD<sub>600</sub> of 0.1 in fresh BB media and used as the working culture. Metal salts to be tested were diluted from 0.5 M aqueous stock solutions into BB media to 20 mM working solutions and serially diluted from right to left along the rows of a clear, flat-bottomed, 96-well plate. Aliquots of 100 µL of the working culture were added to the inner wells of the 96-well plate to a final OD<sub>600</sub> of 0.05 and final volume of 200 µL. Aliquots of 100 µL of fresh BB media were added to the wells of the top and bottom rows to achieve a final volume of 200 µL. The top and bottom rows of the plate serve as metal dilution controls to allow for background subtraction of colored metal solutions (i.e., copper, cobalt, nickel, etc.). The right and left columns of the plate contained only 200 µL media and served as sterility controls for the assay. Bacterial growth was evaluated via OD<sub>600</sub> using

a Tecan plate reader set at 30 °C, over a 72-hour period with readings taken every 10 minutes with constant double orbital shaking (1.5 mm). OD<sub>600</sub> values were normalized to the positive growth control and adjusted for both background signal and metal signals using either the values from the right and left columns or the top and bottom rows, respectively. Data presented are representative of biological triplicates with error calculated as standard deviation represented by error bars in the figures.

#### 4.4.4 Metal Detoxification Assays

A single colony of *M. atlanticus* was used to inoculate 30 mL of BB medium in a 50 mL centrifuge tube prior to incubation at 30 °C in an angled rack (~45 °), 225 rpm for 18-24 h. This was completed two additional times for a total of three biological replicates. For each metal of interest (Cr, Cd, Co, Cu, Ni, Mn, Mo, W, V, and Zn), a high (A) and a low (B) concentration were selected based off the results of the metal tolerance assays (**Figure 14 and Figure 15**) Each concentration was prepared in a 50 mL centrifuge tube by diluting the aqueous metal stocks (Section 4.4.3.1) into 30 mL of BB medium. Initial metal concentrations were recorded by removing 1 mL aliquots from each tube which were subsequently labeled X.Y.Z.T where X represents the metals being tested (Cr, Cd, Co, Cu, Ni, Mn, Mo, W, V, or Zn), Y represents the metal concentration (either A or B), Z indicates the biological replicate (1-3), and T indicates the timepoint number. To measure basal metal content, 1 mL aliquots of each overnight culture was taken immediately prior to inoculating the full sample set.

Each batch, meaning one biological replicate of all ten metals of both metal concentrations, was inoculated with 1.3 mL of liquid culture (final OD<sub>600</sub> of ~0.05). Due to the large number of samples (63 total), inoculation and sampling were completed in batches and in the same order each time to reduce discrepancies in sample timing. Samples were taken at 6, 18, 24, 48, and 72 h to capture the entire growth cycle.

Samples collected for ICP-OES were collected as follows: 1.5 mL aliquots were taken from each respective tubes at the previously indicated timepoints and stored in 2 mL snap-cap tubes which were labeled as previously described. These samples were centrifuged at 6000 rpm for five minutes, both the supernatant and the cell pellet were collected. Further sample treatment is detailed below in Section 4.4.5.2.

## **4.4.5 Inductively Coupled Plasma Optical Emission Spectroscopy (ICP-OES)**

### **4.4.5.1 Sample Preparation**

Samples for ICP-OES were made gravimetrically in acid-rinsed (3% HNO<sub>3</sub> in double-distilled 18.2 MΩ water, ddH<sub>2</sub>O), labeled, 15 mL centrifuge tubes with masses recorded. Collected supernatants were passed through a 0.22 μm filter to remove any solid particulates. Filtered samples were aliquoted into the pre-weighed tubes and diluted to 10 mL in 3% HNO<sub>3</sub> with masses recorded before and after dilution.

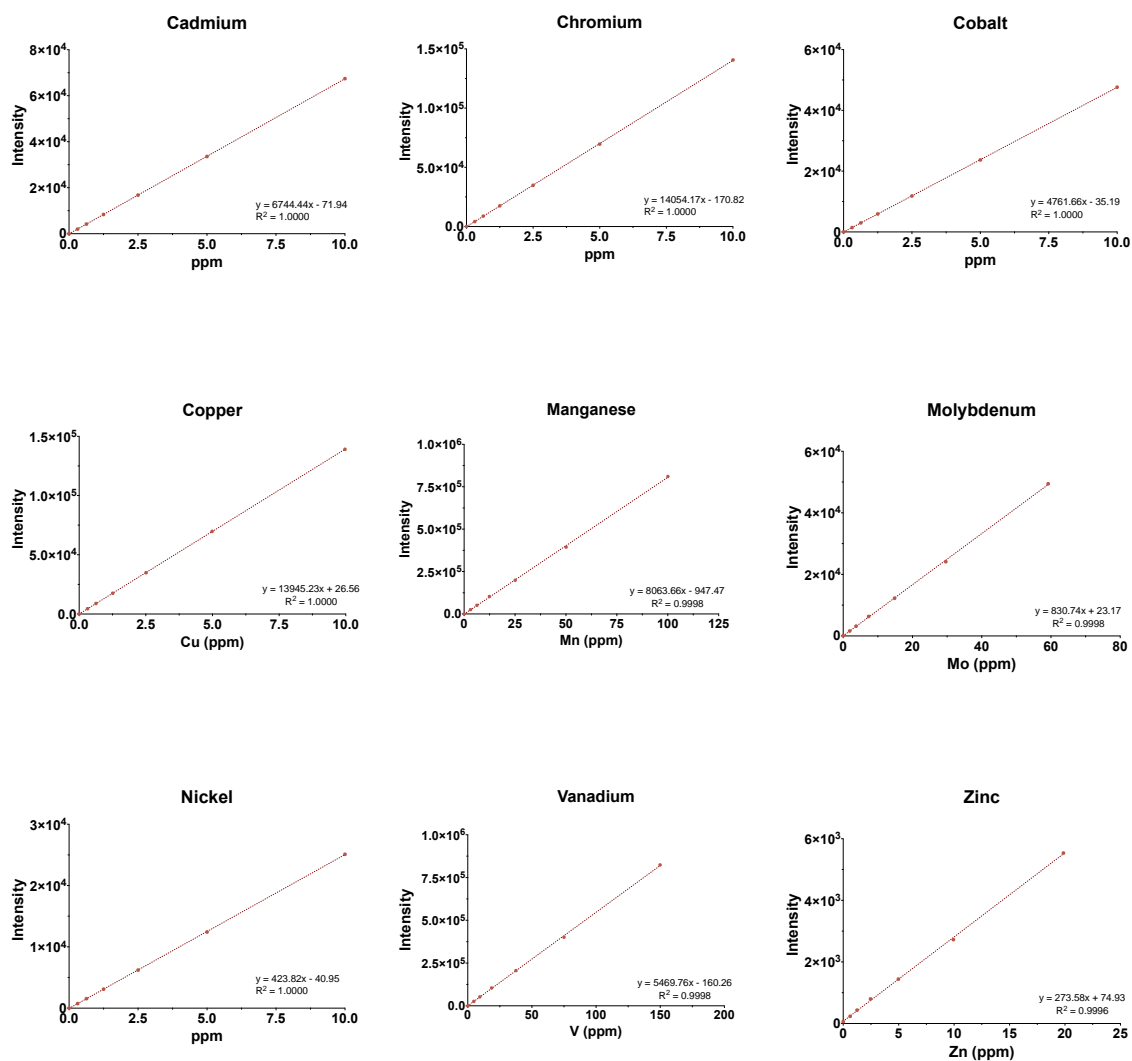
### **4.4.5.2 Calibration Curves and Analysis Parameters**

Multi-metal calibration curves were designed to have the highest metal concentration at least one serial dilution above the highest sampled concentration and

one serial dilution below the lowest sampled concentration. Calibration curves were prepared gravimetrically in 3% HNO<sub>3</sub> in ddH<sub>2</sub>O metal standards purchased from Inorganic Ventures. Initial metal concentrations were made at 2x the highest desired concentration in 50 mL volumetric flasks with 3% HNO<sub>3</sub> and serially diluted to create a 6-point standard curve. Samples were processed in batches and calibration curves were prepared immediately prior to analysis in the same matrix.

Elemental analysis was performed on an Agilent 5800 ICP-OES system. Instrument calibration occurred initially and after each single-metal sample set (36 samples). For each metal of interest, multiple wavelengths were selected to ensure adequate signal resolution and the wavelength with the highest linearity and lowest error in the calibration curve was chosen for data analysis (Cd = 227 nm, Cr = 268 nm, Co = 236 nm, Cu = 324 nm,, Ni = 216 nm, Mn = 261 nm, Mo= 205 nm, V= 292 nm, Zn= 335 nm). Each sample was measured in triplicate with the average intensity reported by the instrument. Raw intensities were converted to concentration (in ppm) using the line-of-best-fit generated from the prepared calibration curves.

## 4.5 Supplemental Materials



Supplemental Figure 2: Calibration curves generated from prepared metal stocks used in the *M. atlanticus* metal detoxification assay. The line of best fit for each metal ion was used to convert raw intensities to ppm.

## **5. Investigating metal modulation on the antimicrobial activity of Clavanin A and Clavanin C to describe the role of biometals in primitive innate immunity**

### ***5.1 Introduction***

Tunicates are filter-feeding marine invertebrates that are solely reliant on innate immunity for defense against pathogens present within their environment.<sup>64</sup> As the closest living relatives of vertebrates, tunicates hold an optimal evolutionary position for the investigation of the role of innate immunity.<sup>66, 158</sup> Belonging to the same phylum as humans, tunicates can serve as primitive models for studying innate immunological mechanisms.<sup>69, 159</sup> A defining difference between vertebrate and invertebrate organisms is the presence of the adaptive immune response. Invertebrate organisms lack specific, anticipatory long-term immunological memory and somatic recombination; the ability to produce and develop pathogen-specific antigens.<sup>62-68, 159</sup> Apart from this, there are multiple similarities between vertebrate and invertebrate immune systems, such as the presence of phagocytotic cells, production of antimicrobial peptides (AMPs), signaling receptors that modulate immune responses, and pattern-recognition receptors.<sup>63-68, 159, 160</sup> AMPs play two critical roles in innate immunity, as direct, broad-spectrum antimicrobial agents and as effector molecules to trigger immune responses.<sup>161-164 161-164</sup>

The clavanin family of AMPs was discovered in the hemocytes, cells analogous to the red and white blood cells found in vertebrates, of the tunicate *Styela clava*.<sup>165, 166</sup> This family is composed of alpha-helical AMPs with sequences rich in histidine,

phenylalanine and valine.<sup>165</sup> The original five peptides have approximately 80% sequence homology and the sixth member, discovered through the prepropeptide region of the genome, has approximately 50% homology (sequences listed in **Table 5**).<sup>165, 167, 168</sup> Clavanin A (clavA) is the most well studied member of the clavanin family,<sup>165, 168-171</sup> though recent literature has begun exploring the other peptides.<sup>172</sup> Like most other AMPs, the clavanin peptides are cationic and amphipathic in nature to facilitate membrane interactions. The sequences contain an abundance of aliphatic residues, such as glycine and phenylalanine, which are pivotal in facilitating membrane interactions, which is a common mechanism of action for AMPs.<sup>165, 167, 168, 170, 173-175</sup>

**Table 5: Sequences of Clavanin Antimicrobial Peptides**

Peptide	Sequence
Clavanin A <sup>165</sup>	VFQFLGKIIHHVGNFVHGFSHVF
Clavanin B <sup>165</sup>	VFQFLGRIIHHVGNFVHGFSHVF
Clavanin C <sup>165</sup>	VFHLLGKIIHHVGNFV $\hat{Y}$ GFSHV <sup>a</sup>
Clavanin D <sup>165</sup>	AFHLLGKIIHHVGNFV $\hat{Y}$ GFSHV <sup>a</sup>
Clavanin E <sup>167</sup>	LFKLLGKIIHHVGNFVHGFSHVF
Clvaspirin <sup>168</sup>	FLRFIGSVIHGIGHLVHHIGVAL

<sup>a</sup>  $\hat{Y}$  – post translationally modified tyrosine residue.

ClavA has been shown to utilize distinctly different mechanisms of action that are entirely dependent on pH.<sup>169-172</sup> Given the proportion of histidine residues in the sequence; the pH-dependent mechanism of action is not surprising. Under neutral conditions (pH 7.4), it was found that clavA induces non-specific membrane damage

which likely induces the leakage of cellular contents and the loss of the proton motive force.<sup>169, 171</sup> In an acidic environment (pH 5.5), clavA has been shown to interact with an unknown membrane embedded ion-channel to inflict damage on pathogenic cells.<sup>169-171</sup> ClavA has also been shown to have strong membrane interactions under acidic conditions which may facilitate translocation of the peptide into the cytoplasm to enable DNA binding and inhibition of DNA synthesis.<sup>169</sup> Interestingly, the antimicrobial effects of ClavA are improved against *E. coli* MG1655 when supplemental Zn<sup>2+</sup> ions are present which is attributed to the presence of a putative Zn binding motif in the sequence.

Putative metal binding sites within peptide sequences have garnered attention as more antimicrobial peptides with metal-regulated activities have been investigated. Histatin-5, a human salivary peptide, has potent candidacidal activity against *C. albicans* that is modulated upon addition of copper or zinc.<sup>94, 176, 177</sup> Piscidin 1, an AMP isolated from teleosts, has enhanced bactericidal effects in the presence of copper.<sup>178</sup> These metal induced effects have been attributed to metal interactions with specific amino acid sequences such as the amino-terminal Cu(II) Ni(II) (ATCUN) motif,<sup>90, 91, 179</sup> the HX<sub>3</sub>H site involved in Zn(II) binding,<sup>180, 181</sup> and the *bis*-His site commonly associated with Cu(I) binding.<sup>93, 182</sup> The peptides in the Clavanin family possess these metal binding sites, while the presence of these motifs does not confirm that metal ions will enhance or impede peptide activity the potential is worth investigation. Understanding the

interplay between metal ions, particularly those of biological importance like Cu and Zn, and antimicrobial peptides may allow for fine-tuning of peptide-based therapeutics.

This study aims to continue the investigation of the Clavanin family of AMPs by expanding our knowledge of potential metal-modulated antimicrobial activity of both ClavA and ClavC against fungal strains *Candida albicans* (*C. albicans*) strain SC5314 and *Cryptococcus neoformans* (*C. neoformans*) H99 and against *Escherichia coli* (*E. coli*) strain BW25113 which is the parent strain for the Keio library. Broth microdilution techniques were employed to challenge the growth of these microbes against independent peptide (ClavA or ClavC) and against peptide-metal combinations where Cu and Zn were the metal ions of interest. In accordance with previous literature, ClavC exhibited more potent antimicrobial activity than ClavA against *Escherichia coli*. We also observed increased activity for both peptides under acidic conditions. Conversely, we did not observe the significant metal-dependent increases in peptide antibacterial activity that have previously been reported.<sup>169</sup>

## ***5.2 Results and Discussion***

### ***5.2.1 Antifungal Activity of Clavanin A and Clavanin C against *Candida albicans*.***

Normally, *Candida albicans* is a commensal fungal organism that inhabits the mucosal surfaces of the gastrointestinal and genitourinary tracts in most humans.<sup>183-185</sup> *C. albicans* is not problematic in healthy individuals as it is a key member of a

'normal' gut microbiota. However, under certain conditions, *C. albicans* can transition into a pathogenic state and, in this form, is the primary cause of invasive candidiasis and blood stream infections.<sup>184, 186</sup> *Candida* species in general are leading causes of nosocomial infections and drug resistant strains have earned an "urgent threat" label by the Centers for Disease Control and Prevention (CDC).<sup>184, 187</sup> The continued emergence of drug resistant strains coupled with limited therapeutic options for aggressive fungal infections highlights the need for continued investigation into antifungal treatment methods.

The vast majority of literature regarding Clavanin peptides revolves around their antibacterial activity despite early reports of their broad-spectrum abilities.<sup>165-167, 169-173, 188</sup> In efforts to expand our understanding of these peptides in different systems, two-dimensional broth microdilution assays were used to assess the activity of ClavA and ClavC against the fungal species *Candida albicans* while also testing the impact of metal supplementation. ClavA exhibited a minimum inhibitory condition (MIC) of 50  $\mu$ M under neutral conditions and 25  $\mu$ M under acidic conditions. The antifungal activity of ClavA in the literature is incredibly limited with very little overlap between results from different groups. The MIC obtained here for ClavA under neutral conditions is in accordance with previous literature,<sup>170, 188</sup> however there is deviation when it comes to the behavior of ClavA in low pH environments. An early report indicated that ClavA had potent antifungal activity (MIC < 4  $\mu$ M) only at pH 5.5.<sup>170</sup> Here, an increase in

activity is observed, but the impact of pH is not as drastic. This discrepancy may potentially be due to different fungal strains as the strain used in the original paper is not defined. Alternatively, differences in activity may be due to experimental design. Original literature utilized radial diffusion assays to determine the MIC while microdilutions were employed here, while both methods are acceptable there are likely differences in the fungal burden experienced by ClavA upon initial exposure.

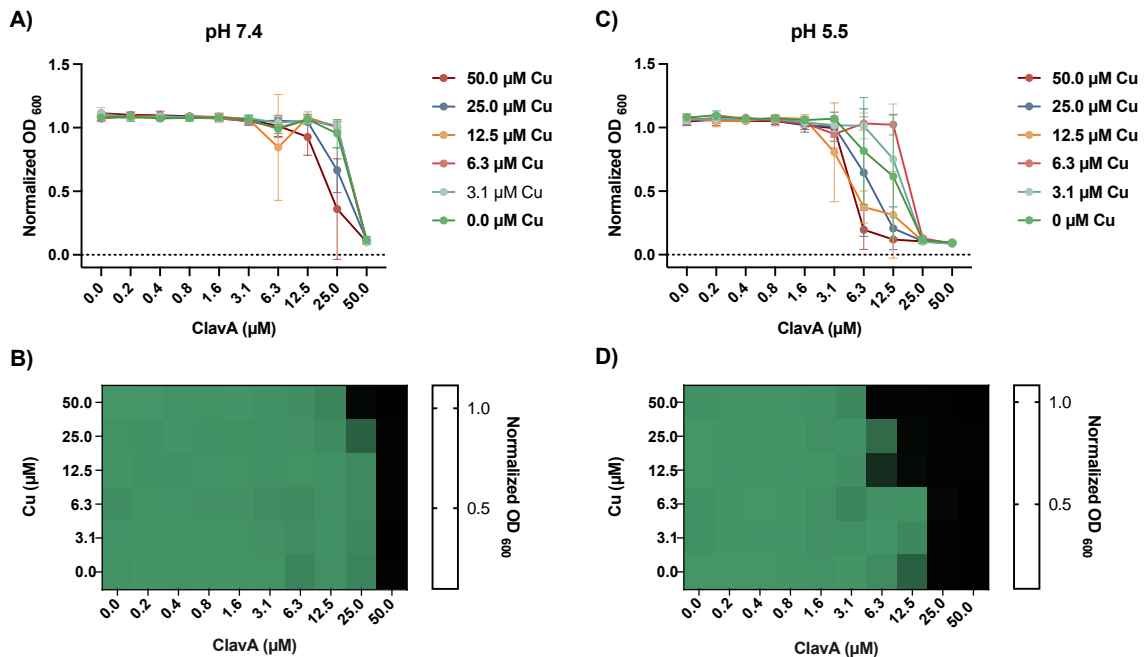


**Figure 17: Antifungal activity of ClavA with Cu<sup>2+</sup> Supplementation Against *C. albicans*.** Fungal cells were preincubated in either PPB at pH 7.4 (A and B) or MES buffer at pH 5.5 (C and D) for 90 min at 37 °C with increasing concentrations of ClavA and Cu<sup>2+</sup>. Aliquots were resuspended in SD+ buffered with either Tris (pH 7.4) or MES (pH 5.5) and fungal growth was measured after incubation for 48 h at 30 °C. Data reported represent the average of three biological replicates. Error was calculated as standard deviation and represented by error bars in A and C.

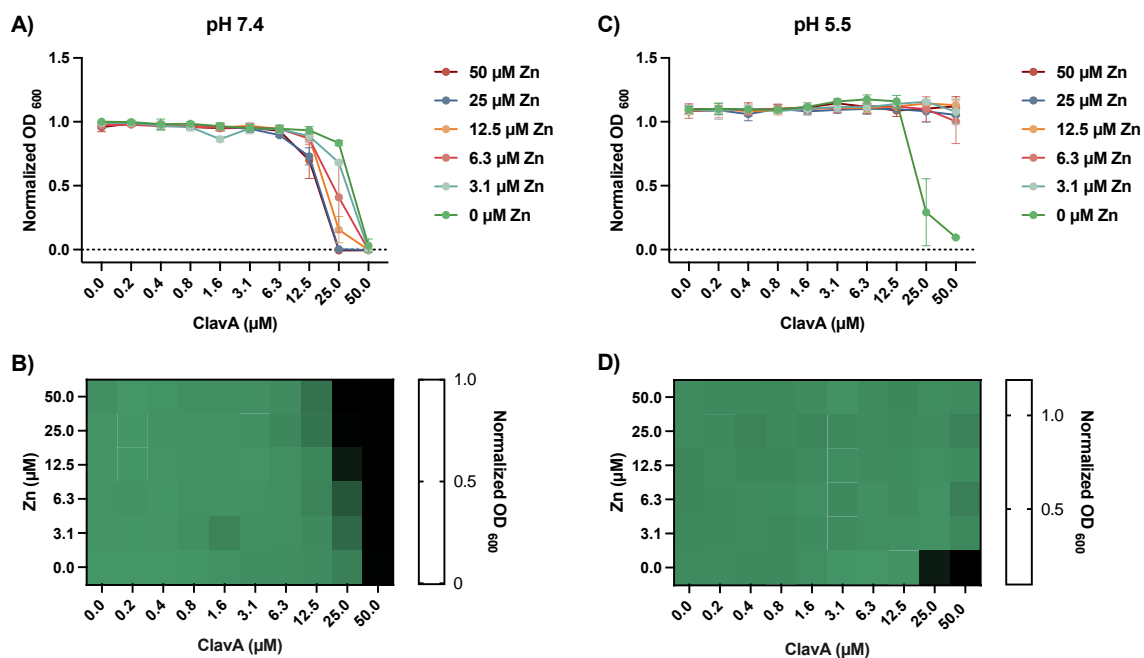


**Figure 18: Antifungal activity of ClavA with Zn<sup>2+</sup> Supplementation Against *C. albicans*.** Fungal cells were preincubated in either PPB at pH 7.4 (A and B) or MES buffer at pH 5.5 (C and D) for 90 min at 37 °C with increasing concentrations of ClavA and Zn<sup>2+</sup>. Aliquots were resuspended in SD+ buffered with either Tris (pH 7.4) or MES (pH 5.5) and fungal growth was measured after incubation for 48 h at 30 °C. Data reported represent the average of three biological replicates. Error was calculated as standard deviation and represented by error bars in A and C.

When co-treated with Cu<sup>2+</sup>, ClavA exhibits no significant increase in activity under neutral conditions and a minor increase in activity (MIC = 6.3 μM) upon an addition of 50 μM Cu<sup>2+</sup> (Figure 17). The combination of ClavA and Zn<sup>2+</sup> induced a 2-fold decrease in a not induce significant improvements in observed MIC under neutral conditions and, at pH 5.5, the addition of supplemental Zn<sup>2+</sup> appeared to inhibit all peptide activity (Figure 18). Of the limited literature regarding the antifungal activity of ClavA, only one instance includes the effect of metal supplementation on peptide

performance. However, the peptide sequences used previously have been modified to remove the C-terminal amide thus presenting a free carboxylate group which could increase Zn-binding potential. That study reported that Cu supplementation had no impact on ClavA, but indicated a Zn mediated 2-fold increase in ClavA activity against *C. albicans* under neutral conditions.<sup>172</sup>

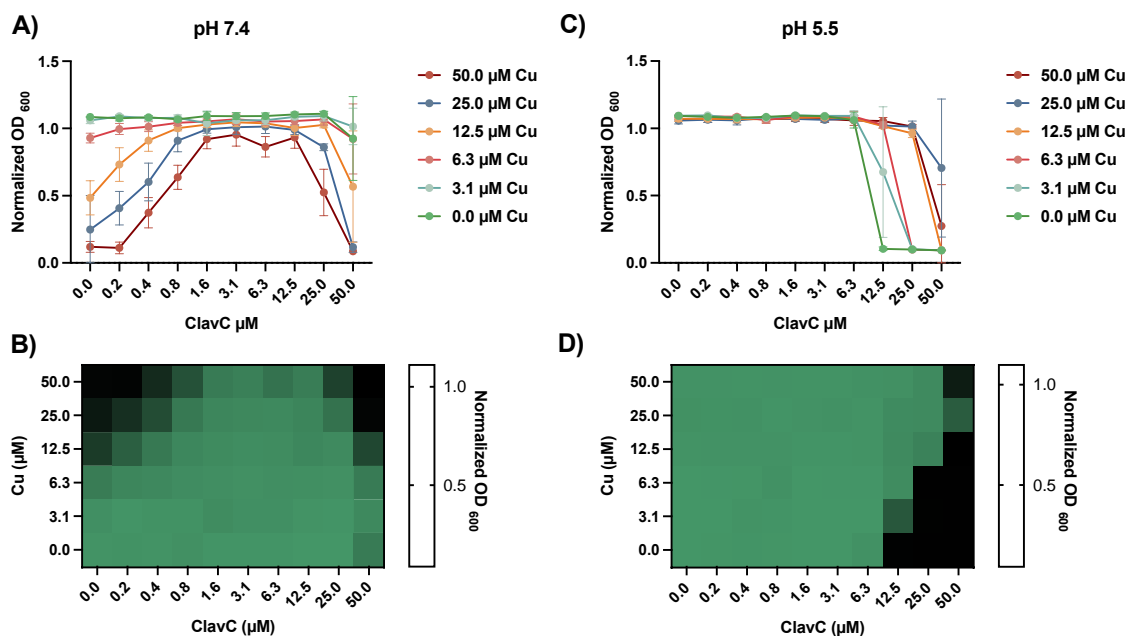


**Figure 19: Antifungal activity of ClavC with Cu<sup>2+</sup> Supplementation Against *C. albicans*.** Fungal cells were preincubated in either PPB at pH 7.4 (A and B) or MES buffer at pH 5.5 (C and D) for 90 min at 37 °C with increasing concentrations of ClavC and Cu<sup>2+</sup>. Aliquots were resuspended in SD+ buffered with either Tris (pH 7.4) or MES (pH 5.5) and fungal growth was measured after incubation for 48 h at 30 °C. Data reported represent the average of three biological replicates. Error was calculated as standard deviation and represented by error bars in A and C.

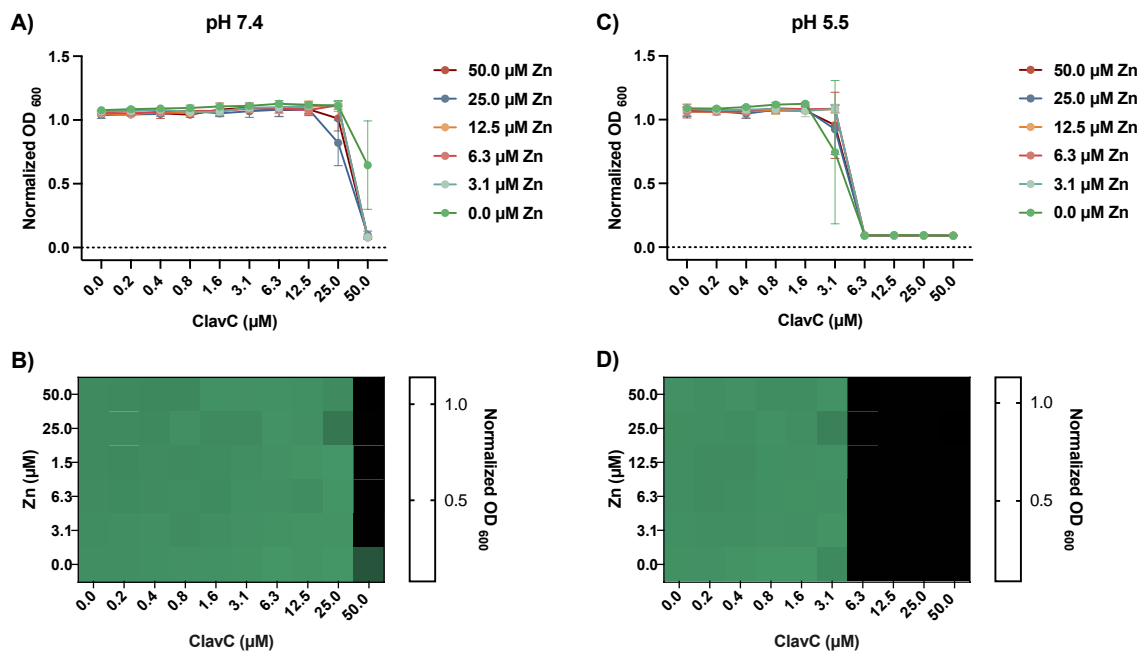


**Figure 20: Antifungal activity of ClavC with Zn<sup>2+</sup> Supplementation Against *C. albicans*.** Fungal cells were preincubated in either PPB at pH 7.4 (A and B) or MES buffer at pH 5.5 (C and D) for 90 min at 37 °C with increasing concentrations of ClavC and Zn<sup>2+</sup>. Aliquots were resuspended in SD+ buffered with either Tris (pH 7.4) or MES (pH 5.5) and fungal growth was measured after incubation for 48 h at 30 °C. Data reported represent the average of three biological replicates. Error was calculated as standard deviation and represented by error bars in A and C.

Treatment of *C. albicans* cells with ClavC indicated an antifungal MIC of > 50 μM in a neutral environment and 12.5 μM under acidic conditions. Literature revolving around ClavC is limited, early reports simply indicate that ClavC is approximately 3 to 5 times more effective than ClavA against *C. albicans* at a pH of 6.5.<sup>165</sup> A more recent report with modified peptide sequences, which are discussed above, indicates that ClavC has modest activity with an MIC of 25 μM at pH 7.4. In the same study, cotreatment of ClavC with Zn increased peptide efficacy with a new MIC of approximately 6.3 μM. The

increase in activity upon Zn addition is most likely due to enhanced Zn affinity resulting from the removal of the C-terminal amide. The study also reports no Cu induced changes in ClavC activity which is mildly surprising given the presence of the ATCUN motive which is known to bind Cu.<sup>90, 179</sup> Here, supplementation with Cu<sup>2+</sup> did not have a significant impact on peptide activity under neutral conditions and Cu<sup>2+</sup> addition in acidic media decreased the efficacy of the peptide (**Figure 19**). Cotreatment of ClavC and supplemental Zn<sup>2+</sup> appeared to have no significant impact on peptide activity (**Figure 20**).

### **5.2.2 Clavanin A and Clavanin C Retain Candidacidal Activity in the Absence of Cu and Zn.**

The lack of metal-modulated antifungal activity of ClavA and ClavC was surprising given the literature precedent, especially between ClavA and Zn.<sup>165, 169, 170</sup> We hypothesized that perhaps the synthetic defined media in use contained sufficient levels of metal ions so that the metal content in the untreated peptide control was enough to induce changes in peptide activity. To investigate this possibility, one-dimensional microdilutions were prepared in metal drop-out media. In **Figure 21** both ClavA and ClavC were tested against *C. albicans* in either complete synthetic defined media (SD+), synthetic defined media with Cu dropped out (SD-Cu), or synthetic defined media with Zn dropped out (SD-Zn).

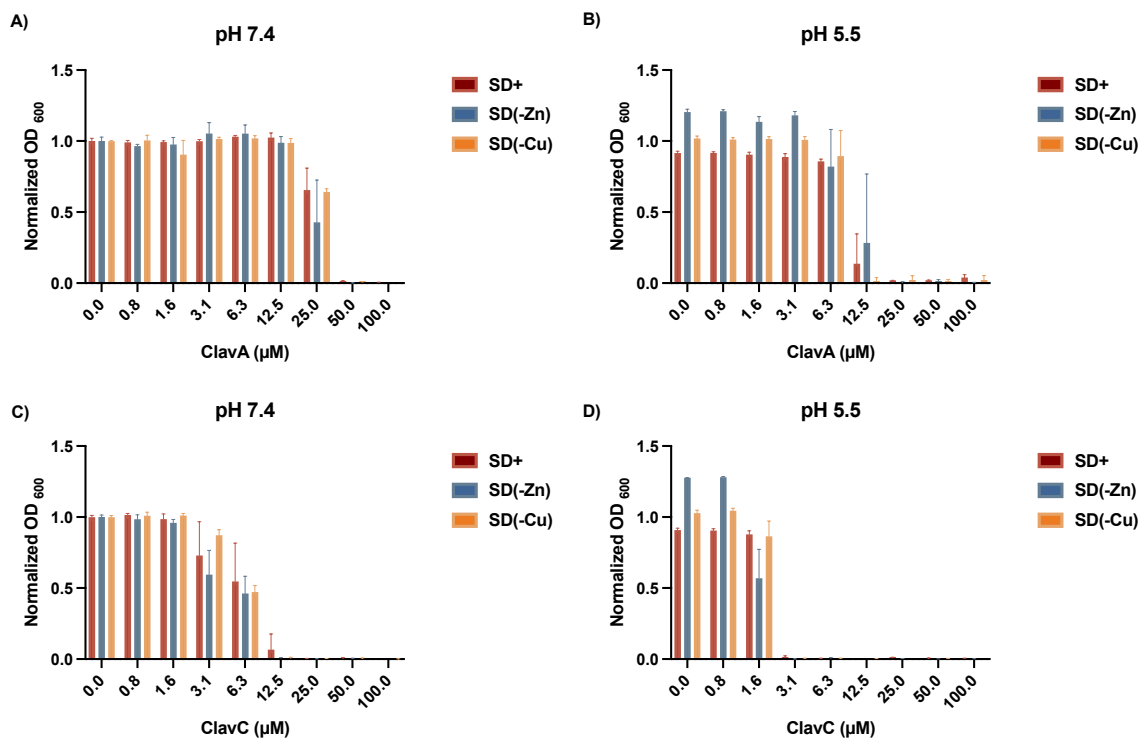


**Figure 21: Candidacidal Activity of Clavanin A and Clavanin C under Metal Complete, Zinc Deplete, and Copper Deplete Conditions.** The activity of ClavA (top) and ClavC (bottom) against *C. albicans* in complete SD+ (red), SD-Zn (blue), and SD-Cu (yellow) media to evaluate potential requirements for labile metals in solution. Fungal cells were preincubated in either PPB at pH 7.4 (A and C) or MES at pH 5.5 (B and D) for 90 min at 37 °C with increasing concentrations of either ClavA or ClavC. Aliquots were resuspended in respective media and incubated for 48 h at 30 °C. Data are representative of the average of three biological replicates. Error was calculated as standard deviation and is represented by the error bars above.

Both ClavA and ClavC retain their antifungal activity against *C. albicans* regardless of bioavailable Cu or Zn. These results suggest that ClavA and ClavC use mechanisms of action against *C. albicans* that is not dependent on metal availability and is not influenced by metal ions present in the concentration ranges assayed here. ClavA and ClavC are alpha-helical peptides whose secondary structures demonstrate spatial

segregation of hydrophobic and charged residues. These structural characteristics, which are known to aid in facilitating membrane interactions,<sup>102, 163, 171, 175, 189</sup> and the data presented here suggest that these AMPs may be utilizing mechanisms of action that involve interactions with the cell-surface under these conditions. There are multiple known models that have been defined to explain how AMPs may interact and damage the target cell surface. Models such as the barrel-stave or toroidal pore involve the aggregation of AMPs which accumulate on the cell surface and insert to disrupt the surface integrity which subsequently impacts electrochemical balances and, depending on size, cause the loss of cellular contents.<sup>189</sup> Other models suggest interactions between peptides and components of the cell wall will result in deleterious effects. An example of this is the interaction between the salivary peptide histatin 5 (Hist-5) which interacts with beta-glucan and with heat shock proteins to exert antifungal activity.<sup>176, 177</sup> To draw a better conclusion regarding the mechanisms in use by both ClavA and ClavC against *C. albicans* will require further investigation into the specific type of surface interactions involved.

### **5.2.3 Antifungal Activity of Clavanin A Against *Cryptococcus neoformans* H99 is Potentiated under Acidic Conditions**

As of 2023, *Cryptococcus neoformans* is placed at the top of the critical priority group of fungal pathogens.<sup>190, 191</sup> This opportunistic pathogen originated as an environmental pathogen and now has a global distribution with mortality rates of up to 61%.<sup>192</sup> *C. neoformans* is one of the major species responsible for causing life-threatening

cryptococcal meningitis, while these infections are usually connected to immunocompromised patients, reports of infections in immunocompetent individuals are emerging.<sup>191, 192</sup> Treatment for *C. neoformans* infections face challenges similar to those previously discussed for *C. albicans* as antifungal resistant strains are becoming increasingly prevalent and treatment options are generally limited.<sup>186, 187, 190, 191</sup> Clavanin peptides are reported to have broad-spectrum activity, but have not yet been tested against *C. neoformans*.

To evaluate potential activity against *C. neoformans* two-dimensional broth microdilutions were used to not only test the activity of ClavA independently, but also with metal supplementation. Though ClavA activity was not dependent on Cu or Zn availability against *C. albicans*, the peptide may utilize a different mechanism of action or have different requirements for base function against a different fungal species. Against *C. neoformans*, ClavA exhibited poor activity under neutral conditions (MIC > 50  $\mu$ M), however under acidic conditions activity greatly improved (MIC = 3.1  $\mu$ M).

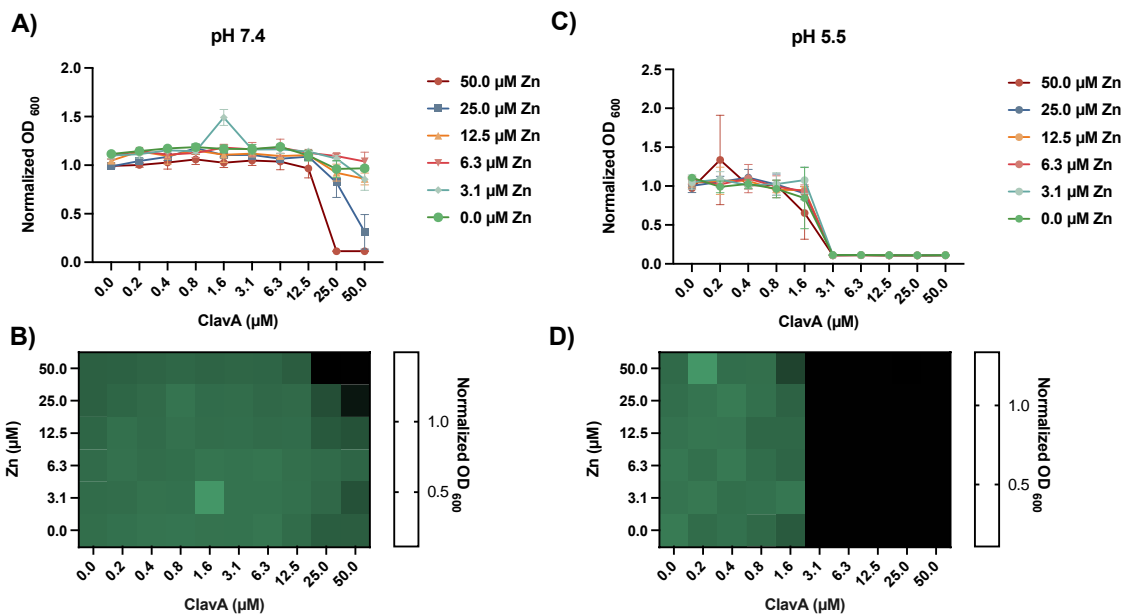


**Figure 22: Antifungal Activity of ClavA against *C. neoformans* is Impacted by Zn<sup>2+</sup> Supplementation.** Fungal cells were pre-incubated in either PPB at pH 7.4 (A and B) or MES at pH 5.5 (A and B) for 90 min at 37 °C with increasing concentrations of ClavA and Zn<sup>2+</sup>. Aliquots were resuspended in SD+ buffered with either Tris (pH 7.4) or MES (pH 5.5) and fungal growth was measured after incubation for 48 h at 30 °C. Data are representative of the average of three biological replicates. Error was calculated as standard deviation and is represented by the error bars above.

When cotreated with high concentrations (>12.5 μM) Zn, ClavA activity against *C. neoformans* increases slightly with a new inhibitory concentration of 25 μM in the presence of 50 μM supplemental Zn (**Figure 22**). Interestingly, treatment of both ClavA and Cu exhibited increased antifungal activity in both neutral and acidic environments (**Figure 23**). High concentrations of Cu in culture media appear to have substantial antifungal effects against *C. neoformans* as can be seen in the zero-peptide condition where 6.3 μM and 25 μM Cu inhibits fungal growth at neutral pH and acidic pH, respectively.

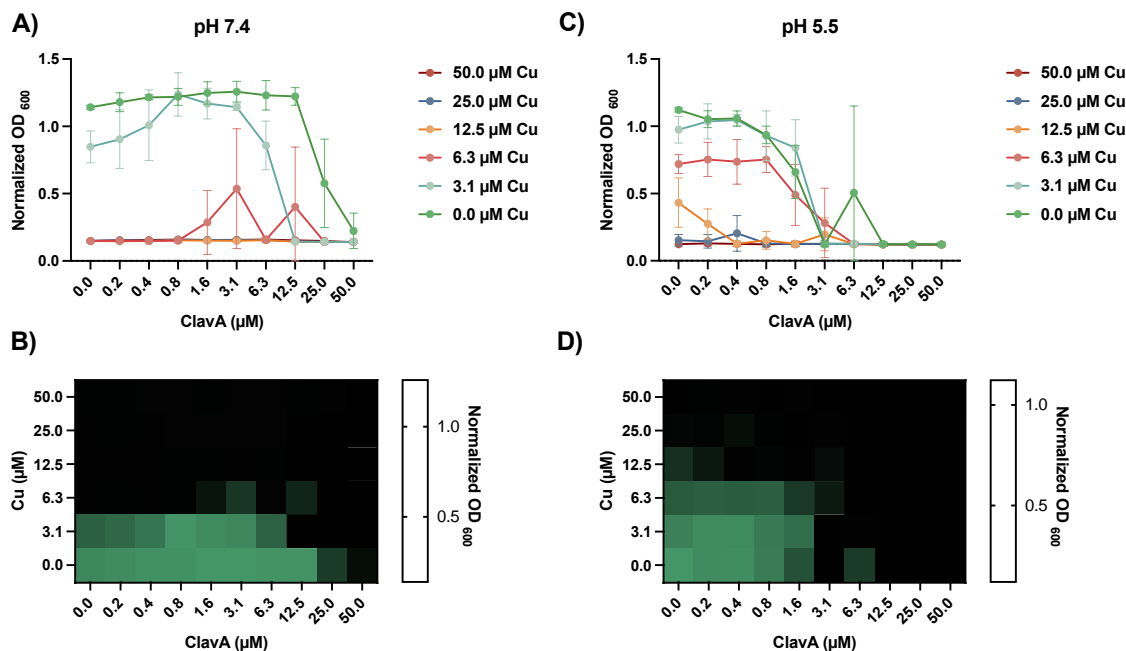


**Figure 23: Antifungal Activity of ClavA against *C. neoformans* is Increased by Cu<sup>2+</sup> Supplementation.** Fungal cells were pre-incubated in either PPB at pH 7.4 (A and B) or MES at pH 5.5 (A and B) for 90 min at 37 °C with increasing concentrations of ClavA and Cu<sup>2+</sup>. Aliquots were resuspended in SD+ buffered with either Tris (pH 7.4) or MES (pH 5.5) and fungal growth was measured after incubation for 48 h at 30 °C. Data are representative of the average of three biological replicates. Error was calculated as standard deviation and is represented by the error bars above.

### 5.2.4 Antibacterial Activity of Clavanin and Clavanin C Against *Escherichia coli* strain BW25113

*Escherichia coli* is commonly used in bacterial investigations as it is incredibly well studied and understood. The *E. coli* strain BW25113 is the parent strain for the Keio collection which is a library of gene knockout strains provided by the National Institute of Genetics, Mishima, Shizuoka, Japan that are single-gene deletion mutants for all non-essential *E. coli* K-12 genes.<sup>193, 194</sup> This strain was chosen for these initial investigations to allow for future antibacterial assays which may utilize the

various knockout strains to dig deeper into metal dependence, membrane interactions, and other relevant phenomena.

Two-dimensional broth microdilution “checkerboard” assays were performed to gain a comprehensive understanding of the effect of supplemental  $\text{Cu}^{2+}$  or  $\text{Zn}^{2+}$  on the antibacterial activity of ClavA under neutral and acidic conditions and of ClavC under acidic conditions. In all assays, bacterial cells suspended in either PPB (pH 7.4) or MES buffer (pH 5.5) were exposed to varying concentrations of either ClavA or ClavC and  $\text{Cu}^{2+}$  or  $\text{Zn}^{2+}$ . Preincubation protocols were implemented to ensure that cells were exposed to a combination treatment of peptide and supplemental metal ion.

Under neutral conditions, ClavA exhibits increased antibacterial activity in the presence of  $\text{Cu}^{2+}$  (**Figure 24A-B**) and in the presence of  $\text{Zn}^{2+}$  (**Figure 24C-D**). ClavA alone exhibited modest antibacterial activity against *E. coli* cells with a MIC value of 50  $\mu\text{M}$ . Supplementation with 25  $\mu\text{M}$   $\text{Cu}^{2+}$  greatly increased the antibacterial activity with 6.3  $\mu\text{M}$  peptide required. We note that the top concentration of supplemental copper added, 50  $\mu\text{M}$ , may exhibit its own antibacterial effects under these conditions which can be seen clearly by the substantial decrease in cell growth in **Figure 24A**. The antibacterial activity of ClavA also increases with an addition of 3.1  $\mu\text{M}$   $\text{Zn}^{2+}$ . While the Zn-induced activity is not as drastic as presented in recent studies,<sup>165, 169, 170</sup> our results are in support of the claims that ClavA exhibits increased antibacterial in the presence of Zn. These differences in the degree of peptide efficacy could simply be due to differences between

*E. coli* strains as *E. coli* B25113 is related to, but not identical to *E. coli* K-12 used in previous literature.

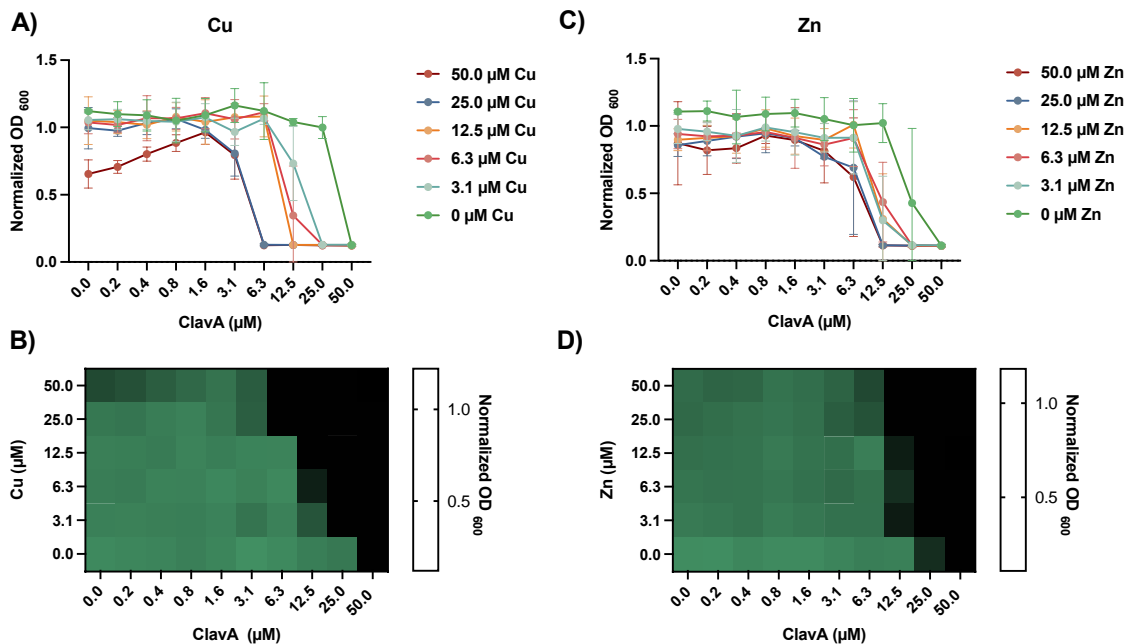


**Figure 24: Antibacterial Activity of Clavanin A with Supplemental Cu<sup>2+</sup> or Zn<sup>2+</sup> against *Escherichia coli* strain BW25113.** *E. coli* cells were pre-incubated in PPB at pH 7.4 for 90 min at 37 °C with increasing concentrations of supplemental Cu<sup>2+</sup> (A and B) or Zn<sup>2+</sup> (C and D). Aliquots were resuspended in fresh buffered MHB and bacterial growth was measured after incubation for 20 h at 37 °C. Data represent the average of three biological replicates. Error was calculated as standard deviation and is represented by error bars in the figure (A and C).

When *E. coli* cells were exposed to ClavA under acidic conditions (pH 5.5), treatments of peptide alone expressed moderate antibacterial activity (**Figure 14**). These results agree with existing literature indicating that ClavA has enhanced activity in more acidic environments.<sup>169-171</sup> Interestingly, at this pH supplementation with either Cu<sup>2+</sup> or Zn<sup>2+</sup> had no impact on peptide activity. Under these conditions, the charge of the peptide increases which may induce a conformation that is not conducive to metal

interactions. Additionally, the histidine residues typically implicated in facilitating peptide-metal interactions are protonated under these conditions.

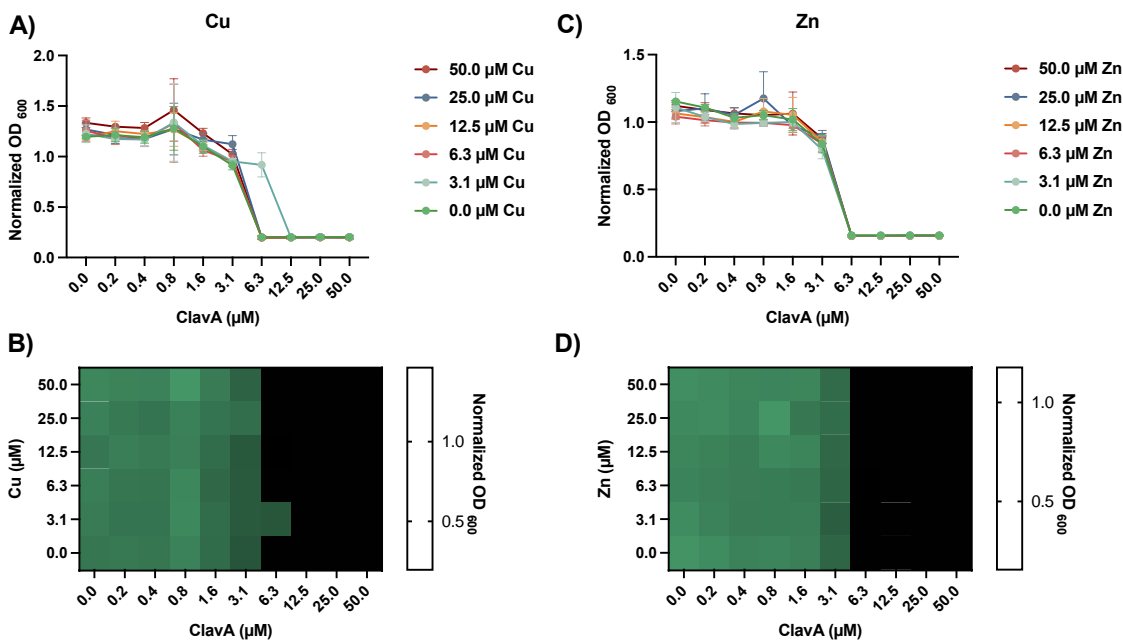


**Figure 25: Antibacterial Activity of Clavanin A with Supplemental  $\text{Cu}^{2+}$  or  $\text{Zn}^{2+}$  against *Escherichia coli* strain BW25113.** *E. coli* cells were pre-incubated in MES at pH 5.5 for 90 min at 37 °C with increasing concentrations of supplemental  $\text{Cu}^{2+}$  (A and B) or  $\text{Zn}^{2+}$  (C and D). Aliquots were resuspended in fresh buffered MHB and bacterial growth was measured after incubation for 20 h at 37 °C. Data represent the average of three biological replicates. Error was calculated as standard deviation and is represented by error bars in the figure (A and C).

ClavC exhibited an MIC value of 1.6  $\mu\text{M}$  against *E. coli* under acidic conditions (Figure 26). The activity of ClavC is not impacted by the supplemental concentrations of  $\text{Cu}^{2+}$  or  $\text{Zn}^{2+}$  tested. While the sequence of ClavC possesses putative binding sites for Cu and Zn, the protonation of the involved histidine residues under these conditions likely prevents and peptide-metal interactions. This result may suggest that, like ClavA, ClavC

may also have the ability to utilize more than one mechanism of action to attack pathogenic cells.

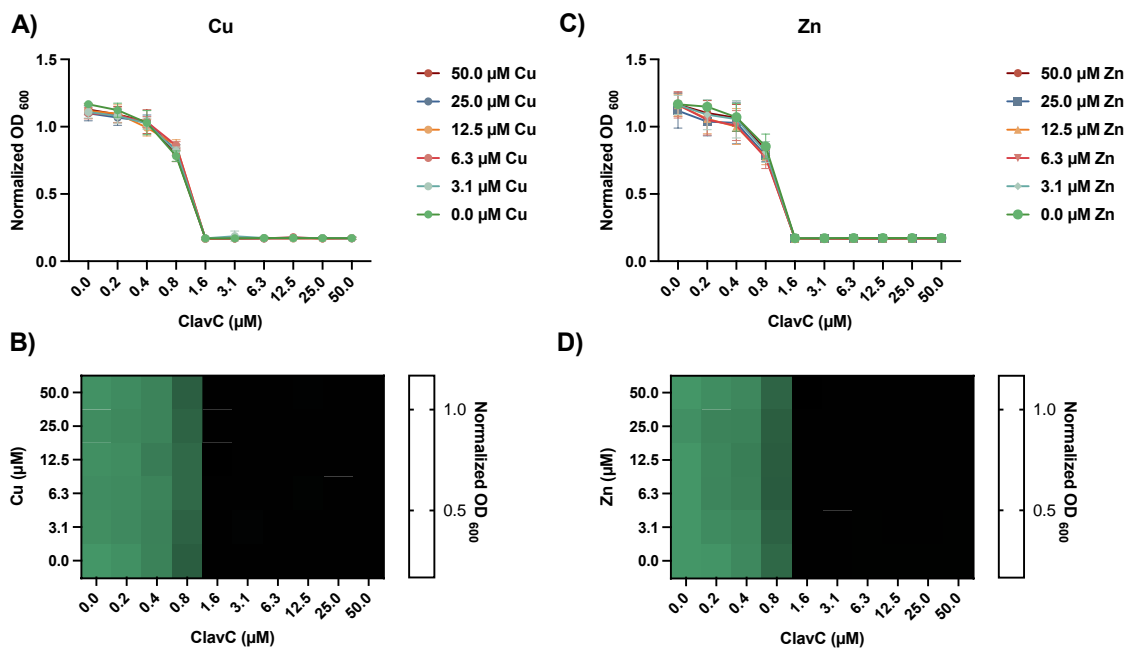


**Figure 26: Antibacterial Activity of Clavanin C with Supplemental Cu<sup>2+</sup> or Zn<sup>2+</sup> against *Escherichia coli* strain BW25113.** *E. coli* cells were pre-incubated in MES at pH 5.5 for 90 min at 37 °C with increasing concentrations of supplemental Cu<sup>2+</sup> (A and B) or Zn<sup>2+</sup> (C and D). Aliquots were resuspended in fresh buffered MHB and bacterial growth was measured after incubation for 20 h at 37 °C. Data represent the average of three biological replicates. Error was calculated as standard deviation and is represented by error bars in the figure (A and C).

### 5.3 Conclusions and Future Directions

In this section, we have successfully characterized the antifungal activity of ClavA against two opportunistic fungal pathogens *C. albicans* and *C. neoformans*. Against *C. albicans*, the MIC of ClavA was >50 µM for neutral conditions and 25 µM for acidic conditions. ClavA showed very little metal-induced changes in antifungal activity.

Additionally, the antifungal activity of ClavA is not dependent on the presence of labile Cu or Zn as activity was retained in the absence of these metals. Antifungal activity against *C. neoformans* under neutral conditions yielded and MIC > 50  $\mu\text{M}$  for ClavA, however under acidic conditions the antifungal activity was potentiated to yield an MIC of 6.3  $\mu\text{M}$ . Under neutral conditions, high levels of bioavailable Zn (>25  $\mu\text{M}$ ) induces a slight increase in peptide activity (MIC = 25  $\mu\text{M}$ ), but Zn supplementation has no effect under acidic conditions. Supplementation with  $\text{CuSO}_4$  yielded interesting effects, results suggest that copper concentrations above 12.5  $\mu\text{M}$  may inhibit fungal growth independent of peptide co-treatment. In a neutral environment, supplementation with 3.1  $\mu\text{M}$  Cu increased ClavA activity (MIC = 12.5  $\mu\text{M}$ ). In the presence of 3.1  $\mu\text{M}$  Cu at low pH, the activity of ClavA is slightly improved (MIC = 3.1  $\mu\text{M}$ ), when the concentration of Cu is increased to 12.5  $\mu\text{M}$ , ClavA is substantially increased (MIC = 0.2  $\mu\text{M}$ ). Antifungal characterization efforts were extended to ClavC against *C. albicans*. In the absence of additional metal supplementation ClavC exhibited an MIC of 50  $\mu\text{M}$  at pH 7.4 and 25  $\mu\text{M}$  at pH 5.5. Under neutral conditions, concentrations of Zn and Cu above 12.5  $\mu\text{M}$  were independently able to induce a 2-fold increase in ClavC activity. In acidic environments, supplementation with increasing amount of either Zn or Cu decreased peptide activity.

ClavA and ClavC were also tested for antibacterial activity against *E. coli* strain BW23115. The results presented here, to an extent, agree with previously published

literature. ClavC is more effective than ClavA as an antibacterial agent and the activity of both peptides is potentiated under acidic conditions. The antibacterial activity of ClavA is potentiated by both Cu and Zn under neutral conditions, but the effect of supplemental metal is nonexistent under acidic conditions. ClavC also demonstrated no metal-related activity under acidic conditions.

Overall, we present new antifungal activity for ClavA and ClavC and further build up upon the antibacterial characterization for both peptides. The body of work currently associated with this family of antimicrobial peptides is sparse and spans nearly 30 years. There are contradictory conclusions regarding how metals such as copper and zinc may impact peptide function.

## ***5.4 Methods***

### **5.4.1 Materials and General Methods**

Chemicals and solvents were obtained from commercial supplies and used as received unless otherwise noted.

### **5.4.2 Peptide Synthesis**

Peptides were synthesized on a Protein Technologies PS3 automated peptide synthesizer using rink amide MBHA low-loaded resin (Chem-Impex International Inc.) on a 0.1 mmol scale. All Fmoc-protected amino acids were purchased from Chem-Impex International Inc. Amino acid coupling was achieved using HBTU [o-benzotriazole-N,N,N',N'-tetramethyluronium hexafluorophosphate] in N,N'-dimethylformamide

(DMF) using N-methylmorpholine as an activator for 30 min cycles. Piperidine (20 % (v/v) in DMF) was applied as a deprotecting agent throughout the synthesis. Prior to cleavage, the resin was washed three times with approximately 2 mL each of dichloromethane, glacial acetic acid, and methanol. Side chain deprotection and cleavage was completed using 5-7 mL of cleavage solution (95% trifluoroacetic acid, 2.5% ethanedithiol, and 2.5% triisopropylsilane) for 3-5 h under N<sub>2</sub> gas to yield peptides with N-terminal free amines and C-terminal amides. Cleavage solution was evaporated down to 2 mL under a nitrogen jet to precipitate peptide. Resulting precipitate was pelleted (5 min, 6000 rpm), washed three times with diethyl ether, and left to air dry overnight.

### 5.4.3 Peptide Purification

Peptides were purified using a Waters 1524 reverse-phase Binary HPLC Pump on a Waters XBridge Prep C18 column (18 μM OBD, 19mm x 250 mm) with a 40 min linear gradient from 3 to 97% acetonitrile in water with 0.1% TFA. Peptides were detected using a photodiode array set to 280 nm and 257 nm. Purity was validated to >95% by HPLC on a Waters XBridge Peptide BEH C18 column (130Å, 10 μm, 4.6 mm x 250 mm) and peptides masses were confirmed by electrospray ionization mass spectrometry (ESI-MS).

Clavanin A: VFQFLGKIIHHVGNFVHGFSHVF, calculated mass: 2665.6 m/z, found [M+2H]<sup>2+</sup> 1333.8, [M+3H]<sup>3+</sup> 889.4 m/z, and [M+4]<sup>4+</sup> 667.6 m/z.

Clavanin C: VFHLLGKIIHHVGNFVYGFSHVF calculated mass: 2666.4 m/z, found  $[M+2H]^{2+}$  1334.4,  $[M+3H]^{3+}$  889.4 m/z, and  $[M+4]^{4+}$  667.2 m/z.

#### 5.4.4 Preparation and Quantification of Stock Solutions

Peptide stock solutions were prepared by dissolving ~50 mg of lyophilized peptide in 1 mL of Milli-Q water. Solution concentrations were determined using the Edelhoch method.<sup>195, 196</sup> In short, 4  $\mu$ L of peptide stock was diluted into 396  $\mu$ L Milli-Q water to obtain an absorbance reading at 280 nm (for Tyr and Trp residues) or 257 (for Phe residues) between 0.1 and 1 absorbance units. Absorption spectra were recorded in 1 cm quartz cuvettes on a Varian Cary 50 UV-Vis spectrophotometer. Peptide stock solutions were stored at -20 °C in sealed cryogenic storage vials.

Copper (II) stock solutions were prepared by dissolving copper sulfate (Sigma-Aldrich) in Milli-Q water and standardizing by EDTA titration in an ammonium buffer to a murexide endpoint. Zinc (II), Iron (III) and nitrilotriacetic acid (NTA) stock solutions were completed by dissolving powders in Milli-Q water.

#### 5.4.5 Bacterial Strains, Yeast Strains, and Culture Conditions

Bacterial stocks were maintained in 25% glycerol in LB at -80 °C. Experiments were performed with *Escherichia coli* reference strain BW25113. Prior to all experiments, bacterial species were streaked from frozen glycerol stocks onto MHB agar plates and grown at 37 °C for 20 h. A single colony was used to inoculate 3 mL of MHB media prior to incubation at 37 °C, 200 rpm overnight. Optical density at 600 nm (OD<sub>600</sub>)

measurements were taken prior to all experiments to ensure culture growth was as expected.

Fungal stocks were maintained in 25% glycerol in YPD at -80 °C. Experiments were performed with *Candida albicans* clinical isolate SC5314 or *Cryptococcus neoformans* isolate H99. Fungal species were streaked from frozen glycerol stocks onto YPD agar plates and grown at 30 °C for 24 h. A single colony was used to inoculate 5 mL YPD or synthetic defined (SD) media prior to incubation at 30 °C, 200 rpm overnight. OD<sub>600</sub> measurements were taken prior to all experiments to ensure adequate culture growth.

#### **5.4.6 Synthetic Defined (SD+) Media**

Experiments conducted at pH 5.5 were conducted with MES buffer (Sigma-Aldrich) and all experiments conducted at pH 7.4 were conducted with Tris-HCl buffer. All buffered synthetic defined media formulations were prepared from Chelex-treated Milli-Q water with appropriate additions of media components to tightly regulate metal content. Milli-Q water utilized in this process was treated with Chelex-100 resin (100-200 mesh sodium form) using the batch method (50 g/L Bio-Rad Laboratories). A 10x concentrated batch of metal-free SD media was prepared in Chelex-treated Milli-Q water by adding glucose and yeast nitrogen base ingredients (YNB) at 10x concentrations. YNB components were added individually to prevent trace metals present in commercially available powders. To prepare working 1X SD, the 10x metal-free SD was diluted (1:10 v/v) into Chelex-treated Milli-Q water and MES buffer (Sigma Aldrich) was added to a

final concentration of 50 mM. The pH of the media was adjusted to either pH 5.5 or pH 7.4 using 1.0 M HCl or NaOH pellets and the pH corrected medium was then sterilized by vacuum filtration (0.22  $\mu\text{m}$ ). Finally, metal salts such as  $\text{CuSO}_4$ ,  $\text{FeCl}_3$ ,  $\text{MnCl}_2$ , and  $\text{ZnCl}_2$  were added. For assays utilizing metal drop-out media such as SD(-Cu) or SD(-Zn), the above protocol was followed exactly but the metal salts added in the last step were modified to reflex the desired drop-out condition.

## **5.4.7 Antibacterial and Antifungal Activity Assays**

### **5.4.7.1 Antibacterial Microdilution Assays**

*E. coli* reference strain BW25113 was cultured overnight in MHB, as described above, and diluted to an  $\text{OD}_{600}$  of 0.2 in either MES buffer (pH 5.5) or PPB (pH 7.4) to be used as the working culture. Peptides to be tested were serially diluted 2-fold in either 100  $\mu\text{L}$  MES or PPB from aqueous stock into a clear, flat-bottomed 96 well plate. Under metal supplemented conditions, 10  $\mu\text{L}$  of either  $\text{CuSO}_4$  or  $\text{ZnCl}_2$  were added to the bottom half of the plate. 100  $\mu\text{L}$  of the working culture were added to the 96-well plate containing buffer and peptide to achieve an  $\text{OD}_{600}$  of 0.1 and a final volume of 200  $\mu\text{L}$  per well. This initial plate was incubated at 37  $^\circ\text{C}$ , 200 rpm for 90 min to allow time peptide-cell (and metal if included), interactions to occur. After incubation, 50  $\mu\text{L}$  of the initial plate was added to a new 96-well plate containing 50  $\mu\text{L}$  of MHB to obtain a final well volume of 100  $\mu\text{L}$  and a final OD of 0.05. The final plate was incubated at 37  $^\circ\text{C}$ , 200 rpm for 20 h. Final peptide concentrations are indicated on figure axes. For each experiment,

a positive peptide-free control and a cell-free negative control were included. Bacterial growth was measured via OD<sub>600</sub> using a PerkinElmer Victor3 V multilabel plate reader at 0 and 20 h. OD<sub>600</sub> values were normalized to the positive growth control and adjusted by subtracting the 0 h timepoint readings from the final, 20 h timepoint, to remove any background signals from MHB medium. Data are representative of three biological replicates, each with three technical replicates per experiment. For each assay, each of three replicate conditions were averaged and error was calculated as standard deviation which is represented by error bars in the figures.

#### **5.4.7.2 Antifungal Two-Dimensional Microdilution Assays**

Either *C. albicans* or *C. neoformans* were cultured overnight in YPD, as described above, and diluted to an optical density at 600 nm (OD<sub>600</sub>) of 0.07 in either MES (pH 5.5) or PPB (pH 7.4) and used as the working culture. Peptides to be tested were serially diluted 2-fold from aqueous stocks horizontally from right to left along the wells of a clear, flat-bottomed, 96-well plate. Under metal supplemented conditions Under metal supplemented conditions, 10 µL of either CuSO<sub>4</sub> or ZnCl<sub>2</sub> were added to the bottom half of the plate. 100 µL of the working culture were added to the 96-well plate containing buffer and peptide to achieve an OD<sub>600</sub> of 0.035 and a final volume of 200 µL per well. This initial plate was incubated at 37 °C, 200 rpm for 90 min to allow time peptide-cell (and metal if included), interactions to occur. After initial incubation, 10 µL of the first plate were added to a new 96-well plate containing 190 µL YPD. The final plate was

incubated at 30 °C, 200 rpm for 48 hours. For each experiment, a positive peptide-free control and a cell-free negative control were included. Fungal growth was measured via OD<sub>600</sub> using a PerkinElmer Victor3 V multilabel plate reader at 0, 24, and 48 h. OD<sub>600</sub> values were normalized to the positive growth control and adjusted by subtracting the 0 h timepoint readings from the final, 48 h timepoint, to remove any background signals from YPD medium. Data are representative of three biological replicates, each with three technical replicates per experiment. For each assay, each of three replicate conditions were averaged and error was calculated as standard deviation which is represented by error bars in the figures.

#### **5.4.7.3 Antibacterial Two-Dimensional Microdilution Assays**

*E. coli* reference strain BW25113 (Keio) was cultured overnight in MHB, as described above, and diluted to an OD<sub>600</sub> of 0.2 in either MES buffer (pH 5.5) or PPB (pH 7.4) to be used as the working culture. Peptides to be tested were serially diluted 2-fold from aqueous stock along the bottom row of a clear, flat-bottomed 96 well plate. The metal to be tested was serially diluted 2-fold from aqueous stock down the rightmost column. To each well, 180 µL of the working culture, 10 µL aliquots from the rightmost column were distributed to all column (except the leftmost column) and 10 µL aliquots from the bottom row were distributed to all rows (except the top row). This allowed for a checkerboard style of treatment where each well contains a different ratio of peptide to metal. This initial plate contained a final volume of 200 µL and an OD<sub>600</sub> of 0.1 and was

incubated at 37 °C, 200 rpm for 90 min to allow time peptide-cell (and metal if included), interactions to occur. After incubation, 50  $\mu$ L from the initial plate was used to inoculate three new 96-well plates containing 50  $\mu$ L of MHB to obtain a final well volume of 100  $\mu$ L. The final plate was incubated at 37 °C, 200 rpm for 20 h. Final peptide concentrations are indicated on figure axes. For each experiment, a positive peptide-free control and a cell-free negative control were included. Bacterial growth was measured via OD<sub>600</sub> using a PerkinElmer Victor3 V multilabel plate reader at 0 and 20 h. OD<sub>600</sub> values were normalized to the positive growth control and adjusted by subtracting the 0 h timepoint readings from the final, 20 h timepoint, to remove any background signals from MHB medium. Data are representative of three biological replicates, each with three technical replicates per experiment. For each assay, each of three replicate conditions were averaged and error was calculated as standard deviation which is represented by error bars in the figures.

#### **5.4.7.4 Antifungal Two-Dimensional Microdilution Assays**

Either *C. albicans* or *C. neoformans* were cultured overnight in either YPD or SD+ media, as described previously, and diluted down to an OD<sub>600</sub> of 0.07 in PPB (pH 7.4) or MES (pH 5.5) as the working culture. Peptides to be tested were serially diluted 2-fold from aqueous stocks along the bottom row of a clear, flat bottomed 96-well plate. The metal to be tested was serially diluted 2-fold from aqueous stock down the rightmost column. To each well, 180  $\mu$ L of the working culture was added, 10  $\mu$ L aliquots from the

rightmost column were distributed to all column (except the leftmost column) and 10  $\mu$ L aliquots from the bottom row were distributed to all rows (except the top row). This allowed for a checkerboard style of treatment where each well contains a different ratio of peptide to metal. This initial plate contained a final volume of 200  $\mu$ L and an OD<sub>600</sub> of 0.06 and was incubated for 90 min at 37 °C, 200 rpm. Final concentrations of peptide and metal are indicated in figure axes. Following incubation, 10  $\mu$ L aliquots from the initial plate were used to inoculate three new plates containing 190  $\mu$ L of fresh media (either YPD or SD+) to a final volume of 200  $\mu$ L. Final plates were covered with AeraSeal film and incubated for 48 h at 30 °C, fungal growth measurements were taken as described in the microdilution assays section (Section 5.4.7.2). OD<sub>600</sub> values were normalized to the positive growth control and adjusted by subtracting the 0 hr timepoint from the 48 h timepoint to remove any background signals. Data are representative of three biological replicates, each with three technical replicates per experiment. GraphPad Prism 10 (version 10.2.3) was used to visualize data through the generation of heatmaps which depict the average OD<sub>600</sub> values from the biological replicates at the final timepoint.

## 6. Conclusion

This work aimed to explore the interactions between marine bacteria and heavy metal ions. Chapter 2 and chapter 3 presented two different approaches to investigating the current decline in a popular Cu-based self-polishing antifouling coating. In chapter 2, we designed a highly customizable lab-scale method to investigate how solution components impact surface composition and Cu-release. Here, we determined that in the presence of media components Cu release from coated glass substrates was increased by approximately 500% over a 2-week timeframe when compared to deionized Milli-Q water. We also built the foundation for upcoming work that will focus on determining how the presence of different bacterial species may alter Cu release or impact the surface of the coating. In chapter 3, we deployed coated panels to different field sites to allow for the collection, isolation, and identification of bacterial species believed to play important roles in facilitating biofouling. As a result, we created a library of isolates to begin to understand community diversity in early biofouling communities and we have begun building copper tolerance profiles for isolated bacterial species.

In chapter 4, we assessed the ability of *Marinobacter atlanticus*, an electroactive marine bacterium, to tolerate concentrations of essential and non-essential heavy metals prevalent in aquatic environments. We present the first assessment of metal tolerance for this species and have presented a unique interaction with vanadium that will be

explored in future work. As *M. atlanticus* demonstrated admirable abilities at tolerating heavy metals, we evaluated its ability to detoxify metal contaminated solutions, but our results were inconclusive. Ultimately, this work introduces a novel direction of study between *M. atlanticus* and vanadium and contributes to the foundation of research in support of developing *M. atlanticus* as a biosensor.

Finally, in chapter 5 we provided contributions to the growing body of research surrounding the Clavanin family of antimicrobial peptides. These peptides, first isolated almost 30 years ago, were reported to have broad spectrum activity yet current research emphasizes the antibacterial capabilities of ClavA. In light of the rising problem of drug resistant fungal pathogens and the currently limited therapeutic options we assessed the antifungal activity of ClavA and ClavC against the opportunistic fungal pathogen *Candida albicans* and found modest antifungal activity. We utilized metal-deplete media conditions to determine that neither ClavA nor ClavC require Cu or Zn to exert antifungal activity against *C. albicans*. *Cryptococcus neoformans* activity for ClavA was also assessed and we discovered strong anticryptococcal activity under acidic conditions. Additionally, we presented additional antibacterial data against a different strain of *Escherichia coli* (BW25113) in which we did not observe metal modulated changes in peptide activity.

## References

1. Morel, F. M. M.; Milligan, A. J.; Saito, M. A., Marine Bioinorganic Chemistry: The Role of Trace Metals in the Oceanic Cycles of Major Nutrients. *Treatise on Geochemistry* **2003**, *6*, 113-143.
2. Shah, S. B., Heavy Metals in the Marine Environment – An Overview. In *Heavy Metals in Scleractinian Corals*, Springer International Publishing: Cham, 2021; pp 1-26.
3. Jakimska, A.; Konieczka, P.; Krzysztof, S.; Namieśnik, J., Bioaccumulation of Metals in Tissues of Marine Animals, Part I: the Role and Impact of Heavy Metals on Organisms. *Polish Journal of Environmental Studies* **2011**, *20* (5), 1117-1125.
4. Jomova, K.; Makova, M.; Alomar, S. Y.; Alwasel, S. H.; Nepovimova, E.; Kuca, K.; Rhodes, C. J.; Valko, M., Essential metals in health and disease. *Chemico-Biological Interactions* **2022**, *367*, 110173.
5. Richir, J.; Gobert, S., Trace elements in marine environments: occurrence, threats and monitoring with special focus on the Costal Mediterranean. *Journal of environmental and analytical toxicology* **2016**, *6* (1).
6. Nordberg, G. F.; Nordberg, M.; Costa, M., Toxicology of metals: overview, definitions, concepts, and trends. *Handbook on the Toxicology of Metals* **2022**, 1-14.
7. Pande, V.; Pandey, S. C.; Sati, D.; Bhatt, P.; Samant, M., Microbial Interventions in Bioremediation of Heavy Metal Contaminants in Agroecosystem. *Front Microbiol* **2022**, *13*, 824084.
8. Romano, E.; Bergamin, L.; Croudace, I. W.; Pierfranceschi, G.; Sesta, G.; Ausili, A., Measuring anthropogenic impacts on an industrialised coastal marine area using chemical and textural signatures in sediments: A case study of Augusta Harbour (Sicily, Italy). *Science of The Total Environment* **2021**, *755*, 142683.

9. Sonker, S.; Fulke, A. B.; Monga, A., Recent trends on bioremediation of heavy metals; an insight with reference to the potential of marine microbes. *International Journal of Environmental Science and Technology* **2024**.
10. Ardila, P. A. R.; Alonso, R. Á.; Valsero, J. J. D.; García, R. M.; Cabrera, F. Á.; Cosío, E. L.; Laforet, S. D., Assessment of heavy metal pollution in marine sediments from southwest of Mallorca island, Spain. *Environmental Science and Pollution Research* **2023**, 30 (7), 16852-16866.
11. Kumudu, R. V. B.; Pathmalal, M. M., Heavy Metal Contamination in the Coastal Environment and Trace Level Identification. In *Marine Pollution*, Monique, M.; Mohamed, H. H. A.; Teresa, B.; Ahmed, A. A., Eds. IntechOpen: Rijeka, 2022; p Ch. 1.
12. Mortvedt, J. J., Heavy metal contaminants in inorganic and organic fertilizers. *Fertilizer research* **1995**, 43 (1), 55-61.
13. Zhang, P.; Yang, M.; Lan, J.; Huang, Y.; Zhang, J.; Huang, S.; Yang, Y.; Ru, J., Water Quality Degradation Due to Heavy Metal Contamination: Health Impacts and Eco-Friendly Approaches for Heavy Metal Remediation. *Toxics* **2023**, 11 (10).
14. Bighiu, M. A.; Eriksson-Wiklund, A. K.; Eklund, B., Biofouling of leisure boats as a source of metal pollution. *Environ Sci Pollut Res Int* **2017**, 24 (1), 997-1006.
15. Lagerstrom, M.; Ytreberg, E.; Wiklund, A. E.; Granhag, L., Antifouling paints leach copper in excess - study of metal release rates and efficacy along a salinity gradient. *Water Res* **2020**, 186, 116383.
16. Lagerstrom, M.; Norling, M.; Eklund, B., Metal contamination at recreational boatyards linked to the use of antifouling paints-investigation of soil and sediment with a field portable XRF. *Environ Sci Pollut Res Int* **2016**, 23 (10), 10146-57.
17. Ayobami, A. O., An assessment of trace metal pollution indicators in soils around oil well clusters. *Petroleum Research* **2022**, 7 (2), 275-285.

18. Tsamos, P.; Stefanou, S.; Noli, F., Assessment of distribution of heavy metals and radionuclides in soil and plants nearby an oil refinery in northern Greece. *Case Studies in Chemical and Environmental Engineering* **2024**, *9*, 100593.
19. Houessionon, M. G. K.; Ouendo, E. D.; Bouland, C.; Takyi, S. A.; Kedote, N. M.; Fayomi, B.; Fobil, J. N.; Basu, N., Environmental Heavy Metal Contamination from Electronic Waste (E-Waste) Recycling Activities Worldwide: A Systematic Review from 2005 to 2017. *Int J Environ Res Public Health* **2021**, *18* (7).
20. Chakraborty, S. C.; Qamruzzaman, M.; Zaman, M. W. U.; Alam, M. M.; Hossain, M. D.; Pramanik, B. K.; Nguyen, L. N.; Nghiem, L. D.; Ahmed, M. F.; Zhou, J. L.; Mondal, M. I. H.; Hossain, M. A.; Johir, M. A. H.; Ahmed, M. B.; Sithi, J. A.; Zargar, M.; Moni, M. A., Metals in e-waste: Occurrence, fate, impacts and remediation technologies. *Process Safety and Environmental Protection* **2022**, *162*, 230-252.
21. Alabssawy, A. N.; Hashem, A. H., Bioremediation of hazardous heavy metals by marine microorganisms: a recent review. *Archives of Microbiology* **2024**, *206* (3), 103.
22. Wang, H.; Fan, Z.; Kuang, Z.; Yuan, Y.; Liu, H.; Huang, H., Heavy Metals in Marine Surface Sediments of Daya Bay, Southern China: Spatial Distribution, Sources Apportionment, and Ecological Risk Assessment. *Frontiers in Environmental Science* **2021**, *9*.
23. Raza'i, T. S.; Thamrin; Nofrizal; Amrifo, V.; Pardi, H.; Pangestiansyah Putra, I.; Febrianto, T.; Fadhli Ilhamdy, A., Accumulation of essential (copper, iron, zinc) and non-essential (lead, cadmium) heavy metals in *Caulerpa racemosa*, sea water, and marine sediments of Bintan Island, Indonesia. *F1000Res* **2021**, *10*.
24. Zhou, B.; Zhang, T.; Wang, F., Microbial-Based Heavy Metal Bioremediation: Toxicity and Eco-Friendly Approaches to Heavy Metal Decontamination. *Applied Sciences* **2023**, *13* (14), 8439.
25. Choudhury, S.; Chatterjee, A., Microbial application in remediation of heavy metals: an overview. *Archives of Microbiology* **2022**, *204* (5), 268.

26. Abo-Alkasem, M. I.; Hassan, N. m. H.; Abo Elsoud, M. M., Microbial bioremediation as a tool for the removal of heavy metals. *Bulletin of the National Research Centre* **2023**, *47* (1), 31.
27. Ruczaj, A.; Brzóska, M. M., Environmental exposure of the general population to cadmium as a risk factor of the damage to the nervous system: A critical review of current data. *Journal of Applied Toxicology* **2023**, *43* (1), 66-88.
28. Siddiquee, S.; Rovina, K.; Azad, S. A.; Naher, L.; Suryani, S.; Chaikaew, P., Heavy metal contaminants removal from wastewater using the potential filamentous fungi biomass: a review. *J Microb Biochem Technol* **2015**, *7* (6), 384-395.
29. Vullo, D. L.; Ceretti, H. M.; Daniel, M. A.; Ramírez, S. A. M.; Zalts, A., Cadmium, zinc and copper biosorption mediated by *Pseudomonas veronii* 2E. *Bioresource Technology* **2008**, *99* (13), 5574-5581.
30. Chatterjee, A.; Das, R.; Abraham, J., Bioleaching of heavy metals from spent batteries using *Aspergillus nomius* JAMK1. *International Journal of Environmental Science and Technology* **2020**, *17* (1), 49-66.
31. Dafforn, K. A.; Lewis, J. A.; Johnston, E. L., Antifouling strategies: history and regulation, ecological impacts and mitigation. *Mar Pollut Bull* **2011**, *62* (3), 453-65.
32. Lewis, J. A. In *Marine biofouling and its prevention*, Materials Forum, 1998; pp 41-61.
33. McElroy, D. J.; Hochuli, D. F.; Doblin, M. A.; Murphy, R. J.; Blackburn, R. J.; Coleman, R. A., Effect of copper on multiple successional stages of a marine fouling assemblage. *Biofouling* **2017**, *33* (10), 904-916.
34. Andrewartha, J.; Perkins, K.; Sargison, J.; Osborn, J.; Walker, G.; Henderson, A.; Hallegraef, G., Drag force and surface roughness measurements on freshwater biofouled surfaces. *Biofouling* **2010**, *26* (4), 487-96.

35. Jin, H.; Tian, L.; Bing, W.; Zhao, J.; Ren, L., Bioinspired marine antifouling coatings: Status, prospects, and future. *Progress in Materials Science* **2022**, *124*, 100889.
36. Almeida, E.; Diamantino, T. C.; de Sousa, O., Marine paints: The particular case of antifouling paints. *Progress in Organic Coatings* **2007**, *59* (1), 2-20.
37. Hu, P.; Xie, Q.; Ma, C.; Zhang, G., Silicone-Based Fouling-Release Coatings for Marine Antifouling. *Langmuir* **2020**, *36* (9), 2170-2183.
38. Watermann, B. T.; Daehne, B.; Sievers, S.; Dannenberg, R.; Overbeke, J. C.; Klijstra, J. W.; Heemken, O., Bioassays and selected chemical analysis of biocide-free antifouling coatings. *Chemosphere* **2005**, *60* (11), 1530-1541.
39. Fears, K. P.; Barnikel, A.; Wassick, A.; Ryou, H.; Schultzhause, J. N.; Orihuela, B.; Scancella, J. M.; So, C. R.; Hunsucker, K. Z.; Leary, D. H.; Swain, G.; Rittschof, D.; Spillmann, C. M.; Wahl, K. J., Adhesion of acorn barnacles on surface-active borate glasses. *Philosophical Transactions of the Royal Society B: Biological Sciences* **2019**, *374* (1784), 20190203.
40. Blossom, N., Copper in the ocean environment. *Am Chemet Corp* **2007**, 1-8.
41. Arboleda-Baena, C.; Osiadacz, N.; Parragué, M.; González, A. E.; Fernández, M.; Finke, G. R.; Navarrete, S. A., Assessing Efficacy of “Eco-Friendly” and Traditional Copper-Based Antifouling Materials in a Highly Wave-Exposed Environment. *Journal of Marine Science and Engineering* **2023**, *11* (1), 217.
42. Abe, K.; Nomura, N.; Suzuki, S., Biofilms: hot spots of horizontal gene transfer (HGT) in aquatic environments, with a focus on a new HGT mechanism. *FEMS Microbiol Ecol* **2020**, *96* (5).
43. Fu, S.; Wang, Q.; Wang, R.; Zhang, Y.; Lan, R.; He, F.; Yang, Q., Horizontal transfer of antibiotic resistance genes within the bacterial communities in aquacultural environment. *Science of The Total Environment* **2022**, *820*, 153286.

44. Barzkar, N.; Sukhikh, S.; Babich, O., Study of marine microorganism metabolites: new resources for bioactive natural products. *Frontiers in Microbiology* **2024**, *14*.
45. Ameen, F.; AlNadhari, S.; Al-Homaidan, A. A., Marine microorganisms as an untapped source of bioactive compounds. *Saudi J Biol Sci* **2021**, *28* (1), 224-231.
46. Falco, A.; Adamek, M.; Pereiro, P.; Hoole, D.; Encinar, J. A.; Novoa, B.; Mallavia, R., The Immune System of Marine Organisms as Source for Drugs against Infectious Diseases. *Mar Drugs* **2022**, *20* (6).
47. Pomponi, S. A., The bioprocess-technological potential of the sea. In *Progress in Industrial Microbiology*, Osinga, R.; Tramper, J.; Burgess, J. G.; Wijffels, R. H., Eds. Elsevier: 1999; Vol. 35, pp 5-13.
48. Williams, P. G., Panning for chemical gold: marine bacteria as a source of new therapeutics. *Trends Biotechnol* **2009**, *27* (1), 45-52.
49. Ghosh, S.; Sarkar, T.; Pati, S.; Kari, Z. A.; Edinur, H. A.; Chakraborty, R., Novel Bioactive Compounds From Marine Sources as a Tool for Functional Food Development. *Frontiers in Marine Science* **2022**, *9*.
50. Okechukwu, Q. N.; Adepoju, F. O.; Kanwugu, O. N.; Adadi, P.; Serrano-Aroca, Á.; Uversky, V. N.; Okpala, C. O. R., Marine-Derived Bioactive Metabolites as a Potential Therapeutic Intervention in Managing Viral Diseases: Insights from the SARS-CoV-2 In Silico and Pre-Clinical Studies. *Pharmaceuticals* **2024**, *17* (3), 328.
51. Rotter, A.; Barbier, M.; Bertoni, F.; Bones, A. M.; Cancela, M. L.; Carlsson, J.; Carvalho, M. F.; Cegłowska, M.; Chirivella-Martorell, J.; Conk Dalay, M.; Cueto, M.; Dailianis, T.; Deniz, I.; Díaz-Marrero, A. R.; Drakulovic, D.; Dubnika, A.; Edwards, C.; Einarsson, H.; Erdoğan, A.; Eroldoğan, O. T.; Ezra, D.; Fazi, S.; FitzGerald, R. J.; Gargan, L. M.; Gaudêncio, S. P.; Gligora Udovič, M.; Ivošević DeNardis, N.; Jónsdóttir, R.; Kataržytė, M.; Klun, K.; Kotta, J.; Ktari, L.; Ljubešić, Z.; Lukić Bilela, L.; Mandalakis, M.; Massa-Gallucci, A.; Matijošytė, I.; Mazur-Marzec, H.; Mehiri, M.; Nielsen, S. L.; Novoveská, L.; Overlingé, D.; Perale, G.; Ramasamy, P.; Rebours, C.; Reinsch, T.; Reyes, F.; Rinkevich, B.; Robbens, J.; Röttinger, E.; Rudovica, V.; Sabotič, J.; Safarik, I.; Talve, S.; Tasdemir, D.; Theodotou Schneider, X.; Thomas, O. P.;

Toruńska-Sitarz, A.; Varese, G. C.; Vasquez, M. I., The Essentials of Marine Biotechnology. *Frontiers in Marine Science* **2021**, *8*.

52. Ruginescu, R.; Enache, M.; Popescu, O.; Gomoiu, I.; Cojoc, R.; Batrinescu-Moteau, C.; Maria, G.; Dumbravician, M.; Neagu, S., Characterization of Some Salt-Tolerant Bacterial Hydrolases with Potential Utility in Cultural Heritage Bio-Cleaning. *Microorganisms* **2022**, *10* (3), 644.

53. Maldonado-Ruiz, K.; Pedroza-Islas, R.; Pedraza-Segura, L., Blue Biotechnology: Marine Bacteria Bioproducts. *Microorganisms* **2024**, *12* (4).

54. Kennedy, J.; Marchesi, J. R.; Dobson, A. D., Marine metagenomics: strategies for the discovery of novel enzymes with biotechnological applications from marine environments. *Microbial cell factories* **2008**, *7*, 1-8.

55. Sarkar, S.; Pramanik, A.; Mitra, A.; Mukherjee, J., Bioprocessing data for the production of marine enzymes. *Marine Drugs* **2010**, *8* (4), 1323-1372.

56. Brennan, L.; Owende, P., Biofuels from microalgae—A review of technologies for production, processing, and extractions of biofuels and co-products. *Renewable and Sustainable Energy Reviews* **2010**, *14* (2), 557-577.

57. Bhatia, D.; Paul, S.; Acharjee, T.; Ramachairy, S. S., Biosensors and their widespread impact on human health. *Sensors International* **2024**, *5*, 100257.

58. Chang, H. J.; Voyvodic, P. L.; Zuniga, A.; Bonnet, J., Microbially derived biosensors for diagnosis, monitoring and epidemiology. *Microb Biotechnol* **2017**, *10* (5), 1031-1035.

59. Wan, X.; Saltepe, B.; Yu, L.; Wang, B., Programming living sensors for environment, health and biomanufacturing. *Microb Biotechnol* **2021**, *14* (6), 2334-2342.

60. Suttle, C. A., Marine viruses—major players in the global ecosystem. *Nat Rev Microbiol* **2007**, *5* (10), 801-812.

61. Whitman, W. B.; Coleman, D. C.; Wiebe, W. J., Prokaryotes: The unseen majority. *Proceedings of the National Academy of Sciences* **1998**, *95* (12), 6578-6583.
62. Buchmann, K., Evolution of Innate Immunity: Clues from Invertebrates via Fish to Mammals. *Front Immunol* **2014**, *5*, 459.
63. Flajnik, M. F., A cold-blooded view of adaptive immunity. *Nat Rev Immunol* **2018**, *18* (7), 438-453.
64. Franchi, N.; Ballarin, L., Immunity in Protochordates: The Tunicate Perspective. *Front Immunol* **2017**, *8*, 674.
65. Vivier, E.; Malissen, B., Innate and adaptive immunity: specificities and signaling hierarchies revisited. *Nature Immunology* **2005**, *6* (1), 17-21.
66. Cooper, E. L.; Parrinello, N., Immunodefense in Tunicates: Cells and Molecules. In *The Biology of Ascidians*, Sawada, H.; Yokosawa, H.; Lambert, C. C., Eds. Springer Japan: Tokyo, 2001; pp 383-394.
67. Loker, E. S.; Adema, C. M.; Zhang, S. M.; Kepler, T. B., Invertebrate immune systems--not homogeneous, not simple, not well understood. *Immunol Rev* **2004**, *198*, 10-24.
68. Raftos, D. A., Allorecognition and Humoral Immunity in Tunicates. *Annals of the New York Academy of Sciences* **1994**, *712* (1), 227-244.
69. Rinkevich, B., Primitive immune systems: are your ways my ways? *Immunol Rev* **2004**, *198*, 25-35.
70. Rosental, B.; Kowarsky, M.; Seita, J.; Corey, D. M.; Ishizuka, K. J.; Palmeri, K. J.; Chen, S.-Y.; Sinha, R.; Okamoto, J.; Mantalas, G.; Manni, L.; Raveh, T.; Clarke, D. N.; Tsai, J. M.; Newman, A. M.; Neff, N. F.; Nolan, G. P.; Quake, S. R.; Weissman, I. L.; Voskoboynik, A., Complex mammalian-like haematopoietic system found in a colonial chordate. *Nature* **2018**, *564* (7736), 425-429.

71. Auguste, M.; Melillo, D.; Corteggio, A.; Marino, R.; Canesi, L.; Pinsino, A.; Italiani, P.; Boraschi, D., Methodological Approaches To Assess Innate Immunity and Innate Memory in Marine Invertebrates and Humans. *Frontiers in Toxicology* **2022**, *4*.
72. Wiese, J.; Imhoff, J. F., Marine bacteria and fungi as promising source for new antibiotics. *Drug Development Research* **2019**, *80* (1), 24-27.
73. Schneemann, I.; Kajahn, I.; Ohlendorf, B.; Zinecker, H.; Erhard, A.; Nagel, K.; Wiese, J.; Imhoff, J. F., Mayamycin, a Cytotoxic Polyketide from a Streptomyces Strain Isolated from the Marine Sponge Halichondria panicea. *Journal of Natural Products* **2010**, *73* (7), 1309-1312.
74. Shin, D.; Byun, W. S.; Moon, K.; Kwon, Y.; Bae, M.; Um, S.; Lee, S. K.; Oh, D.-C., Coculture of marine Streptomyces sp. with Bacillus sp. produces a new piperazic acid-bearing cyclic peptide. *Frontiers in chemistry* **2018**, *6*, 498.
75. Wiese, J.; Abdelmohsen, U. R.; Motiei, A.; Humeida, U. H.; Imhoff, J. F., Bacicyclin, a new antibacterial cyclic hexapeptide from Bacillus sp. strain BC028 isolated from Mytilus edulis. *Bioorg Med Chem Lett* **2018**, *28* (4), 558-561.
76. Dou, W.; Xu, D.; Gu, T., Biocorrosion caused by microbial biofilms is ubiquitous around us. *Microb Biotechnol* **2021**, *14* (3), 803-805.
77. Rao, P.; Mulky, L., Microbially Influenced Corrosion and its Control Measures: A Critical Review. *Journal of Bio- and Tribo-Corrosion* **2023**, *9* (3), 57.
78. Davidson, I.; Cahill, P.; Hinz, A.; Kluza, D.; Scianni, C.; Georgiades, E., A Review of Biofouling of Ships' Internal Seawater Systems. *Frontiers in Marine Science* **2021**, *8*.
79. Hunsucker, K. Z.; Vora, G. J.; Hunsucker, J. T.; Gardner, H.; Leary, D. H.; Kim, S.; Lin, B.; Swain, G., Biofilm community structure and the associated drag penalties of a groomed fouling release ship hull coating. *Biofouling* **2018**, *34* (2), 162-172.

80. S. R., K. S.; G., S. T., Antimicrobial Resistance in Marine Ecosystem: An Emerging Threat for Public Health. In *Handbook on Antimicrobial Resistance: Current Status, Trends in Detection and Mitigation Measures*, Mothadaka, M. P.; Vaiyapuri, M.; Rao Badireddy, M.; Nagarajrao Ravishankar, C.; Bhatia, R.; Jena, J., Eds. Springer Nature Singapore: Singapore, 2023; pp 1-28.
81. Georgiades, E.; Scianni, C.; Davidson, I.; Tamburri, M. N.; First, M. R.; Ruiz, G.; Ellard, K.; Deveney, M.; Kluza, D., The Role of Vessel Biofouling in the Translocation of Marine Pathogens: Management Considerations and Challenges. *Frontiers in Marine Science* **2021**, *8*.
82. Qian, P. Y.; Cheng, A.; Wang, R.; Zhang, R., Marine biofilms: diversity, interactions and biofouling. *Nat Rev Microbiol* **2022**, *20* (11), 671-684.
83. Elmas, S.; Gedefaw, D. A.; Larsson, M.; Ying, Y.; Cavallaro, A.; Andersson, G. G.; Nydén, M.; Andersson, M. R., Porous PEI Coating for Copper Ion Storage and Its Controlled Electrochemical Release. *Advanced Sustainable Systems* **2020**, *4* (3), 1900123.
84. Tribou, M.; Swain, G., The effects of grooming on a copper ablative coating: a six year study. *Biofouling* **2017**, *33* (6), 494-504.
85. Schröder, L.; Hellweger, F.; Putschew, A., Copper leaching from recreational vessel antifouling paints in freshwater: A Berlin case study. *Journal of Environmental Management* **2022**, *301*, 113895.
86. Lagerström, M.; Lindgren, J. F.; Holmqvist, A.; Dahlström, M.; Ytreberg, E., In situ release rates of Cu and Zn from commercial antifouling paints at different salinities. *Marine Pollution Bulletin* **2018**, *127*, 289-296.
87. Ytreberg, E.; Lagerström, M.; Holmqvist, A.; Eklund, B.; Elwing, H.; Dahlström, M.; Dahl, P.; Dahlström, M., A novel XRF method to measure environmental release of copper and zinc from antifouling paints. *Environmental Pollution* **2017**, *225*, 490-496.

88. Król, A.; Mizerna, K.; Bożym, M., An assessment of pH-dependent release and mobility of heavy metals from metallurgical slag. *Journal of Hazardous Materials* **2020**, *384*, 121502.
89. Koontz, J. L.; Liggans, G. L.; Redan, B. W., Temperature and pH affect copper release kinetics from copper metal foil and commercial copperware to food simulants. *Food Addit Contam Part A Chem Anal Control Expo Risk Assess* **2020**, *37* (3), 465-477.
90. Sankararamkrishnan, R.; Verma, S.; Kumar, S., ATCUN-like metal-binding motifs in proteins: identification and characterization by crystal structure and sequence analysis. *Proteins* **2005**, *58* (1), 211-21.
91. Laussac, J. P.; Sarkar, B., Characterization of the copper(II)- and nickel(II)-transport site of human serum albumin. Studies of copper(II) and nickel(II) binding to peptide 1-24 of human serum albumin by <sup>13</sup>C and <sup>1</sup>H NMR spectroscopy. *Biochemistry* **1984**, *23* (12), 2832-8.
92. Lee, J.; Dennison, C., Cytosolic Copper Binding by a Bacterial Storage Protein and Interplay with Copper Efflux. *Int J Mol Sci* **2019**, *20* (17).
93. Schwab, S.; Shearer, J.; Conklin, S. E.; Alies, B.; Haas, K. L., Sequence proximity between Cu(II) and Cu(I) binding sites of human copper transporter 1 model peptides defines reactivity with ascorbate and O<sub>2</sub>. *Journal of Inorganic Biochemistry* **2016**, *158*, 70-76.
94. Conklin, S. E.; Bridgman, E. C.; Su, Q.; Riggs-Gelasco, P.; Haas, K. L.; Franz, K. J., Specific Histidine Residues Confer Histatin Peptides with Copper-Dependent Activity against *Candida albicans*. *Biochemistry* **2017**, *56* (32), 4244-4255.
95. Grogan, J.; McKnight, C. J.; Troxler, R. F.; Oppenheim, F. G., Zinc and copper bind to unique sites of histatin 5. *FEBS Lett* **2001**, *491* (1-2), 76-80.
96. Krishna, D. N. G.; Philip, J., Review on surface-characterization applications of X-ray photoelectron spectroscopy (XPS): Recent developments and challenges. *Applied Surface Science Advances* **2022**, *12*, 100332.

97. Scofield, J. H., Hartree-Slater subshell photoionization cross-sections at 1254 and 1487 eV. *Journal of Electron Spectroscopy and Related Phenomena* **1976**, 8 (2), 129-137.
98. Tanuma, S.; Powell, C. J.; Penn, D. R., Calculations of electron inelastic mean free paths. V. Data for 14 organic compounds over the 50–2000 eV range. *Surface and Interface Analysis* **1994**, 21 (3), 165-176.
99. Powell, C. J.; Jablonski, A., Electron effective attenuation lengths for applications in Auger electron spectroscopy and x-ray photoelectron spectroscopy. *Surface and Interface Analysis* **2002**, 33 (3).
100. Petrovykh, D. Y.; Kimura-Suda, H.; Whitman, L. J.; Tarlov, M. J., Quantitative analysis and characterization of DNA immobilized on gold. *J Am Chem Soc* **2003**, 125 (17), 5219-26.
101. NIST, NIST X-Ray Photoelectron Spectroscopy Database, NIST Standard Reference Database Number 20. **2024**.
102. Lemire, J. A.; Harrison, J. J.; Turner, R. J., Antimicrobial activity of metals: mechanisms, molecular targets and applications. *Nat Rev Microbiol* **2013**, 11 (6), 371-384.
103. Smethurst, D. G. J.; Shcherbik, N., Interchangeable utilization of metals: New perspectives on the impacts of metal ions employed in ancient and extant biomolecules. *Journal of Biological Chemistry* **2021**, 297 (6).
104. Fu, Y.; Chang, F.-M. J.; Giedroc, D. P., Copper Transport and Trafficking at the Host–Bacterial Pathogen Interface. *Accounts of Chemical Research* **2014**, 47 (12), 3605-3613.
105. Vincent, M.; Duval, R. E.; Hartemann, P.; Engels-Deutsch, M., Contact killing and antimicrobial properties of copper. *J Appl Microbiol* **2018**, 124 (5), 1032-1046.
106. Hans, M.; Mathews, S.; Mucklich, F.; Solioz, M., Physicochemical properties of copper important for its antibacterial activity and development of a unified model. *Biointerphases* **2016**, 11 (1).

107. Gomes, I. B.; Simoes, M.; Simoes, L. C., Copper Surfaces in Biofilm Control. *Nanomaterials-Basel* **2020**, *10* (12).
108. Brown, R. J.; Galloway, T. S.; Lowe, D.; Browne, M. A.; Dissanayake, A.; Jones, M. B.; Depledge, M. H., Differential sensitivity of three marine invertebrates to copper assessed using multiple biomarkers. *Aquat Toxicol* **2004**, *66* (3), 267-78.
109. Levy, J. L.; Angel, B. M.; Stauber, J. L.; Poon, W. L.; Simpson, S. L.; Cheng, S. H.; Jolley, D. F., Uptake and internalisation of copper by three marine microalgae: Comparison of copper-sensitive and copper-tolerant species. *Aquatic Toxicology* **2008**, *89* (2), 82-93.
110. Moenne, A.; Gómez, M.; Laporte, D.; Espinoza, D.; Sáez, C. A.; González, A., Mechanisms of Copper Tolerance, Accumulation, and Detoxification in the Marine Macroalga *Ulva compressa* (Chlorophyta): 20 Years of Research. *Plants (Basel)* **2020**, *9* (6).
111. Giachino, A.; Waldron, K. J., Copper tolerance in bacteria requires the activation of multiple accessory pathways. *Mol Microbiol* **2020**, *114* (3), 377-390.
112. Hadley, R. C.; Zhitnitsky, D.; Livnat-Levanon, N.; Masrati, G.; Vigonsky, E.; Rose, J.; Ben-Tal, N.; Rosenzweig, A. C.; Lewinson, O., The copper-linked *Escherichia coli* AZY operon: Structure, metal binding, and a possible physiological role in copper delivery. *Journal of Biological Chemistry* **2022**, *298* (1).
113. Chaturvedi, K. S.; Henderson, J. P., Pathogenic adaptations to host-derived antibacterial copper. *Front Cell Infect Mi* **2014**, *4*.
114. Outten, F. W.; Outten, C. E.; Hale, J.; O'Halloran, T. V., Transcriptional activation of an *Escherichia coli* copper efflux regulon by the chromosomal MerR homologue, CueR. *Journal of Biological Chemistry* **2000**, *275* (40), 31024-31029.
115. Rensing, C.; Fan, B.; Sharma, R.; Mitra, B.; Rosen, B. P., CopA: An *Escherichia coli* Cu(I)-translocating P-type ATPase. *Proc Natl Acad Sci U S A* **2000**, *97* (2), 652-6.

116. Outten, F. W.; Huffman, D. L.; Hale, J. A.; O'Halloran, T. V., The independent cue and cus systems confer copper tolerance during aerobic and anaerobic growth in *Escherichia coli*. *Journal of Biological Chemistry* **2001**, 276 (33), 30670-30677.
117. Grass, G.; Rensing, C., CueO is a multi-copper oxidase that confers copper tolerance in *Escherichia coli*. *Biochem Biophys Res Commun* **2001**, 286 (5), 902-8.
118. Holm, E. R.; Wendt, D. E.; Brewer, L.; Connolly, J.; Kowalke, G.; Swain, G.; Connelly, P.; Kavanagh, C.; Teo, S.; Lim, C.; Hadfield, M. G.; Huggett, M.; Nedved, B. T. *Characterization of Fouling at Field Test Sites of the ONR Biofouling Program: Background Information and Results for 2006-2007*; NAVAL SURFACE WARFARE CENTER CARDEROCK DIVISION: Bethesda, MD, 2008.
119. Tuck, B.; Watkin, E.; Somers, A.; Machuca, L. L., A critical review of marine biofilms on metallic materials. *Npj Mat Degrad* **2022**, 6 (1).
120. Camps, M.; Barani, A.; Gregori, G.; Bouchez, A.; Le Berre, B.; Bressy, C.; Blache, Y.; Briand, J. F., Antifouling coatings influence both abundance and community structure of colonizing biofilms: a case study in the Northwestern Mediterranean Sea. *Appl Environ Microbiol* **2014**, 80 (16), 4821-31.
121. Lang, J. M.; Erb, R.; Pechal, J. L.; Wallace, J. R.; McEwan, R. W.; Benbow, M. E., Microbial Biofilm Community Variation in Flowing Habitats: Potential Utility as Bioindicators of Postmortem Submersion Intervals. *Microorganisms* **2016**, 4 (1).
122. Besemer, K., Biodiversity, community structure and function of biofilms in stream ecosystems. *Research in Microbiology* **2015**, 166 (10), 774-781.
123. Hunsucker, K. Z.; Koka, A.; Lund, G.; Swain, G., Diatom community structure on in-service cruise ship hulls. *Biofouling* **2014**, 30 (9), 1133-40.
124. Briand, J. F.; Barani, A.; Garnier, C.; Réhel, K.; Urvois, F.; LePoupon, C.; Bouchez, A.; Debroas, D.; Bressy, C., Spatio-Temporal Variations of Marine Biofilm Communities Colonizing Artificial Substrata Including Antifouling Coatings in Contrasted French Coastal Environments. *Microb Ecol* **2017**, 74 (3), 585-598.

125. Sokal, R. R.; Michener, C. D., A statistical method for evaluating systematic relationships. *University of Kansas Science Bulletin* **1958**, *38*, 1409-1438
126. Cao, Y.; Mu, H.; Liu, W.; Zhang, R.; Guo, J.; Xian, M.; Liu, H., Electricigens in the anode of microbial fuel cells: pure cultures versus mixed communities. *Microbial Cell Factories* **2019**, *18* (1), 39.
127. Yang, Z.; Li, H.; Li, N.; Sardar, M. F.; Song, T.; Zhu, H.; Xing, X.; Zhu, C., Dynamics of a Bacterial Community in the Anode and Cathode of Microbial Fuel Cells under Sulfadiazine Pressure. *Int J Environ Res Public Health* **2022**, *19* (10).
128. Bretschger, O.; Obraztsova, A.; Sturm, C. A.; Chang, I. S.; Gorby, Y. A.; Reed, S. B.; Culley, D. E.; Reardon, C. L.; Barua, S.; Romine, M. F.; Zhou, J.; Beliaev, A. S.; Bouhenni, R.; Saffarini, D.; Mansfeld, F.; Kim, B. H.; Fredrickson, J. K.; Nealson, K. H., Current production and metal oxide reduction by *Shewanella oneidensis* MR-1 wild type and mutants. *Appl Environ Microbiol* **2007**, *73* (21), 7003-12.
129. Bond, D. R.; Lovley, D. R., Electricity production by *Geobacter sulfurreducens* attached to electrodes. *Appl Environ Microbiol* **2003**, *69* (3), 1548-55.
130. Verma, M.; Singh, V.; Mishra, V., Moving towards the enhancement of extracellular electron transfer in electrogens. *World Journal of Microbiology and Biotechnology* **2023**, *39* (5), 130.
131. Aiyer, K.; Doyle, L. E., Capturing the signal of weak electricigens: a worthy endeavour. *Trends in Biotechnology* **2022**, *40* (5), 564-575.
132. Bond, D. R.; Holmes, D. E.; Tender, L. M.; Lovley, D. R., Electrode-Reducing Microorganisms That Harvest Energy from Marine Sediments. *Science* **2002**, *295* (5554), 483-485.
133. Onderko, E. L.; Phillips, D. A.; Eddie, B. J.; Yates, M. D.; Wang, Z.; Tender, L. M.; Glaven, S. M., Electrochemical Characterization of *Marinobacter atlanticus* Strain

CP1 Suggests a Role for Trace Minerals in Electrogenic Activity. *Frontiers in Energy Research* **2019**, *7*.

134. Snider, R. M.; Strycharz-Glaven, S. M.; Tsoi, S. D.; Erickson, J. S.; Tender, L. M., Long-range electron transport in *Geobacter sulfurreducens* biofilms is redox gradient-driven. *Proc Natl Acad Sci U S A* **2012**, *109* (38), 15467-72.

135. Bird, L. J.; Mickol, R. L.; Eddie, B. J.; Thakur, M.; Yates, M. D.; Glaven, S. M., *Marinobacter*: A case study in bioelectrochemical chassis evaluation. *Microb Biotechnol* **2023**, *16* (3), 494-506.

136. Wang, Z.; Leary, D. H.; Malanoski, A. P.; Li, R. W.; Hervey, W. J.; Eddie, B. J.; Tender, G. S.; Yanosky, S. G.; Vora, G. J.; Tender, L. M.; Lin, B.; Strycharz-Glaven, S. M., A Previously Uncharacterized, Nonphotosynthetic Member of the Chromatiaceae Is the Primary CO<sub>2</sub>-Fixing Constituent in a Self-Regenerating Biocathode. *Applied and Environmental Microbiology* **2015**, *81* (2), 699-712.

137. Eddie, B. J.; Malanoski, A. P.; Onderko, E. L.; Phillips, D. A.; Glaven, S. M., *Marinobacter atlanticus* electrode biofilms differentially regulate gene expression depending on electrode potential and lifestyle. *Biofilm* **2021**, *3*, 100051.

138. Phillips, D. A.; Bird, L. J.; Eddie, B. J.; Yates, M. D.; Tender, L. M.; Voigt, C. A.; Glaven, S. M., Activation of Protein Expression in Electroactive Biofilms. *ACS Synth Biol* **2020**, *9* (8), 1958-1967.

139. Bird, L. J.; Leary, D. H.; Hervey, J.; Compton, J.; Phillips, D.; Tender, L. M.; Voigt, C. A.; Glaven, S. M., Marine Biofilm Engineered to Produce Current in Response to Small Molecules. *ACS Synth Biol* **2023**, *12* (4), 1007-1020.

140. Yates, M. D.; Bird, L. J.; Eddie, B. J.; Onderko, E. L.; Voigt, C. A.; Glaven, S. M., Nanoliter scale electrochemistry of natural and engineered electroactive bacteria. *Bioelectrochemistry* **2021**, *137*, 107644.

141. Mohapatra, R. K.; Parhi, P. K.; Patra, J. K.; Panda, C. R.; Thatoi, H. N., Biotransformation of Toxic Heavy Metals by Marine Metal Resistant Bacteria- A Novel

Approach for Bioremediation of the Polluted Saline Environment. In *Microbial Biotechnology: Volume 1. Applications in Agriculture and Environment*, Patra, J. K.; Vishnuprasad, C. N.; Das, G., Eds. Springer Singapore: Singapore, 2017; pp 343-376.

142. Dash, H. R.; Mangwani, N.; Chakraborty, J.; Kumari, S.; Das, S., Marine bacteria: potential candidates for enhanced bioremediation. *Appl Microbiol Biotechnol* **2013**, *97* (2), 561-71.

143. De, J.; Ramaiah, N.; Vardanyan, L., Detoxification of Toxic Heavy Metals by Marine Bacteria Highly Resistant to Mercury. *Marine Biotechnology* **2008**, *10*.

144. Mickol, R.; Yates, M. D.; Glaven, S. In *Comparison of protocols for extraction of lubricant precursors from marine bacteria*, Symposium on Biomaterials, Fuels, and Chemicals, 2023.

145. Mickol, R.; Yates, M. D.; Tolsma, J.; Beasley, M. A.; Glaven, S. In *Development of *Marinobacter atlanticus* as a biomanufacturing chassis organism*, Society for Industrial Microbiology and Biotechnology, 2023.

146. Yates, M. D.; Mickol, R.; Glaven, S. In *Development of Marine-Based Biomanufacturing Processes*, Symposium on Biomaterials, Fuels, and Chemicals, 2023.

147. Lohan, M. C.; Tagliabue, A., Oceanic Micronutrients: Trace Metals that are Essential for Marine Life. *Elements* **2018**, *14* (6), 385-390.

148. Hansel, C. M., Manganese in Marine Microbiology. *Adv Microb Physiol* **2017**, *70*, 37-83.

149. Yuliani, D.; Morishita, F.; Imamura, T.; Ueki, T., Vanadium Accumulation and Reduction by Vanadium-Accumulating Bacteria Isolated from the Intestinal Contents of *Ciona robusta*. *Marine Biotechnology* **2024**, *26* (2), 338-350.

150. Rehder, D., The role of vanadium in biology. *Metallomics* **2015**, *7* (5), 730-742.

151. Singh, V.; Singh, J.; Singh, N.; Rai, S. N.; Verma, M. K.; Verma, M.; Singh, V.; Chivate, M. S.; Bilal, M.; Mishra, V., Simultaneous removal of ternary heavy metal ions by a newly isolated Microbacterium paraoxydans strain VSVM IIT(BHU) from coal washery effluent. *BioMetals* **2023**, *36* (4), 829-845.
152. Chojnacka, K., Biosorption and bioaccumulation – the prospects for practical applications. *Environment International* **2010**, *36* (3), 299-307.
153. Feng, L.; Liu, B.; Yao, J.; Li, M.; Zhu, J.; Zhao, Y.; Wu, Y., Extracellular bioreduction is the main Cr(VI) detoxification strategy of *Bacillus* sp. HL1. *Journal of Environmental Management* **2024**, *358*, 120870.
154. Gu, Y.; Chen, X.; Liu, L.; Wang, S.; Yu, X.; Jia, Z.; Zhou, X., Cr (VI)-bioremediation mechanism of a novel strain *Bacillus paramycoides* Cr6 with the powerful ability to remove Cr (VI) from contaminated water. *Journal of Hazardous Materials* **2023**, *455*, 131519.
155. Tan, H.; Wang, C.; Zeng, G.; Luo, Y.; Li, H.; Xu, H., Bioreduction and biosorption of Cr (VI) by a novel *Bacillus* sp. CRB-B1 strain. *Journal of hazardous materials* **2020**, *386*, 121628.
156. Luria, S. E.; Burrous, J. W., Hybridization between *Escherichia coli* and *Shigella*. *J Bacteriol* **1957**, *74* (4), 461-76.
157. Bird, L. J.; Wang, Z.; Malanoski, A. P.; Onderko, E. L.; Johnson, B. J.; Moore, M. H.; Phillips, D. A.; Chu, B. J.; Doyle, J. F.; Eddie, B. J.; Glaven, S. M., Development of a Genetic System for *Marinobacter atlanticus* CP1 (sp. nov.), a Wax Ester Producing Strain Isolated From an Autotrophic Biocathode. *Front Microbiol* **2018**, *9*, 3176.
158. Delsuc, F.; Brinkmann, H.; Chourrout, D.; Philippe, H., Tunicates and not cephalochordates are the closest living relatives of vertebrates. *Nature* **2006**, *439* (7079), 965-8.
159. Goldstein, O.; Mandujano-Tinoco, E. A.; Levy, T.; Talice, S.; Raveh, T.; Gershoni-Yahalom, O.; Voskoboynik, A.; Rosental, B., *Botryllus schlosseri* as a Unique

Colonial Chordate Model for the Study and Modulation of Innate Immune Activity. *Mar Drugs* **2021**, *19* (8).

160. Ballarin, L.; Cima, F.; Sabbadin, A., Phagocytosis in the colonial ascidian *Botryllus schlosseri*. *Dev Comp Immunol* **1994**, *18* (6), 467-81.

161. Duarte-Mata, D. I.; Salinas-Carmona, M. C., Antimicrobial peptides immune modulation role in intracellular bacterial infection. *Front Immunol* **2023**, *14*, 1119574.

162. Zharkova, M. S.; Orlov, D. S.; Golubeva, O. Y.; Chakchir, O. B.; Eliseev, I. E.; Grinchuk, T. M.; Shamova, O. V., Application of Antimicrobial Peptides of the Innate Immune System in Combination With Conventional Antibiotics-A Novel Way to Combat Antibiotic Resistance? *Front Cell Infect Microbiol* **2019**, *9*, 128.

163. Zhang, Q. Y.; Yan, Z. B.; Meng, Y. M.; Hong, X. Y.; Shao, G.; Ma, J. J.; Cheng, X. R.; Liu, J.; Kang, J.; Fu, C. Y., Antimicrobial peptides: mechanism of action, activity and clinical potential. *Mil Med Res* **2021**, *8* (1), 48.

164. Wang, J.; Dou, X.; Song, J.; Lyu, Y.; Zhu, X.; Xu, L.; Li, W.; Shan, A., Antimicrobial peptides: Promising alternatives in the post feeding antibiotic era. *Med Res Rev* **2019**, *39* (3), 831-859.

165. Lee, I. H.; Zhao, C.; Cho, Y.; Harwig, S. S.; Cooper, E. L.; Lehrer, R. I., Clavanins, alpha-helical antimicrobial peptides from tunicate hemocytes. *FEBS Lett* **1997**, *400* (2), 158-62.

166. Lehrer, R. I.; Lee, I. H.; Menzel, L.; Waring, A.; Zhao, C., Clavanins and stylins, alpha-helical antimicrobial peptides from the hemocytes of *Styela clava*. *Adv Exp Med Biol* **2001**, *484*, 71-6.

167. Zhao, C.; Liaw, L.; Hee Lee, I.; Lehrer, R. I., cDNA cloning of Clavanins: antimicrobial peptides of tunicate hemocytes. *FEBS Letters* **1997**, *410* (2-3), 490-492.

168. In, I.-H.; Zhao, C.; Nguyen, T.; Menzel, L.; Waring, A. J.; Lehrer, R. I.; Sherman, M. A., Clavaspilin, an antibacterial and haemolytic peptide from *Styela clava*. *The Journal of Peptide Research* **2001**, *58* (6), 445-456.
169. Juliano, S. A.; Pierce, S.; deMayo, J. A.; Balunas, M. J.; Angeles-Boza, A. M., Exploration of the Innate Immune System of *Styela clava*: Zn<sup>2+</sup> Binding Enhances the Antimicrobial Activity of the Tunicate Peptide Clavanin A. *Biochemistry* **2017**, *56* (10), 1403-1414.
170. Lee, I. H.; Cho, Y.; Lehrer, R. I., Effects of pH and salinity on the antimicrobial properties of clavanins. *Infect Immun* **1997**, *65* (7), 2898-903.
171. van Kan, E. J.; Demel, R. A.; Breukink, E.; van der Bent, A.; de Kruijff, B., Clavanin permeabilizes target membranes via two distinctly different pH-dependent mechanisms. *Biochemistry* **2002**, *41* (24), 7529-39.
172. Miller, A.; Matera-Witkiewicz, A.; Mikołajczyk, A.; Wieczorek, R.; Rowińska-Żyrek, M., Chemical “Butterfly Effect” Explaining the Coordination Chemistry and Antimicrobial Properties of Clavanin Complexes. *Inorganic Chemistry* **2021**, *60* (17), 12730-12734.
173. Silva, O. N.; Alves, E. S.; de la Fuente-Núñez, C.; Ribeiro, S. M.; Mandal, S. M.; Gaspar, D.; Veiga, A. S.; Castanho, M. A.; Andrade, C. A.; Nascimento, J. M.; Fensterseifer, I. C.; Porto, W. F.; Correa, J. R.; Hancock, R. E.; Korpole, S.; Oliveira, A. L.; Liao, L. M.; Franco, O. L., Structural Studies of a Lipid-Binding Peptide from Tunicate Hemocytes with Anti-Biofilm Activity. *Sci Rep* **2016**, *6*, 27128.
174. Hancock, R. E.; Sahl, H. G., Antimicrobial and host-defense peptides as new anti-infective therapeutic strategies. *Nat Biotechnol* **2006**, *24* (12), 1551-7.
175. Nguyen, L. T.; Haney, E. F.; Vogel, H. J., The expanding scope of antimicrobial peptide structures and their modes of action. *Trends Biotechnol* **2011**, *29* (9), 464-72.

176. Campbell, J. X.; Gao, S.; Anand, K. S.; Franz, K. J., Zinc Binding Inhibits Cellular Uptake and Antifungal Activity of Histatin-5 in *Candida albicans*. *ACS Infectious Diseases* **2022**, *8* (9), 1920-1934.
177. Xu, T.; Levitz, S. M.; Diamond, R. D.; Oppenheim, F. G., Anticandidal activity of major human salivary histatins. *Infect Immun* **1991**, *59* (8), 2549-54.
178. Rai, R. K.; De Angelis, A.; Greenwood, A.; Opella, S. J.; Cotten, M. L., Metal-ion Binding to Host Defense Peptide Piscidin 3 Observed in Phospholipid Bilayers by Magic Angle Spinning Solid-state NMR. *ChemPhysChem* **2019**, *20* (2), 295-301.
179. Portelinha, J.; Duay, S. S.; Yu, S. I.; Heilemann, K.; Libardo, M. D. J.; Juliano, S. A.; Klassen, J. L.; Angeles-Boza, A. M., Antimicrobial Peptides and Copper(II) Ions: Novel Therapeutic Opportunities. *Chem Rev* **2021**, *121* (4), 2648-2712.
180. Krishna, S. S.; Majumdar, I.; Grishin, N. V., Structural classification of zinc fingers: survey and summary. *Nucleic acids research* **2003**, *31* (2), 532-550.
181. Donaghy, C.; Javellana, J. G.; Hong, Y. J.; Djoko, K.; Angeles-Boza, A. M., The Synergy between Zinc and Antimicrobial Peptides: An Insight into Unique Bioinorganic Interactions. *Molecules* **2023**, *28* (5).
182. Pushie, M. J.; Shaw, K.; Franz, K. J.; Shearer, J.; Haas, K. L., Model Peptide Studies Reveal a Mixed Histidine-Methionine Cu(I) Binding Site at the N-Terminus of Human Copper Transporter 1. *Inorganic Chemistry* **2015**, *54* (17), 8544-8551.
183. Martin, H.; Kavanagh, K.; Velasco-Torrijos, T., Targeting adhesion in fungal pathogen *Candida albicans*. *Future Med Chem* **2021**, *13* (3), 313-334.
184. Kim, J.; Sudbery, P., *Candida albicans*, a major human fungal pathogen. *J Microbiol* **2011**, *49* (2), 171-7.
185. Pfaller, M. A.; Diekema, D. J., Epidemiology of invasive candidiasis: a persistent public health problem. *Clin Microbiol Rev* **2007**, *20* (1), 133-63.

186. Cowen, L. E.; Sanglard, D.; Howard, S. J.; Rogers, P. D.; Perlin, D. S., Mechanisms of Antifungal Drug Resistance. *Cold Spring Harb Perspect Med* **2014**, *5* (7), a019752.
187. CDC, Antibiotic Resistance Threats in the United States. *U.S. Department of Health and Human Services, CDC* **2019**.
188. Lima, S. M. F.; Freire, M. S.; Gomes, A. L. O.; Cantuária, A. P. C.; Dutra, F. R. P.; Magalhães, B. S.; Sousa, M. G. C.; Migliolo, L.; Almeida, J. A.; Franco, O. L.; Rezende, T. M. B., Antimicrobial and immunomodulatory activity of host defense peptides, clavansins and LL-37, in vitro: An endodontic perspective. *Peptides* **2017**, *95*, 16-24.
189. Struyfs, C.; Cammue, B. P. A.; Thevissen, K., Membrane-Interacting Antifungal Peptides. *Frontiers in Cell and Developmental Biology* **2021**, *9*.
190. (WHO), W. H. O., WHO Fungal Priority Pathogens List to guide research, development, and public health action. **2022**.
191. Zhao, Y.; Ye, L.; Zhao, F.; Zhang, L.; Lu, Z.; Chu, T.; Wang, S.; Liu, Z.; Sun, Y.; Chen, M.; Liao, G.; Ding, C.; Xu, Y.; Liao, W.; Wang, L., Cryptococcus neoformans, a global threat to human health. *Infect Dis Poverty* **2023**, *12* (1), 20.
192. Iyer, K. R.; Revie, N. M.; Fu, C.; Robbins, N.; Cowen, L. E., Treatment strategies for cryptococcal infection: challenges, advances and future outlook. *Nat Rev Microbiol* **2021**, *19* (7), 454-466.
193. Baba, T.; Ara, T.; Hasegawa, M.; Takai, Y.; Okumura, Y.; Baba, M.; Datsenko, K. A.; Tomita, M.; Wanner, B. L.; Mori, H., Construction of *Escherichia coli* K-12 in-frame, single-gene knockout mutants: the Keio collection. *Molecular Systems Biology* **2006**, *2* (1), 2006.0008.
194. Yamamoto, N.; Nakahigashi, K.; Nakamichi, T.; Yoshino, M.; Takai, Y.; Touda, Y.; Furubayashi, A.; Kinjyo, S.; Dose, H.; Hasegawa, M.; Datsenko, K. A.;

Nakayashiki, T.; Tomita, M.; Wanner, B. L.; Mori, H., Update on the Keio collection of *Escherichia coli* gene deletion mutants. *Molecular Systems Biology* **2009**, *5* (1), 335.

195. Edelhoch, H.; Brand, L.; Wilchek, M., Fluorescence studies with tryptophyl peptides. *Biochemistry* **1967**, *6* (2), 547-559.

196. Edelhoch, H., Spectroscopic determination of tryptophan and tyrosine in proteins. *Biochemistry* **1967**, *6* (7), 1948-1954.

## Biography

Sara M. Tuck graduated from Tarleton State University in 2019 with a bachelor's degree in chemistry with minors in mathematics and criminal justice. She performed undergraduate research under Dr. Lance Whaley. She began her graduate work in the Fall of 2019 in the Department of Chemistry at Duke University and joined the lab of Professor Katherine J. Franz. Her graduate research originally focused on the evaluation of metal-modulated antimicrobial activity for two antimicrobial peptides isolated from the marine tunicate *Styela clava*. During the Summer of 2022, she was selected to participate in the Naval Research Enterprise Internship Program under the guidance of Dr. Andrew Purdy in the materials synthesis and processing section, chemistry division, at the United States Naval Research Laboratory (NRL) in Washington, DC. During this time, she investigated experimental methods to fine-tune the size and morphology of nickel nanowires. In Spring of 2023, Sara was awarded a position in the STEM Student Employment Program (SSEP) which allowed her to return to NRL to pursue a joint research project under the guidance of Dr. Kenan Fears. During her time at NRL as a SSEP student, she spent time in the molecular interfaces and tribology section, chemistry division, before transferring to the Center for Biomolecular Science and Engineering. Her work has been presented at Department of Defense conferences, including the Tri-Service Microbiome Consortium and at Biotechnology for Defense, as well as national conferences hosted by the American Chemical Society and the American Vacuum

Society. Following graduation, Sara is commissioning into the United States Navy to pursue a career in microbiology.